



Διδακτορική Διατριβή

Θέμα

**«Επίδραση μεταβολικών παραγόντων στην ενεργοποίηση
και απενεργοποίηση των μακροφάγων»**

Ελευθερία Ιερωνυμάκη



PhD Thesis

“Effect of metabolic factors on macrophage activation and inactivation”

Eleftheria Ieronymaki

Heraklion, 2019

Τριμελής Συμβουλευτική Επιτροπή

Χρήστος Τσατσάνης: Καθηγητής Κλινικής Χημείας, Τμήμα Ιατρικής, Πανεπιστήμιο Κρήτης.

Αριστείδης Ηλιόπουλος: Καθηγητής Βιολογίας και Γενετικής, Τμήμα Ιατρικής, Εθνικό και Καποδιστριακό Πανεπιστήμιο Αθηνών.

Γεώργιος Χαμηλός: Αναπληρωτής Καθηγητής Κλινικής Μικροβιολογίας - Μικροβιακής Παθογένεσης, Τμήμα Ιατρικής, Πανεπιστήμιο Κρήτης.

Επταμελής Συμβουλευτική Επιτροπή

Χρήστος Τσατσάνης: Καθηγητής Κλινικής Χημείας, Τμήμα Ιατρικής, Πανεπιστήμιο Κρήτης.

Αριστείδης Ηλιόπουλος: Καθηγητής Βιολογίας και Γενετικής, Τμήμα Ιατρικής, Εθνικό και Καποδιστριακό Πανεπιστήμιο Αθηνών.

Γεώργιος Χαμηλός: Αναπληρωτής Καθηγητής Κλινικής Μικροβιολογίας - Μικροβιακής Παθογένεσης, Τμήμα Ιατρικής, Πανεπιστήμιο Κρήτης.

Δημήτρης Καρδάσης: Καθηγητής Βιοχημείας, Τμήμα Ιατρικής, Πανεπιστήμιο Κρήτης.

Μαρία Βενυχάκη: Αναπληρώτρια Καθηγήτρια Κλινικής Χημείας, Τμήμα Ιατρικής, Πανεπιστήμιο Κρήτης.

Γεώργιος Μπερτσιάς: Επίκουρος Καθηγητής Ρευματολογίας - Κλινικής Ανοσολογίας, Τμήμα Ιατρικής, Πανεπιστήμιο Κρήτης.

Θεοδόσιος Φιλιππάτος: Επίκουρος Καθηγητής Παθολογίας, Τμήμα Ιατρικής, Πανεπιστήμιο Κρήτης.

Ευχαριστίες...

Η παρούσα διατριβή εκπονήθηκε στο εργαστήριο κλινικής χημείας υπό την επίβλεψη του καθηγητή Χρήστου Τσατσάνη. Με την ολοκλήρωσή της θα ήθελα να εκφράσω τις ειλικρινείς και θερμές ευχαριστίες μου σε όλους όσους με τη συμβολή τους βοήθησαν να φέρω εις πέρας την εργασία αυτή.

Αρχικά, θα ήθελα να ευχαριστήσω θερμά τον καθηγητή μου Χρήστο Τσατσάνη, η συμβολή του οποίου ήταν ανεκτίμητη τόσο στην ολοκλήρωση της διδακτορικής μου εργασίας, όσο και στην απόκτηση επιστημονικής γνώσης και εμπειρίας. Τον ευχαριστώ θερμά για τις συμβουλές, την κατανόηση και την υποστήριξη καθ' όλη τη διάρκεια της διδακτορικής μου εργασίας. Ευχαριστώ πολύ και την καθηγήτρια Κατερίνα Βαπορίδη για την βοήθεια και την επιστημονική καθοδήγηση.

Ευχαριστώ θερμά για την επιστημονική υποστήριξη και συνεργασία, τους συνεπιβλέποντες καθηγητές Αριστείδη Ηλιόπουλο και Γεώργιο Χαμηλό.

Επίσης, ευχαριστώ τους καθηγητές της επταμελούς επιτροπής Δημήτρη Καρδάση, Μαρία Βενυχάκη, Γεώργιο Μπερτσιά και Θεοδόσιο Φιλιππάτος για τον χρόνο τους και τη συμμετοχή τους στην κρίση του διδακτορικού μου.

Πολλά ευχαριστώ τους συνεργάτες και μέλη του εργαστηρίου Ελένη Βεργαδή, Κωνσταντίνα Λυρώνη, Χριστίνα Δοξάκη, Μαρία Δασκαλάκη, Μανώλη Θεοδωράκη, Μαρίνα Αζναούροβα και Ελπίδα Νεοφωτίστου για το ευχάριστο κλίμα και τη βοήθεια τους στα πειράματα. Θα ήθελα να ευχαριστήσω και την Ελένη Λαγουδάκη για την χρήσιμη βοήθειά της στις ιστολογικές αναλύσεις.

Πάνω απ' όλα θέλω να ευχαριστήσω την οικογένειά μου, τον πατέρα μου Κώστα, τη μητέρα μου Αρετή και την αδερφή μου Μαρία για την αμέριστη συμπαράσταση και εμπιστοσύνη που μου δείχνει σε κάθε μου επιλογή, καθώς και τον Άλμπερτ που με στηρίζει και είναι δίπλα μου όποτε τον χρειάζομαι όλα αυτά τα χρόνια.

Table of contents

| | |
|--|----|
| Abstract (in Greek)..... | 7 |
| Abstract (in English)..... | 9 |
| Introduction | 12 |
| Obesity and the metabolic syndrome..... | 12 |
| Obesity and metabolic inflammation..... | 13 |
| The role of adipose tissue in metabolic inflammation and insulin resistance..... | 17 |
| The role of liver, muscle, pancreas, gut and brain in metabolic inflammation and insulin resistance..... | 22 |
| Crosstalk of adipose tissue inflammation and the gut microbiome..... | 24 |
| Insulin signaling pathway in obesity and macrophage polarization..... | 26 |
| Factors that crosstalk with insulin signaling..... | 32 |
| The role of metabolism on macrophage activation and the effect of obesity..... | 38 |
| The concept of trained immunity as a mechanism of changes in innate immune responses..... | 43 |
| The effect of obesity on sepsis..... | 47 |
| Aim of the study | 53 |
| Materials and methods | 54 |
| Diet induced insulin resistance and obesity in mice..... | 54 |
| Primary macrophage isolation and culture..... | 54 |
| Glucose uptake assay..... | 55 |
| Caecal Ligation and Puncture Model of Polymicrobial Sepsis..... | 55 |
| Bronchoalveolar lavage fluid (BALF) and blood serum collection..... | 56 |

| | |
|---|-----------|
| ELISA..... | 56 |
| Lung histology and lung injury score determination..... | 57 |
| Glycolysis assay – Extracellular Acidification..... | 57 |
| RNA isolation and quantitative PCR..... | 58 |
| Measurement of myeloperoxidase (MPO) activity..... | 59 |
| Flow cytometry..... | 59 |
| Western blot analysis..... | 60 |
| Tolerance Test (ITT), Pyruvate Tolerance Test (PTT) and Glucose Tolerance Test (GTT)..... | 61 |
| Statistical analysis..... | 61 |
| Results..... | 62 |
| Macrophages become resistant to insulin and exhibit reduced Akt2 phosphorylation and increased mTORC1 activity..... | 62 |
| Insulin resistant macrophages acquire M2-like activation phenotype (M-InsR)... | 72 |
| Insulin resistant macrophages exhibit increased glycolysis..... | 77 |
| mTORC1 and glycolysis control M2-like phenotype in insulin resistant macrophages..... | 82 |
| Obesity and insulin resistance in macrophages is associated with reduced lung injury in polymicrobial sepsis..... | 84 |
| Insulin resistant macrophages shape gut microbiome..... | 91 |
| Lack of adiponectin results in a pro-inflammatory macrophage phenotype and abolishes the effect of high fat diet on inflammatory responses..... | 92 |
| Discussion..... | 94 |
| Future directions..... | 98 |

References.....99

Περίληψη

Η παχυσαρκία είναι μια πάθηση η οποία έχει λάβει διαστάσεις επιδημίας τα τελευταία χρόνια. Αποτελεί ένα σημαντικό προδιαθεσικό παράγοντα για την ανάπτυξη του μεταβολικού συνδρόμου και μιας πληθώρας άλλων σχετιζόμενων με την παχυσαρκία παθολογικών καταστάσεων, συμπεριλαμβανομένου του διαβήτη τύπου 2, της μη-αλκοολικής στεατοηπατοπάθειας, της καρδιαγγειακής νόσου και διαφόρων τύπων καρκίνου. Η παχυσαρκία προκαλεί μια χρόνια χαμηλού βαθμού μεταβολική φλεγμονή, η οποία χαρακτηρίζεται από υψηλά επίπεδα προφλεγμονωδών κυτταροκινών στην κυκλοφορία.

Τα μακροφάγα αποτελούν σημαντικούς διαμεσολαβητές των φλεγμονωδών αποκρίσεων και οι μεταβολικοί παράγοντες μπορούν να επηρεάσουν άμεσα τη λειτουργία τους. Ανάλογα με τα ερεθίσματα που βρίσκονται στο περιβάλλον τους μπορούν να μεταβάλλουν την κατάσταση ενεργοποίησής τους είτε προς μια προφλεγμονώδη, M1-τύπου ή προς μία αντιφλεγμονώδη, M2-τύπου κατάσταση ενεργοποίησης.

Στην παρούσα μελέτη μελετήθηκε η επίδραση της αντίστασης στην ινσουλίνη στην κατάσταση ενεργοποίησης και στο μεταβολισμό των μακροφάγων. Επιπρόσθετα, εξετάστηκε ο ρόλος των μακροφάγων με αντίσταση στην ινσουλίνη στις οξείες φλεγμονώδεις αποκρίσεις, με τη χρήση ενός μοντέλου πολυμικροβιακής σήψης αλλά και στις εμμένουσες φλεγμονώδεις αποκρίσεις όπως αυτές που ρυθμίζουν το μικροβίωμα του εντέρου. Για το σκοπό αυτό χρησιμοποιήσαμε μακροφάγα με αντίσταση στην ινσουλίνη, δηλαδή μακροφάγα τα οποία εκτέθηκαν σε υψηλές συγκεντρώσεις ινσουλίνης είτε στην καλλιέργεια είτε απομονώθηκαν από ποντίκια τα οποία έλαβαν δίαιτα υψηλή σε λιπαρά και ανέπτυξαν αντίσταση στην ινσουλίνη, όπως επίσης και μακροφάγα με έλλειψη στην κινάση Akt2 ή έλλειψη του υποδοχέα του αναπτυξιακού παράγοντα 1 παρόμοιου προς την ορμόνη ινσουλίνη (Igf1R).

Αρχικά, στα μακροφάγα που προαναφέρθηκαν διερευνήθηκε η ενεργοποίηση του μονοπατιού της ινσουλίνης, το οποίο διαμεσολαβείται μέσω του υποδοχέα της ινσουλίνης είτε μέσω του υποδοχέα του IGF1 και μετέπειτα μέσω της ενεργοποίησης του μονοπατιού Akt/mTOR. Τα αποτελέσματα έδειξαν ότι τα μακροφάγα με αντίσταση στην ινσουλίνη, έπειτα από επαγωγή με ινσουλίνη, παρουσίασαν μειωμένη ενεργοποίηση της κινάσης Akt2, η οποία είναι η κύρια ισομορφή μέσω της οποίας

επάγεται η σηματοδότηση της ινσουλίνης. Αντιθέτως, η ενεργοποίηση της κινάσης Akt1 καθώς και του μετέπειτα στόχου της mTORC1 ήταν σημαντικά αυξημένη στα μακροφάγα με αντίσταση στην ινσουλίνη.

Οι ισομορφές Akt1 και Akt2 συμβάλλουν με διαφορετικό τρόπο στην ενεργοποίηση των μακροφάγων. Η έλλειψη της Akt2 πολώνει τα μακροφάγα προς μια M2-τύπου ενεργοποίηση ενώ η έλλειψη της Akt1 ευνοεί μια M1-τύπου ενεργοποίηση. Το σύμπλοκο 1 του mTOR είναι επίσης σημαντικός ρυθμιστής της ενεργοποίησης και του μεταβολισμού των μακροφάγων. Τα μακροφάγα με αντίσταση στην ινσουλίνη, που ονομάστηκαν M-InsR, απέκτησαν μία M2-τύπου ενεργοποίηση η οποία χαρακτηρίζεται από την αυξημένη έκφραση δεικτών M2-τύπου ενεργοποίησης και μειωμένη έκκριση προφλεγμονωδών κυτταροκινών, έπειτα από επαγωγή με λιποπολυσακχαρίτη. Τα μακροφάγα αυτά έδειξαν επίσης ελαττωμένη αντιμικροβιακή δράση. Επιπλέον τα M-InsR μακροφάγα παρουσίασαν αυξημένη γλυκόλυση, όπως επιβεβαιώθηκε από τον αυξημένο γλυκολυτικό ρυθμό, την αυξημένη έκφραση γονιδίων που συμμετέχουν στη γλυκόλυση και την αυξημένη πρόσληψη γλυκόζης.

Στη συνέχεια, προκειμένου να μελετήσουμε τη συμβολή των μακροφάγων με αντίσταση στην ινσουλίνη στις οξείες φλεγμονώδεις αποκρίσεις, χρησιμοποιήθηκε ένα μοντέλο πολυμικροβιακής σήψης και οξείας βλάβης πνεύμονα που επάγεται από απολίνωση και διάτρηση του τυφλού (CLP) σε ποντίκια που φέρουν μακροφάγα με αντίσταση στην ινσουλίνη (ποντίκια παχύσαρκα λόγω πρόσληψης δίαιτας υψηλής σε λιπάρα, ποντίκια με έλλειψη στην Akt2 κινάση και ποντίκια με έλλειψη του IGF1 μόνο από τα μακροφάγα $LysM^{Cre}Igf1R^{fl/fl}$). Βρέθηκε ότι τόσο η έκκριση προφλεγμονωδών κυτταροκινών τόσο στη συστηματική κυκλοφορία όσο και στον πνεύμονα ήταν σημαντικά μειωμένη στα ποντίκια που έφεραν μακροφάγα με αντίσταση στην ινσουλίνη σε σχέση με τα ποντίκια αναφοράς. Η σοβαρότητα της βλάβης πνεύμονα ήταν βελτιωμένη στα ποντίκια με μακροφάγα με αντίσταση στην ινσουλίνη, όπως μετρήθηκε από την δραστηριότητα της μυελοπεροξειδάσης και από την ιστολογική εξέταση. Αν και η επαγόμενη από το CLP βλάβη πνεύμονα ήταν βελτιωμένη στα ποντίκια που έφεραν μακροφάγα με αντίσταση στην ινσουλίνη, πιθανώς λόγω του αυξημένου βακτηριακού φορτίου που βρέθηκε ότι υπάρχει σε αυτά τα ποντίκια. Τα αποτελέσματα θα μπορούσαν μερικώς να εξηγήσουν τη βελτιωμένη επιβίωση των παχύσαρκων ασθενών με σήψη στη Μονάδα Εντατικής Θεραπείας.

Τέλος, προσπαθώντας να διερευνήσουμε το ρόλο των M-InsR μακροφάγων στις εμμένουσες φλεγμονώδεις αποκρίσεις, όπως αυτές που ελέγχουν το εντερικό μικροβίωμα, εξετάσαμε τη μικροβιακή σύσταση του εντέρου στα ποντίκια που έφεραν μακροφάγα με αντίσταση στην ινσουλίνη καθώς και στα ποντίκια αναφοράς. Βρέθηκε μια σημαντική αύξηση στη συγκέντρωση των βακτηρίων του φύλλου *Firmicutes* και μια αντίστοιχη μείωση των *Bacteroidetes* στα ποντίκια με μακροφάγα με αντίσταση στην ινσουλίνη, ακόμα και στα ποντίκια $\text{LysM}^{\text{Cre}}\text{Igf1R}^{\text{fl/fl}}$, υποδεικνύοντας ότι τα μακροφάγα με αντίσταση στην ινσουλίνη μπορούν να διαμορφώσουν το εντερικό μικροβίωμα ανεξάρτητα από τη διαίτα.

Η παρούσα μελέτη περιγράφει την ανάπτυξη ενός είδους μνήμης στα περιφερικά μακροφάγα κατά την παχυσαρκία, η οποία χαρακτηρίζεται από ένα νέο M2-τύπου φαινότυπο ενεργοποίησης, ο οποίος βρίσκεται υπό τον έλεγχο της σηματοδότησης του μονοπατιού Akt1/mTORC1 και του γλυκολυτικού μεταβολισμού. Ο φαινότυπος αυτός ίσως εξηγεί τις διαφορετικές αποκρίσεις των μακροφάγων καθώς και την ανάπτυξη παθολογικών καταστάσεων που εμφανίζονται κατά την παχυσαρκία και το διαβήτη τύπου 2.

Abstract

Obesity is a pathological condition that has reached epidemic proportions in recent years. It constitutes an important risk factor for the development of metabolic syndrome and a variety of other obesity-related pathologic conditions, including Type 2 diabetes, non-alcoholic fatty liver disease, cardiovascular disease and several types of cancer. Obesity induces a chronic low grade metabolic inflammation characterized by high circulating levels of pro-inflammatory cytokines.

Macrophages are important mediators of inflammatory responses and metabolic factors directly act on their function. They can be polarized either towards a pro-inflammatory, M1 phenotype or an anti-inflammatory, M2 phenotype depending on their environmental stimuli.

In the present study we investigated the effect of insulin resistance on macrophage activity and metabolism. Furthermore, we examined the role of these macrophages in acute inflammatory responses, in a model of polymicrobial sepsis and in sustained responses such as those regulating the gut microbiome. For this purpose we employed macrophages that acquired insulin resistance, being macrophages exposed to high insulin concentrations either *in vitro* or *in vivo* in a mouse model of high-fat diet induced insulin resistance, as well as macrophages that lack Akt2 isoform or Insulin-like growth factor 1 receptor (Igf1R).

Firstly, we investigated the activation of the insulin signaling pathway in these macrophages, mediated by either insulin receptor or IGF1 receptor and subsequent activation of the Akt/mTOR pathway. We found that insulin resistant macrophages upon insulin stimulation, showed reduced activation of the Akt2 isoform, the predominant isoform that mediates insulin signals. On the other hand, the activation of Akt1 isoform and its downstream target mTORC1 was significantly elevated in insulin resistant macrophages.

Akt1 and Akt2 isoforms differentially contribute to macrophage polarization. Lack of Akt2 polarizes macrophages towards an M2-like phenotype while absence of Akt1 results in M1 phenotype. mTORC1 is also an important regulator of macrophage function and metabolism. Insulin resistant macrophages obtained an M2-like phenotype, termed M-InsR, that is characterized by increased expression of M2

polarization markers and reduced secretion of pro-inflammatory cytokines upon lipopolysaccharide stimulation. These macrophages also showed reduced anti-microbial capacity. We also found that M-InsR macrophages displayed a metabolic shift towards glycolysis, as it was indicated by increased glycolytic rate, increased expression of genes participating in glycolysis and increased basal glucose uptake.

Subsequently, in order to investigate the contribution of insulin resistant macrophages in acute inflammatory responses, an in vivo model of polymicrobial sepsis and lung injury induced by Cecal Ligation and Puncture (CLP) was used in mice bearing insulin resistant macrophages (diet-induced obese mice, Akt2^{-/-} mice and LysM^{Cre}Igf1R^{fl/fl} mice). We found that systemic and pulmonary expression of the pro-inflammatory cytokines significantly lower in mice bearing insulin resistant macrophages compared to control mice. The severity of lung injury, as indicated by myeloperoxidase activity and histological evaluation was ameliorated in mice harboring insulin resistant macrophages. Although CLP-induced Acute Lung Injury (ALI) was reduced, survival was not improved in mice bearing insulin resistant macrophages probably due to the increased bacterial burden found in these mice. These results showing that insulin resistance dampens inflammatory responses, could partially explain the improved short-term survival of obese septic patients in the Intensive Care Unit.

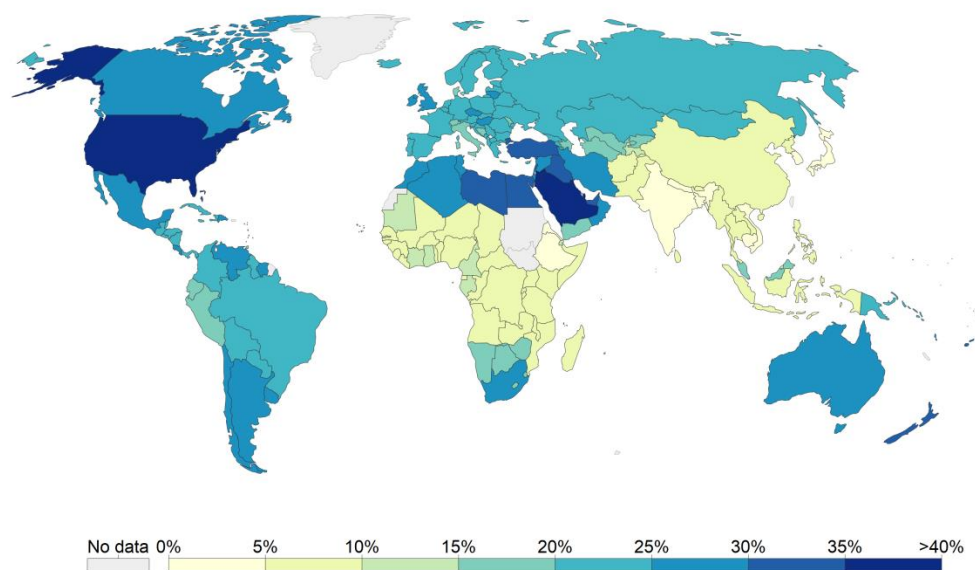
Finally, in order to investigate the role of M-InsR macrophages in sustained responses, such as those regulating the gut microbiome we examined the composition of gut microflora in all mice harboring insulin resistant macrophages. We found that a significant increase in the concentration of the phyla *Firmicutes* and a proportional decrease in *Bacteroidetes* in mice bearing insulin resistant macrophages, even in LysM^{Cre}Igf1R^{fl/fl} mice implying that insulin resistant macrophages can shape microbial composition of the gut irrespective of the diet.

This study describes a kind of innate immune memory in peripheral macrophages characterized by a novel M2-like phenotype, which is under the control of Akt1/mTORC1 signals and glycolytic metabolism. This phenotype may explain changes in macrophage responses and development of related pathologic conditions that occur in obesity and type 2 diabetes.

Introduction

Obesity and the metabolic syndrome

Obesity is a worldwide pathological condition that had reached epidemic proportions in the last few years (Figure 1) (1). Obesity is a chronic medical condition characterized by excess body fat accumulation and predisposes to a variety of diseases and pathological conditions.



Source: WHO, Global Health Observatory

CC BY

Obesity is frequently subdivided into categories according to body mass index (BMI) that is defined as the weight in kilograms divided by the height in meters squared

| Weight Category | Body Mass Index | |
|-----------------------|--|--------------|
| | Children | Adults |
| Underweight | Below 5th percentile* | Below 18.5 |
| Healthy weight | 5th percentile to less than 85th percentile | 18.5 to 24.9 |
| Overweight | 85th percentile to less than 95th percentile | 25 to 29.9 |
| Obese | 95th percentile or above | 30 or above |

Table 1: Weight categories according to BMI.

(BMI = weight (kg)/ height² (m²)). For adults anyone with a BMI over 30 would be classified as obese, while in children is age and sex dependent and is defined as a BMI at or above the 95th percentile according to developmental curves (Table 1).

Waist circumference and waist to hip ratio define the central or abdominal obesity. Increased body fat is considered as a risk factor for the development of cardiovascular diseases independent of BMI. Systemic meta-analysis show a strong association between increased waist to hip ratio (> 0.85 for women and > 0.9 for men) and myocardial infarction but also other chronic cardiovascular conditions, like ischemic heart disease and chronic heart failure (2-4).

Obesity is associated with the development of metabolic syndrome, a complex pathologic condition characterized by high blood glucose levels, arterial hypertension, abdominal obesity and abnormal levels of LDL and triglycerides (5). In addition, it constitutes an important risk factor for the development of Type 2 diabetes, non-alcoholic fatty liver disease, cardiovascular diseases, several types of cancer and a variety of other obesity-related pathologic conditions (6).

However, it is not obesity per se that is responsible for these health disorders but relatively the inflammatory responses that are associated with this condition (7). Obesity induces metabolic inflammation, a low grade inflammation characterized from high circulating levels of pro-inflammatory cytokines. Cytokine levels are gradually increased implying a chronic situation, reaching a 2-3 fold raise compared to homeostatic conditions, instead of acute and dramatically higher levels observed upon infection.

Obesity and metabolic inflammation

Macrophages are important mediators of inflammatory responses and they can be classified according to their activation status as pro-inflammatory or M1-type and anti-inflammatory or M2-type. M1-type macrophages are important for the initiation of inflammation and acute inflammatory response upon infection. Factors like Th1 cytokine interferon- γ (IFN- γ) and toll-like receptor (TLR) ligands can trigger this polarization status (Figure 2). A plethora of pro-inflammatory cytokines and chemokines, such as TNF- α , IL-6, IL-1 β , IL-12, CXCL8, CXCL2 and others are released by M1-type macrophages trying to attract innate and adaptive immune cells

to fight against the invading pathogen. They also have high phagocytic capacity and they produce bactericidal agents, such as reactive oxygen species (ROS) and nitric oxide (NO). NO is synthesized by inducible nitric oxide synthase (iNOS) from arginine.

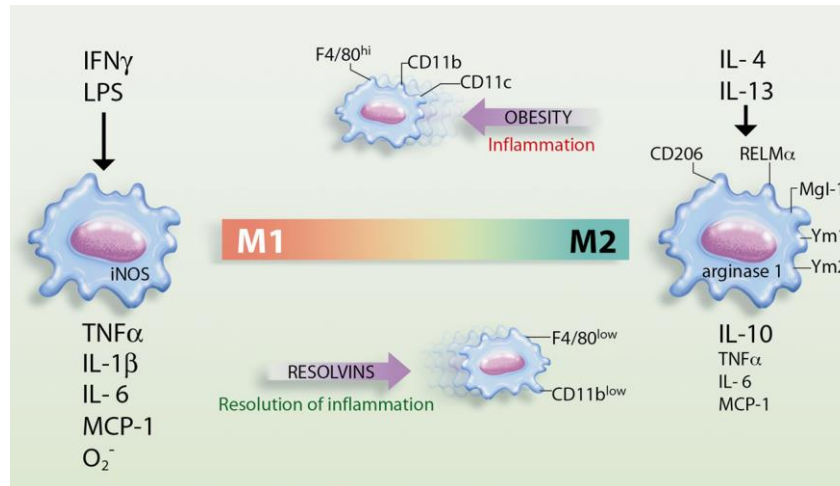


Figure 2: M1-type or Classical activation and M2-type or Alternative activation of macrophages and characteristic polarization markers. (Adapted from Clària, González-Pérez et al. 2011).

After the infection alternatively activated or M2-type macrophages promote resolution of inflammation and tissue remodeling. They are found during helminth infection and they display anti-inflammatory actions. M2-type macrophages are activated by IL-4, IL-13, IL-10 and tumor growth factor β (TGF β) and characterized by the expression of specific markers, like Arginase1, Ym1, Fizz1, IL-10 etc (8, 9).

Macrophages are influenced by a variety of signals originated from the tissue-microenvironment, inducing changes in polarization status and gene expression profile (10). Differential transcription factor activation mediates this dynamic phenotype of macrophages (11). In particular, (lipopolysaccharide (LPS) and free fatty acids (FFAs) through TLR4 and cytokine receptors activate nuclear factor- κ B (NF- κ B), AP1 and Interferon regulatory factor 3 (IRF3) and IRF5 for the expression of M1-type genes. TLR4 engagement results in conformational changes of the receptor that facilitate subsequent recruitment of toll/interleukin-1 receptor (TIR) – domains containing adaptor molecules. There are two major pathways activated, MyD88-dependent and MyD88 – independent (Figure 3). The MyD88-dependent pathway is regulated by MyD88 and TIRAP proteins. Activation of this pathway results in the recruitment of IRAKs (IRAK1 and IRAK4) and TNF Receptor-Associated Factor 6 (TRAF6). TRAF6 activates transforming growth factor- β -

activated kinase 1 (TAK1) and leads to the activation of I κ B Kinase (IKK) and p30, ERK, JNK MAP kinases pathways. Mitogen-Activated Protein Kinase (MAPK) signaling results in the activation of AP-1 transcription factor. IKK (complex of

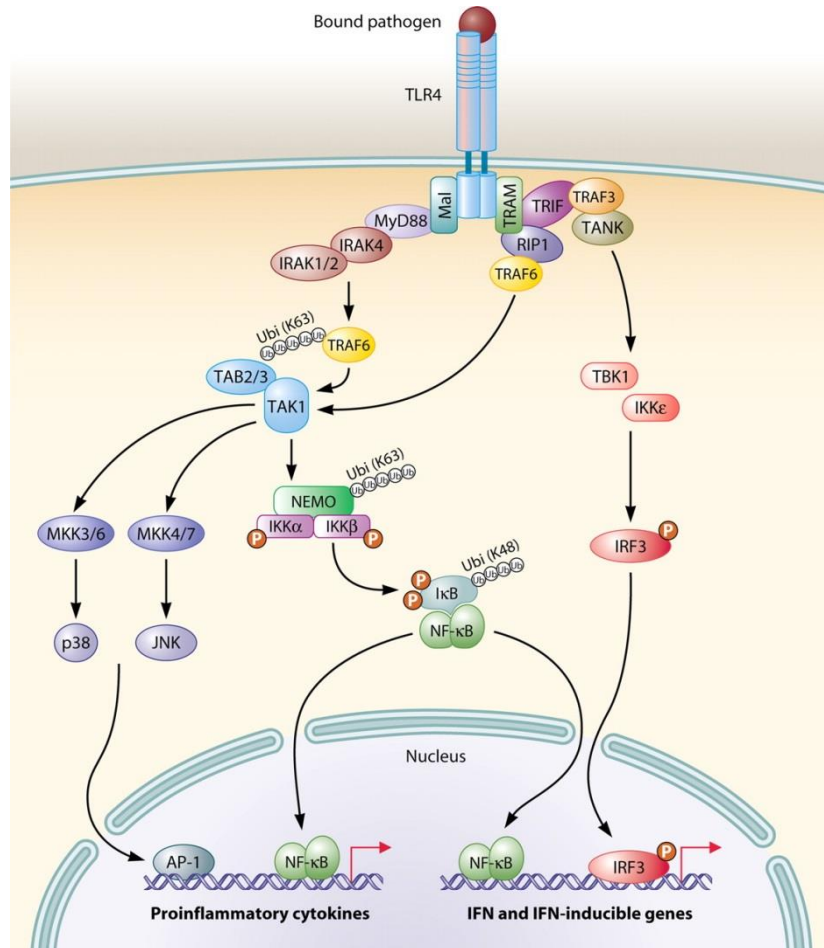


Figure 3: MyD88-dependent and independent Toll-like receptor 4 (TLR4) signaling pathway.

IKK α , IKK β and IKK γ) phosphorylates and promotes ubiquitination and proteasomal degradation of I κ B leading to the release and subsequent translocation of NF- κ B to the nucleus. IRF5 can also be activated by MyD88. In the MyD88- independent pathway TIR-domain-containing adaptor inducing interferon- β (TRIF) and TRIF-related Adaptor Molecule (TRAM) complex activate IRF3 transcription factor, via TRAF3, for the production of type 1 interferons (11, 12).

LPS also could lead to the expression of M2-type genes through C/EBP β , including IL-1 receptor-associated kinase M (IRAK-M) that is a negative regulator of TLR4 signaling (13). IFN- γ through its receptor stimulates signal transducer and activator of transcription 1 and 2 (STAT1 and 2) and IRF5, which enhance M1 polarization

profile. IL-4 binds IL-4R α and mediates the expression of M2 markers through STAT6 and IRF4. Finally, peroxisome proliferator-activated receptor- γ (PPAR- γ) which is triggered by free fatty acids or IL-4 suppresses pro-inflammatory cytokine production (9, 14).

Metabolic inflammation causes impairment of insulin signaling in main metabolic organs, including liver, muscle and adipose tissue leading in systemic hyperglycemia and hyperinsulinemia, features commonly found in obesity.

Insulin is a hormone, which can act directly on macrophage metabolism and function. It is secreted by beta pancreatic cells in response to increased circulating glucose levels, as those found after a meal. Insulin induces anabolic actions, like the conversion of glucose to glycogen in muscle, liver and adipose tissue. In addition, it induces triglyceride storage in adipose tissue. On the contrary, catabolic actions that favor glucose formation, like gluconeogenesis and glycogenolysis in liver and muscle and lipolysis in adipose tissue are suppressed, resulting in energy storage.

Insulin resistance is a pathologic condition, where cells lose their ability to respond to insulin and take up easily glucose from the bloodstream. As a result, pancreatic cells produce higher amount of insulin to overcome cells weak response and keep glucose levels in a healthy range. Prediabetes or borderline is closely tied to obesity and characterized by increased glucose levels in the bloodstream but not high enough to be T2D. It is a metabolic condition that constitutes a pre-diagnosis of T2D.

In the context of obesity, chronic inflammation, particularly in the adipose tissue and liver, constitutes a main contributor to the development of insulin resistance. Chronic inflammation is characterized by three stages. The first phase is associated with an initial trigger that disturbs the organism homeostasis; this disturbance is followed by phase 2, an acute adaptive inflammatory response which eventually results in phase 3, a long term maladaptive stage that leads to complications. Concerning obesity, the trigger might be the disruption of energy balance that poses a homeostatic stress, especially in adipocytes. The response to this stress is associated with cytokine and chemokine release that initiate the catabolic adaptive phase, trying to compensate the hyper-anabolic state induced by the trigger. The adaptive phase results in healthy adipose tissue enlargement and decreased energy storage. Finally, in the maladaptive phase 3 the system trying to restore energy homeostasis reaches a new set point of

weight, blood glucose levels, hormone levels, lipid levels found in the circulation etc. All these changes lead to the complications of obesity including insulin resistance, impaired tissue remodeling and fibrosis (15).

The role of adipose tissue in metabolic inflammation and insulin resistance

Adipose tissue is an endocrine organ important in maintaining energy homeostasis but also contributes to the persistence of inflammation in case of overnutrition. Early after high fat diet feeding, approximately 3-7 days, adipose tissue becomes inflamed and gradually increases, contributing to systemic insulin resistance (16). A complex metabolic and immune interplay between adipocytes and immune cells is responsible for the changes found in adipose tissue microenvironment during obesity.

In lean states, adipocytes secrete adiponectin, an adipokine that promote insulin sensitivity but also possess anti-inflammatory properties (17). Reduced adiponectin levels are linked with insulin resistance (18). Adiponectin affects macrophage sensitivity and suppresses inflammatory responses against pro-inflammatory stimuli, through inhibition of the NF κ B pathway (19). Adiponectin promotes insulin signaling by direct interaction of APPL1 an adaptor protein downstream of adiponectin receptor that mediates proper adiponectin signaling propagation with insulin receptor substrates. Many actions of adiponectin are also mediated through induction of adenosine monophosphate-activated protein kinase (AMPK) downstream adiponectin receptors (18). AMPK is an energy sensor and it is activated by the changes in the AMP/ATP ratio. It is involved in glucose transport, lipid synthesis, protein synthesis and mitochondrial function and biogenesis, promoting insulin sensitivity (20). AMPK activity is reduced in insulin resistance and it is a potent target for diabetes prevention and treatment (21).

Another adipokine that regulates food intake and energy expenditure in the central nervous system is leptin. It also has a role in maintaining insulin sensitivity in insulin responsive tissues. Leptin is increased in obesity but its protective effect is lost due to leptin resistance. Leptin was found to exert pro-inflammatory actions leading to secretion of M1 cytokines from macrophages, contributing to the inflammatory milieu formed in the adipose tissue during obesity (17, 22, 23).

Resistin is a hormone primarily expressed from adipocytes in mice, whereas in humans it is produced from macrophages and it is regulated by the transcription factor PPAR- γ . Resistin levels correlate with the development of obesity, T2D and cardiovascular disease. Increased levels of circulating resistin are found in diet-induced obese or *ob/ob* mice, while treatment with glitazones reduced its secretion both in mice and in humans (24). Resistin can interfere with insulin signaling pathway in liver, muscle and adipose tissue through various mechanisms. High levels of resistin suppress AMPK phosphorylation, but it also induces the expression of SOCS3, a known inhibitor of insulin signaling. Resistin can also interfere with the phosphorylation of insulin receptor substrates and the activation of PI3K/Akt. Resistin is upregulated upon pro-inflammatory stimulation and increases the expression of pro-inflammatory factors, including TNF α , IL-6, IL-12, and monocyte chemoattractant protein (MCP)-1 in PBMCs and macrophages via the NF- κ B pathway (25).

Innate immune system and especially macrophages, possesses an important role in the development of insulin resistance in specific tissues, which eventually leads to systemic insulin resistance. Macrophages are able to sense factors derived from pathogens or from innate and adaptive immune cells or even from specialized cells in the affected tissue. The initial trigger for the development of adipose tissue inflammation could derive from gut microbiome, through a dietary component or metabolite. The initial trigger could also derive from intrinsic signals due to adipose tissue enlargement that result in hypoxia, adipocyte death and mechanical stress due to the interaction with the extracellular matrix (ECM) (15).

Tissue macrophages are classified based on their activation status, into classically activated M1 pro-inflammatory macrophages versus alternatively activated M2 anti-inflammatory cells. Adipose tissue macrophages (ATMs) are the most abundant and can comprise up to 40% of all stromal vascular cells in obese versus 10% in lean adipose tissue, implying their significant role in the regulation of metabolic inflammation (26).

In insulin sensitive adipose tissue, ATMs acquire an anti-inflammatory phenotype and secrete IL-10 that is essential in maintaining tissue metabolic homeostasis. The anti-inflammatory phenotype found in lean state, is preserved due to the presence of Tregs, T (T helper 2-Th2) cells, innate lymphoid cells type 2 (ILC2) cells, eosinophils and

adipocytes that provide anti-inflammatory cytokines IL-4, IL-13, and IL-33 and other anti-inflammatory factors (Figure 4) (27).

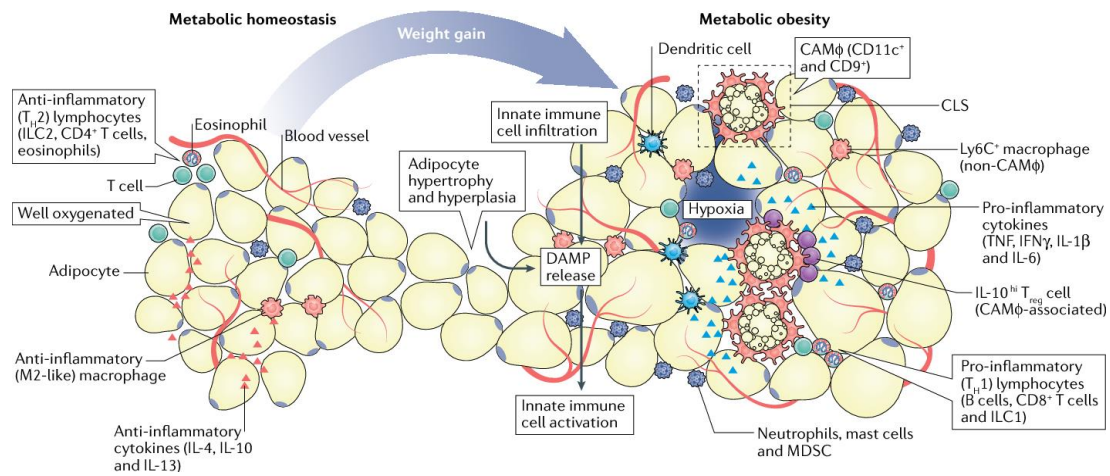


Figure 4: Adipose tissue changes during obesity. In lean adipose tissue ATMs acquire an M2-like phenotype and along with other anti-inflammatory cells, T helper 2 (Th2) cells, innate lymphoid cells type 2 (ILC2) cells, eosinophils they secrete anti-inflammatory cytokines and preserve metabolic homeostasis. After weight gain adipose tissue becomes enlarged and creates hypoxic conditions that result in adipocyte death and subsequent release of damage - associated molecular patterns (DAMPs), Monocytes recruitment combined with the local proliferation results in a pro-inflammatory phenotype of ATMs. Other pro-inflammatory cells are also found in the inflamed adipose tissue, Th1, ILC1 etc. Macrophages secrete pro-inflammatory cytokines and tend to form crown-like structures around dead adipocytes for lipid scavenging. CLS: crown- like structures, CAM ϕ : CLS - associated macrophage, MDSC: myeloid- derived suppressor cells. (Adapted from Lauterbach and Wunderlich 2017).

During obesity, monocyte recruitment along with local proliferation results in a novel pro-inflammatory polarization phenotype of ATMs that express CD11c as surface marker and secrete TNF α and IL-1 β cytokines (27, 28). In the initiation of obesity-induced inflammation, adipocytes are triggered to activate intracellular pro-inflammatory programs with subsequent release of adipokines, cytokines and chemokines. Adipocytes overproduce and secrete pro-inflammatory cytokines, including TNF α and IL-6 contributing to local as well as to systemic inflammation observed during obesity. Adipocytes also secrete chemokines that favor the recruitment of macrophages within inflamed adipose tissue. MCP1-CCR2 signal is important for macrophage infiltration, since deletion of Ccr2 and probably of Ccl2 protects against obesity induced insulin resistance. Other chemotactic signals including leukotriene LTB4-LTB4R1 and Semaphorin3E and its receptor plexinD1 were found to be increased in the adipose tissue of high-fat diet fed mice. Another, mechanism of macrophage chemotaxis to the adipose tissue could be through small

membrane-bound exosomes, produced by dying or palmitate-stimulated adipocytes (29). The recruitment of macrophages and other immune cells results in their activation and subsequent secretion of their own chemokines contributing to the maintenance of this chemoattractant process.

In the early stages of obesity, many changes occur in the adipose tissue microenvironment affecting macrophage activation status. The content of Treg cells is reduced in obese adipose tissue, leading to disruption of inflammatory regulation. Infiltration of CD8⁺ T and Cd4⁺ T helper 1 cells in the obese adipose tissue along with NK and ILC1 accumulation are associated with the production of pro-inflammatory agents, like interferon γ (IFN γ) and adipose tissue inflammation. In addition, recruitment of B cells (B2 cells) promotes a pro-inflammatory state by producing pathogenic IgG antibodies and pro-inflammatory factors. B cells are not the only cells

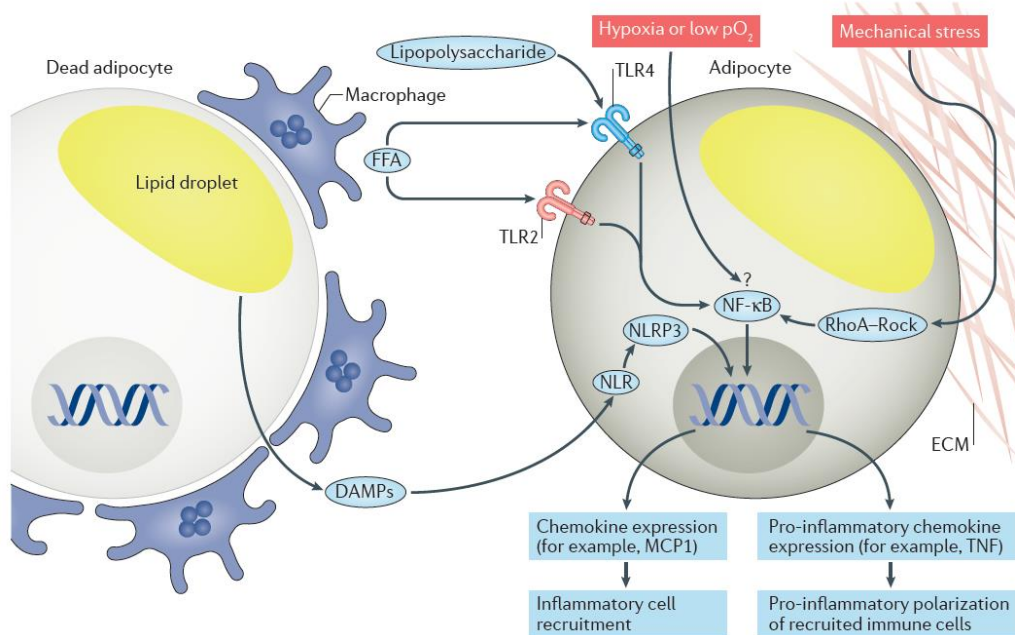


Figure 5: Initial triggers of adipose tissue inflammation. Lipopolysaccharide and FFAs can trigger TLRs and induce pro-inflammatory signaling. Dead adipocytes release damage-associated molecular patterns (DAMPs) that activate NLRP3 inflammasome. Mechanical stress caused due to the interaction of enlarged adipocytes with ECM activates RhoA-Rock that leads to downstream inflammatory signaling. Hypoxia can also trigger inflammation in adipocytes through an unclear mechanism. All these stimuli can lead to the activation of NF-κB, an important regulator for the expression of inflammatory genes. FFA: Free fatty acid, TLR: Toll-like receptor 4, NLR: NOD-like receptor, ECM: Extracellular matrix. (Adapted from Reilly and Saltiel 2017)

that regulate the activity of T cells, adipocytes also possess antigen-presenting capacity. In early stages of obesity, MHC II antigen presentation in adipocytes is observed after only 2 weeks of high-fat feeding in mice. All the aforementioned

events create pro-inflammatory conditions favoring the shift of macrophage polarization from M2 to M1 type, a hallmark of adipose tissue inflammation in obesity. M1 polarization type is characterized by secretion of pro-inflammatory cytokines and tendency to form crown-like structures around the dead adipocytes for lipid scavenging (26, 27).

Obesity is associated with increased intestinal permeability and subsequent higher circulating levels of lipopolysaccharide (LPS), produced by intestinal Gram negative bacteria. Microbial products are recognized by pattern recognition receptors (PRRs) of host immune system, but also from adipocytes. LPS binds to Toll-like receptor 4 (TLR4) and stimulates inflammatory pathways. In addition, free fatty acids (FFAs) derived from dietary sources or from hydrolysis of adipocyte triglyceride stores can trigger inflammation through direct binding to TLR2 and TLR4 receptors. Damage-associated molecular proteins (DAMPs) released from dying adipocytes and recognized by NOD-like receptors (NLRs), result in activation NLRP3 inflammasome activation in leukocytes to reduce tissue damage. Hypoxia in obese adipose tissue can also trigger inflammation. Hypoxic conditions could derive from the uncoupling of mitochondria oxidative metabolism as a result of elevated free fatty acids (FFAs). Oxygen consumption is increased in adipocytes resulting in hypoxia, which is sensed by hypoxia-inducible factor – 1 α (HIF-1 α) promoting the release of pro-inflammatory agents. Hypoxia can also be caused due to lower oxygen perfusion compared to metabolic need in the expanded adipose tissue. Adipocytes are found embedded in a dense network of extracellular matrix (ECM) proteins, especially collagen I. Hypertrophic adipocytes interact with ECM causing mechanical stress, which is sensed by RhoA-Rock pathway and leads to the activation of pro-inflammatory signaling. Many pathways can be triggered by the aforementioned stimuli that lead to activation of NF- κ B, a potent transcription factor responsible for the expression of inflammatory factors (Figure 5) (15).

Macrophages that are found in the inflamed adipose tissue during obesity are often referred to as classically activated due to their pro-inflammatory phenotype. However in the context of obesity, the associated low grade metabolic inflammation is different from acute inflammatory responses against pathogens and consequently macrophages are not identical to the M1 phenotype. During obesity, adipose tissue macrophages are characterized by the expression of specific surface markers and along with the pro-

inflammatory activation and are referred to as metabolically activated, MMe (30). In addition, ATMs acquire a foam cell role, accumulating excess lipid due to dead adipocytes. Foam cells, also found in atheromatic plaques during atherosclerosis, display M2-like characteristics in spite of the inflammatory state (31).

The role of liver, muscle, pancreas, gut and brain in metabolic inflammation and insulin resistance

Liver has an important role in the regulation of glucose homeostasis. Under hyperglycemic conditions, hepatocytes store glucose as glycogen, while during fasting periods glucose is produced to maintain blood glucose levels. In obesity-associated insulin resistance, results to impaired regulation of liver glucose production while its action on *de novo* lipogenesis is enhanced, leading to fasting hyperglycemia and hypertriglyceridemia (27, 32).

Liver becomes inflamed during obesity and contributes to the development of systemic insulin resistance. Activation of liver macrophages has a central role in liver inflammation. Two different macrophage populations are found in the liver, tissue resident macrophages (Kupffer cells –KCs) and recruited macrophages that infiltrate the liver due to the release of chemokines from KCs and steatotic hepatocytes during obesity. Factors that can trigger liver inflammation are the excessive and inappropriate accumulation of fat in the liver and the increased levels of circulating products of gut microbiome (26).

Accumulation of FFAs in the liver due to increased lipolysis of adipose tissue and subsequent excess in circulating fatty acids can cause hepatic insulin resistance and subsequently steatosis and fatty liver diseases. This fat accumulation induces lipotoxicity and eventually leads to liver damage and inflammation. LPS also can enter liver sinusoids through portal vein and stimulate KCs to defend against invading microorganisms (27).

During obesity, the number of resident macrophages remains the same while there is a dramatic increase in recruited liver macrophages. In addition, KCs display a polarization switch towards a pro-inflammatory phenotype and secrete pro-inflammatory cytokines, TNF- α and IL-6, due to increased circulating levels of pro-inflammatory cytokines and LPS found in obesity (26, 27). On the contrary, recent

evidence shows that obesity does not induce a pro-inflammatory phenotypic switch of liver macrophages and recruited macrophages are not able to induce insulin resistance since their recruitment occurs after the development of insulin resistance and their depletion does not improve insulin resistance. This suggests that liver macrophages have a significant role in obesity induced insulin resistance independently of their inflammatory status (33).

Inflammation could be causally linked to the local development of insulin resistance in many other organs, including skeletal muscle, pancreas, central nervous system (CNS) and gut that subsequently can all contribute to systemic insulin resistance (Figure 6).

During obesity, skeletal muscle that has a significant role in glucose homeostasis, also displays metabolic dysfunction. Increased infiltration of pro-inflammatory macrophages is observed in adipose depots of skeletal muscle (intermyocellular or perimuscular) as well as in the surrounding vasculature. These macrophages secrete TNF- α , IL-1 β and other pro-inflammatory factors that could potentially lead to local insulin resistance (26, 32). Accumulation of Ly6C expressing macrophages is also evident in pancreatic islets during obesity. Under the stress of high glucose and FFA levels, β -cells secrete chemotactic agents that promote monocyte recruitment in

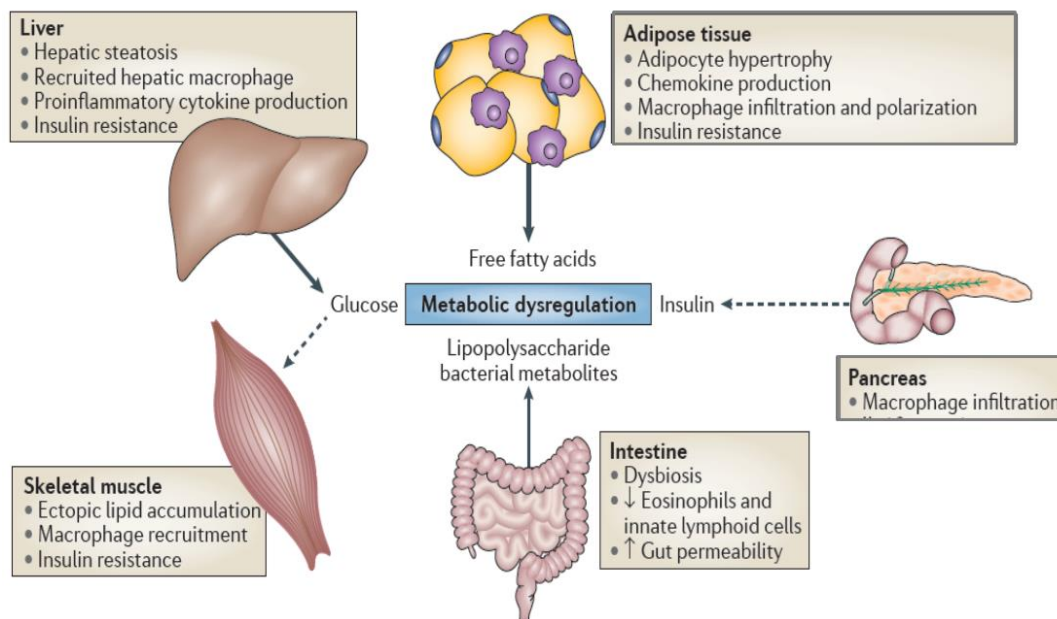


Figure 6: Obesity induces inflammation in adipose tissue, skeletal muscle, liver, pancreas and the intestine. The changes caused by inflammation in each system could eventually lead to metabolic dysregulation. (Adapted from Lackey and Olefsky 2016)

pancreatic islets. Increased pro-inflammatory cytokine secretion found in islet macrophages in obese or T2D states could participate in β -cell dysfunction (29).

The central nervous system, especially hypothalamus, is an important regulator of energy homeostasis in the organism. Studies have shown that obesity-induced inflammation can affect hypothalamus leading to CNS dysfunction and subsequent cognitive decline (34). Hypothalamus senses satiety and nutritional status via median eminence. Median eminence is not protected by blood-brain barrier and this probably increases its vulnerability to circulating FFAs and adipokines found in obese states. Activation of glia soon after high fat diet (HFD) feeding occurs due to recognition of saturated fatty acids (SFAs) by TLR4 expressing microglial cells and results in pro-inflammatory signaling propagation and gliosis. Increased hypothalamic inflammatory signaling leads to leptin-resistance and alters satiety control, leading to decreased inhibition of feeding and weight gain (26).

Crosstalk of adipose tissue inflammation and the gut microbiome

The gut microbiome produces large numbers of metabolites that play a significant role in maintenance of energy homeostasis. Changes in microbial composition and consequently of metabolite expression profile are linked with obesity and can influence host homeostasis and immune system.

In the gut dietary fibers are metabolized by commensal bacteria producing bioactive metabolites, like short-chain fatty acids (SCFAs). SCFAs, including propionate, acetate and butyrate play an important role in modulating adiposity, inflammation and insulin secretion. They also regulate appetite, either directly or through stimulation of enteroendocrine cells and subsequent secretion of gut hormones that act on the CNS via the gut-brain axis (35). Treatment of obese mice or humans with SCFAs or with activators of GPCRs, which are known to become activated by SCFAs, results in improved insulin sensitivity. In addition, microbiome converts primary to secondary and tertiary bile acids, which activate many GPCRs and nuclear hormone receptors, including the bile acid receptor 1 (TGR5) and farnesoid X receptor (FXR), to modulate inflammation and metabolism. Changes in bile acids content is observed in obese mice and could be an additional factor that contributes to disturbance of insulin signaling. Apart from dietary metabolites, microbial endotoxin constitutes an important factor in the impairment of insulin sensitivity. The role of colonic

macrophages is also important, as their infiltration during HFD feeding is linked with increased intestinal inflammation and permeability (36).

In most individuals intestine is colonized by five phyla, Bacteroidetes and Firmicutes being the most abundant, but also by Actinobacteria, Proteobacteria, and Verrucomicrobia. Obesity introduces important changes in the composition of gut microbiome, leading to altered *Firmicutes/Bacteroidetes* ratio and eventually to dysbiosis. Studies employing genetic and diet-induced mouse models of obesity reveal a significant reduction in the amount of *Bacteroidetes* with a proportional increase in *Firmicutes* in obese mice compared to non-obese mice. Clinical studies also confirm this shift towards *Firmicutes* that have increased energy harvest capability, thus promoting more efficient absorption of calories and subsequent weight gain (37).

The presence of bacteria and archaea of the genera *Faecalibacterium*, *Bifidobacterium*, *Lactobacillus*, *Coprococcus*, and *Methanobrevibacter*, which are important producers of SCFAs, is associated with lower tendency to develop metabolic dysregulation and inflammation and consequently T2D and cardiovascular diseases (37, 38). Decline of several key butyrate-producing taxa and consequently reduced potential for butyrate synthesis was associated with many metabolic disorders, including obesity, T2D and cardiometabolic disorders (39). In addition, studies show that *Akkermansia muciniphila* is markedly reduced and inversely associated with obesity, diabetes, cardiometabolic diseases and low grade inflammation (40). In metabolic syndrome, elevated levels of LPS associated with reduction of *Bifidobacteria*, a potential down-regulator of intestinal endotoxin (41).

Absence or elimination of gut microbial content coincides with improved insulin sensitivity and low risk for the development of obesity. Microbiome modulation through dietary administration of probiotics or prebiotics show promising results in animal models. Ingestion of prebiotics inulin or oligofructose utilized mainly by *Roseburia* and *Clostridium* cluster XIVa, show reduced adiposity (42). Arabinoxyylan increases the concentration of specific bacteria, like *Bifidobacterium*, *Roseburia*, and *Bacteroides* display protective effects against high fat diet induced obesity in mice (43, 44). In addition, administration of bacterial-synthesized CLA (conjugated linoleic acid) or CLA-producing bacteria such as *Lactobacillus rhamnosus* markedly reduced

plasma cholesterol, triglycerides and white adipose tissue in animal models (41). Finally, administration of butyrate, a microbiome derived metabolite, shows alleviation of obesity and insulin resistance in mice (45). Accordingly, oral supplementation with butyrate in patients with metabolic syndrome affected trained immunity in peripheral monocytes resulting in reduced metabolic inflammation (46).

Insulin signaling pathway in obesity and macrophage polarization

Insulin is secreted from the pancreatic beta cells in order to regulate glucose homeostasis, fat metabolism and cell growth. Its signaling is mediated through insulin

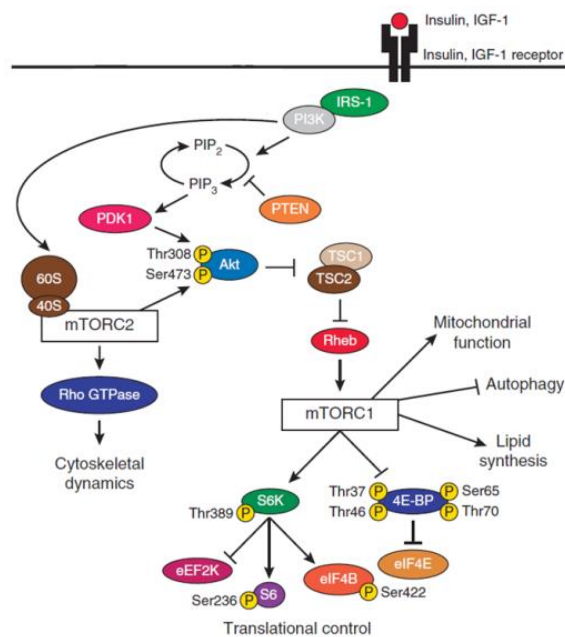


Figure 7: Insulin signaling pathway. Insulin binds to insulin receptor or IGF1 receptor and activates Akt/mTOR pathway.

receptor (IR), which has two isoforms IR α and IR β but also through its homologous insulin-like growth factor 1 receptor (IGF1R) (Figure 7). Engagement of IR or IGF1R results in the phosphorylation of insulin receptor substrate 1/2 (IRS1/2) at its tyrosine residues and in the subsequent activation of two main pathways, the phosphatidylinositol 3-kinase (PI3K) and AKT pathway and the mitogen activated protein kinase (MAPK) pathway (47). Akt is activated mainly by PIP3 that is generated from PI3K class I through conversion of PIP2 at the membrane. Class I PI3K is subdivided into class IA and Class IB. Class IA members PI3K α , PI3K β and PI3K δ have a p110 catalytic subunit and a SH2 containing p85 regulatory subunit. Class IA members are activated by receptor tyrosine kinases, like growth factor

receptors and insulin receptor. PI3K γ a member of class IB becomes activated by G protein-coupled receptors (GPCRs) that recognize cytokines, chemokines and bacterial byproducts. PI3K δ and PI3K γ are the isoforms expressed in hematopoietic lineage (48, 49). The accumulation of PIP3 and PIP2 is also controlled by PI phosphatases, both phosphatase and tensin homolog (PTEN) and SH2 domain-containing inositol-5'-phosphatase 1 (SHIP1), catalyze the conversion of PIP3 to PIP2. PTEN antagonizes the action of PI3K and is a negative regulator of insulin signaling (50).

Akt is a serine/threonine kinase encoded by three highly homologous isoforms (Akt1, Akt2 and Akt3). It is phosphorylated by phosphoinositide-dependent protein kinase-1 (PDK1) and mammalian target of rapamycin complex 2 (mTORC2) to induce many factors, like glucose transporter (Glut), glycogen synthase kinase 3 (GSK3) and forkhead box O1 transcription factor (FoxO1) and mammalian target of rapamycin complex 1 (mTORC1), involved in glucose uptake, glycogen synthesis and protein synthesis (51). Activation of mTORC1 from Akt is mediated indirectly through

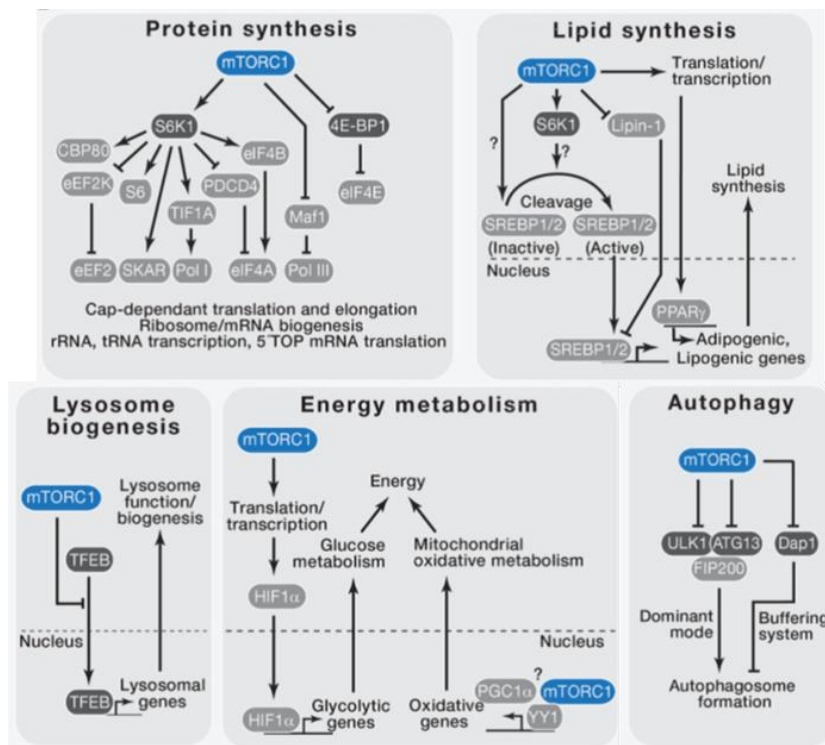


Figure 8: mTORC1 is implicated in lysosome biogenesis, energy metabolism, autophagy and lipid and protein synthesis. (Adapted from Laplante and Sabatini, 2012).

phosphorylation and inactivation of tuberous sclerosis complex 2 (TSC2). TSC2 is a tumor suppressor that forms a complex with TSC1. Inactivation of TSC1-TSC2

complex activates mTORC1, via interaction with active Ras homolog enriched in brain (Rheb). The mTOR complex 1 is involved in multiple cellular functions, via phosphorylation of a variety of downstream targets (Figure 8). Phosphorylation of ribosomal protein S6 kinase (S6K) and 4E-binding protein 1 (4E-BP1) promotes protein synthesis; ULK1 phosphorylation results in suppression of the canonical pathway of autophagy. mTORC1 mediates nuclear association of PPAR- γ coactivator 1a (PGC-1 α) with transcription factor Ying-Yang 1 (YY1) that enhances mitochondrial biogenesis and fatty acid oxidation but also HIF-1 α activation and glycolytic gene expression. It also inactivates transcription factor EB (TFEB) an important regulator of lysosome biogenesis, through phosphorylation and cytosolic localization. It also controls SREBPs transcriptional activity by phosphorylation and inhibition of lipin-1 entry into the nucleus thus inducing lipid synthesis (52).

Obese mice display increased mTORC1 activation in many tissues, likely due to increased levels of circulating insulin, amino acids, and pro-inflammatory cytokines. Prolonged mTORC1 signaling locally in tissues contributes to the development of systemic insulin resistance due to feedback inhibition of PI3K/Akt pathway (Figure 9). S6K suppresses mTOR activation and eventually insulin signaling, through the phosphorylation-dependent degradation of insulin receptor substrate 1 (IRS1), this inhibition is abolished in mice lacking S6K1/2 (53). Hyperinsulinaemia and inflammation induce also other serine kinases, namely JNK and IKK β and lead to phosphorylation and degradation of IRS.

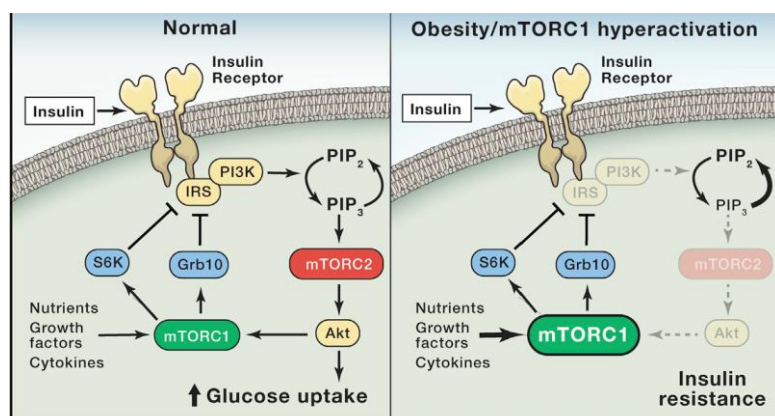


Figure 9: During obesity mTORC1 is hyperactivated and mediates feedback inhibition of insulin signaling pathway via IRS phosphorylation and degradation through S6K. (Adapted from Saxton and Sabatini, 2017).

Macrophages express all components of insulin signaling cascade, indicating a functional insulin signaling but also they can develop insulin resistance in the context of systemic insulin resistance. Insulin signaling through PI3K/Akt pathway has a crucial role in macrophage activation status.

Early studies show that monocytes/macrophages in response to insulin change their antimicrobial capacity through enhancement of phagocytic ability and production of hydrogen peroxide (H₂O₂), but also alter their metabolism towards increased glucose and reduced glutaminase metabolism (54). In addition, insulin and IGF-1 can potentially induce TNF α synthesis in murine and human macrophages (55). In addition, glucose, insulin and palmitate treatment of human monocyte-derived macrophages results in a metabolically activated phenotype (MMe). These macrophages express scavenger receptor CD36, ATP-binding cassette transporter1 (ABCA1) and Perilipin (PLIN) as membrane markers, through PPAR γ activation, but not M1 markers (56).

In animal models, myeloid specific deletion of IR protects mice against HFD-induced obesity and promotes an anti-inflammatory signature of macrophages (57, 58). *LysM^{Cre}Igf1r^{fl/fl}* mice on the other hand show increased adiposity and insulin resistance upon HFD feeding, suggesting an important role for IGF-1R by maintaining an M2 like profile of macrophages during obesity. These animals also show delayed resolution of helminth infection that is in agreement with the upregulation of *Igf1r* observed upon IL-4 treatment (59). Deletion of IGF1R promotes a more inflammatory phenotype in response to pro-inflammatory stimuli, though functionally macrophages display reduced phagocytic capacity (60). Myeloid specific deletion of both receptors IGF1R/IR in mice, protects against skin inflammation and causes attenuation of the pro-inflammatory and an induction of the non-inflammatory macrophage phenotype (61). Loss of IRS2 from myeloid lineage enhances adipose tissue sympathetic nerve function and limits obesity (62). During obesity, hyperinsulinemia promotes downregulation of *Irs2* that causes impairment of IL-4 induced M2a subtype macrophage activation (63). However, there is evidence showing that IRS2 suppresses alternative activation of macrophages (64).

PI3K an upstream regulator of Akt is important for anti-inflammatory polarization of macrophages. Genetic ablation of *Pi3kr1* from macrophages results in increased

expression of TNF α , IL-6 and tissue factor (TF) in response to lipopolysaccharide (65). In addition, the activation of PI3K/Akt pathway in human monocytic cells suppresses the LPS dependent induction of pro-inflammatory factors (66). Alternative activation state of alveolar macrophages is also mediated through activation of PI3K (67). Induction of Arg1 activity and M2 phenotype in SHIP-deficient macrophages depends on PI3K δ activity (48). In the human monocytic cell line THP-1, p110a PI3K was found to regulate phagocytosis, oxidative burst and cytokine production in an isoform specific manner (68). Another study shows that deletion of p85 α regulatory subunit of PI3K results in impaired nitric oxide and IL-12 production upon LPS or IFN- γ stimulation (69). PI3K δ and γ coordinate the effects of C5aR and Fc γ R important mediators of acute inflammation to IgG immune complexes (70). Anti-inflammatory effects of magnesium sulfate are mediated through activation of PI3K β , δ and γ isoforms (71). PI3K δ and γ are also important for naloxone dependent anti-inflammatory action (72).

PTEN is implicated in macrophage polarization by inhibiting a shift towards an anti-inflammatory phenotype. PTEN^{-/-} macrophages become alternatively activated, characterized by increased Arg1 expression mediated by the activation of C/EBP β and STAT3 (73). SHIP is also important in macrophage reprogramming and its deletion results in M2 polarization (74). PIP3 facilitates the recruitment of Akt to the cell membrane, where it gets phosphorylated and activated by PDK-1. PDK-1 deletion in myeloid cells results in enhanced pro-inflammatory response upon TLR4 stimulation and increased susceptibility to septic shock (75). In contrast, evidence suggests that deletion of PDK1 enhances M2 macrophage activation through reduction of aerobic glycolysis and eventually inflammatory responses (76).

Deletion of Akt specific isoforms results in differential polarization status of macrophages. Absence of Akt1 renders macrophages M1 prone and display increased responsiveness to LPS and abolishment of endotoxin tolerance (77). LPS-stimulated Akt1^{-/-} macrophages express high levels of nitric oxide (NO), TNF α and IL-6 (78). This M1 macrophage shift was found to be dependent to miR155 induction and subsequent inhibition of SOCS1 (77). Reduced activity of Akt1 isoform also prevents intracellular growth of various bacteria and enhances the anti-microbial capacity of macrophages (79, 80). Inhibition of Akt1 and subsequent inactivation of mTORC1 results in induction of autophagy and therefore contributes to host immunity against

bacteria (81). Absence of Akt1 is protective in an experimental model of pulmonary fibrosis, through impairment of mitophagy (82). Adiponectin suppresses LPS responses via Akt1 dependent induction of IRAKM (19). In addition, vasoactive intestinal peptide suppresses TLR4 responses via Akt1 (83). Loss of Akt1 in macrophages in mouse models of atherosclerosis showed no effect in the development of atherosclerosis and foam cell formation (84, 85).

Akt2 isoform constitutes the predominant isoform in insulin signaling propagation. Absence of Akt2 from macrophages results in a M2-like polarization phenotype. Macrophages that lack Akt2 show increased expression of M2 polarization markers Arg1, Ym1 and Fizz1 and they also exhibit increased C/EBP β expression (78). In addition, genetic ablation of Akt2 results in upregulation of miR-146 α that suppresses TLR4 signaling pathway via targeting IRF5, TRAF6 and IRAK1 (86). Finally, human macrophages in response to LPS and other pro-inflammatory stimuli induce Akt2 activity and the production of cytokines that typify M1 type polarization (87). Macrophage ablation of Akt2 results in reduced atherosclerosis and foam cell formation in Ldlr^{-/-} mice (85).

Akt promotes indirect activation of mTORC1 that is essential for insulin signaling propagation. *In vivo* and *in vitro* studies also support the importance of mTORC1 in macrophage activation status. Myeloid specific deletion of the mTORC1 specific protein Raptor elevates M2 macrophage population in LysM^{Cre}Raptor^{fl/fl} mice (88). In accordance loss of TSC1 enhances LPS responses and favors M1 polarization phenotype, while it suppresses M2 phenotype activation upon IL-4 stimulation (89, 90). However, there are also studies showing that lack of TSC1 results in both M1 and M2 polarization (91). Furthermore, deletion of Tsc1 in myeloid cells protects mice from high fat diet induced obesity, insulin resistance and adipose tissue inflammation, via mTORC1 dependent M2 macrophage polarization (92). Sustained mTORC1 activation due to the lack of TSC2 in macrophages also enhances the expression of M2 polarization markers (93). Treatment with rapamycin, a suppressor of mTORC1 has been found to promote an M1-like phenotype, both in human and murine macrophages and to block the anti-inflammatory potency of glucocorticoids in myeloid immune cells via increased JNK and NF- κ B activation (94).

The mTORC2 also regulates macrophage activation and deletion of its specific protein Rictor results in increased pro-inflammatory response upon LPS stimulation and higher sensitivity in septic shock (95). In addition, mTORC2 upregulates the M2 surface markers, CD206 and CD163, through Akt1 thus leading to tumor growth and metastasis in mammary tumor models, both in in vitro and in mice (96). Finally selective deletion of Rictor in macrophages prevents M2 differentiation and clearance of a parasitic helminth infection in mice (97). *MRictor*^{-/-} macrophages exhibit reduced survival that leads to reduction of atherosclerosis in *Ldlr* null mice (98).

Macrophages try to adapt to a variety of stimuli found during the development of obesity, acquiring distinct phenotypes that exhibit either pro-inflammatory or anti-inflammatory characteristics or both. Besides the high levels of FFAs, insulin, glucose and bioactive products, oxidative stress is also increased during obesity. Increased levels of reactive oxygen species and nitrogen species result in the oxidation of phospholipids. Oxidized phospholipids (OxPLs) are found on oxidized LDL and on apoptotic cell membranes and are recognized by macrophages promoting either antioxidant or pro-inflammatory phenotype depending on their species. Full length enrichment over truncated species associate with the development of obesity and result in highly activated bioenergetics in ATMs of obese adipose tissue and an M1/M2 hybrid phenotype CD11c⁺CD206⁺, exhibiting both pro- and anti-inflammatory characteristics (99). Atherosclerosis is associated with increased accumulation of oxidized phospholipids that results in the Mox phenotype that is different from both M1 and M2 polarization and is characterized by reduced phagocytic and chemotactic capacity and the expression of Nrf2 target genes involved in the regulation of oxidative status (100). In agreement to this anti-inflammatory phenotype, cholesterol loading to macrophages and foam cell formation results in deactivation of inflammatory responses (101). Transcription analysis of the cells found in atherosclerotic aorta showed that foam cells are less inflammatory compared to their non-foamy counterparts (102).

Metabolic and inflammatory factors that crosstalk with insulin signaling

The inflammatory response triggered by obesity involves a variety of factors that are implicated in the impairment of insulin signaling pathway. As aforementioned, obesity increases the number of circulating free fatty acids due to the excess nutrient

intake. Dietary ω -3 polyunsaturated fatty acids (PUFA), eicosapentaenoic acid (EPA) or docosahexaenoic acid (DHA) exhibit anti-obesity effects, seeing that supplementation of HFD with ω -3 fatty acids results in less weight gain in mice fed supplemented diet compared to HFD fed control mice, especially when they are introduced from the start of the feeding period. However, they also have weight-independent benefits, since they improve insulin sensitivity in mice fed a supplemented diet compared to control HFD, despite weight gain. PUFAs display important anti-inflammatory properties via suppression of NF- κ B and reduction of TNF- α , IL-6 and IL-1 β levels. Omega-3 can bind and activate Free Fatty Acid receptor 4 (FFA4), also known as GPR120 that couples with β -arrestin and the resultant complex can further interact with the transforming growth factor kinase protein (TAK1) and binding protein (TAB-1). This interaction negatively regulates LPS – mediated release of pro-inflammatory cytokines in the macrophage cell line RAW264.7. The GPR120 - β -arrestin complex can also interact and inhibit NLRP3 inflammasome and subsequent pro-inflammatory cytokine release (Figure 10) (103, 104).

Omega-3 metabolites resolvins, protectins and maresins are derived from EPA and DHA and mediate their signaling through GPCRs in order to preserve insulin signaling. Obese mice treated with resolvins acquire improved insulin sensitivity and reduced adipose and hepatic inflammation due to polarization of macrophages

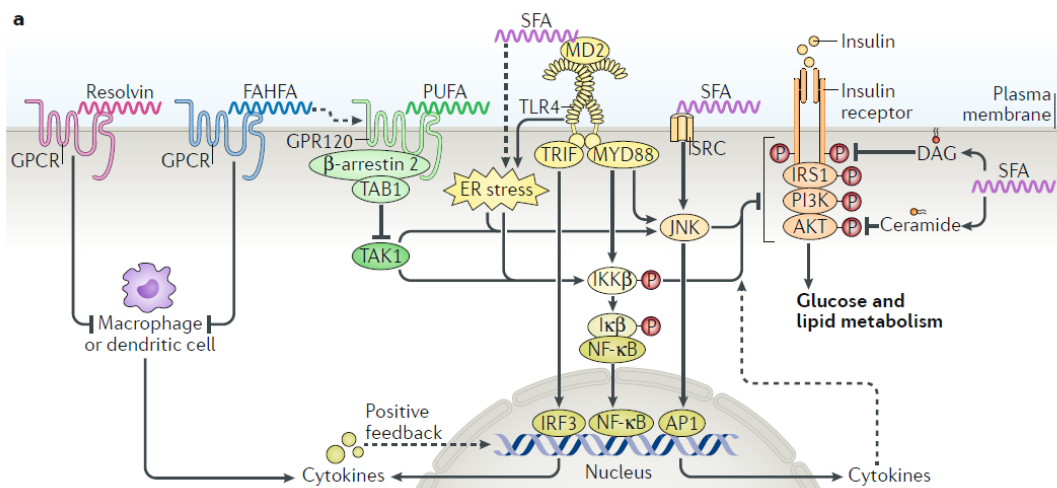


Figure 10: Several signalling lipids, including fatty acids, fatty acid esters of hydroxy fatty acids (FAHFAs), diacylglycerol (DAG) and ceramides, regulate intracellular pathways to influence insulin signaling. SFAs: Saturated fatty acids, PUFA: Polyunsaturated fatty acids, GPCRs: G protein- coupled receptors. (Adapted from Yang, Vijayakumar et al. 2018)

towards an alternatively activated phenotype. Branched fatty acid esters of hydroxy fatty acids (FAHFAs) also mediate their anti-inflammatory actions through GPCRs. Monounsaturated fatty acids (MUFAs), particularly oleic acid is associated with improved glucose homeostasis and inhibition of pro-inflammatory JNK and NF- κ B activation (104).

On the other hand ω -6 PUFA arachidonic acid (ARA) is a precursor of pro-inflammatory mediators including prostaglandins and leukotrienes. ARA has an important contribution to the fatty acid composition of cell membrane phospholipids, modulating raft assembly and promoting pro-inflammatory signals in inflammatory cells, as it was observed in humans fed a western diet (105). Saturated fatty acids are either short-chain containing 4–12 carbon chains, mid-chain containing 13–16 carbon chains and long-chain fatty acids of 17–26 carbon chains. Diets with high composition of SFAs, especially long chain SFAs (lcSFAs), like palmitate associate with obesity-induced inflammation and related disorders.

Apart from dietary intake, the raise in FFAs could also be attributed to the increased release from hypertrophic adipose tissue and reduced clearance. Fatty acids once transported into the cell they can either be re-esterified and stored as triacylglycerol or can be used for β -oxidation to produce energy in the form of ATP. Obese individuals display increased basal lipolysis in response to increased triglyceride depots, thus releasing FFAs and glycerol in the bloodstream. Resistance to antilipolytic effects of insulin and inability of adipocytes to re-esterify and recycle FFAs, further promotes this process.

Hyperlipidemia and increased levels of saturated fatty acids associate with lower insulin sensitivity and inflammation. They enter to the cell, via CD36 and other mediators, and induce production of cytosolic and mitochondrial reactive oxygen species (ROS). Oxidative stress triggers aberrant endoplasmic reticulum (ER) Ca^{2+} release and depletion accompanied by impairment of protein folding machinery leading to accumulation of misfolded proteins and increase in ER ROS production. The unfolded protein response (UPR) signaling results in the activation of IKK β and JNK1 (106, 107). The disruption of Ca^{2+} homeostasis can induce mitochondrial dysfunction leading to apoptosis (108). SFAs also impair insulin signaling through activation of NLRP3 inflammasome pathway and subsequent inactivation of AMPK,

which results in defective autophagy and the generation of mitochondrial ROS (109, 110).

Excess availability of saturated fatty acids in combination with impaired FFAs metabolism results in the accumulation of metabolic intermediates, including DAG and ceramides. Diacylglycerol (DAG), an intermediate of lipolysis and fatty acid esterification which can activate members of the protein kinase C (PKC) family that has an inhibitory effect on insulin signaling pathway via phosphorylation and degradation of insulin receptor substrate (IRS) (111). Ceramide, which is composed of sphingosine and a fatty acid, can interfere with insulin signaling by allosterically activating protein phosphatase 2A (PP2A) and subsequent dephosphorylation of AKT at Thr308 and Ser473 (112), but also through direct activation of PKC, which inhibits AKT membrane recruitment and activation (113). In macrophages ceramides activate NLRP3 inflammasome and the production of pro-inflammatory cytokines.

In addition, SFAs enhance the production of pro-inflammatory cytokines via direct binding to TLR4 and TLR2 receptors (114). Recent evidence suggests that SFAs are not TLR4 agonists, though TLR4 regulates lcsFAs-induced inflammation via priming and metabolic reprogramming of macrophages (115) (Figure 11).

The integrity of epithelial barrier in the intestine is important for preserving a symbiotic relationship with commensal bacteria. In obesity, increased intestinal permeability is associated with impairment of tight junctions between epithelial cells, reduced thickness of the mucosal layer, increased epithelial cell nutrient absorption and translocation of bacterial derived LPS and other byproducts. Macrophages can be stimulated upon TLR4 engagement with circulating LPS derived from altered gut microbiome. TLR ligands can induce serine protein kinases IKK β and JNK1 that phosphorylate IRS1 on Ser307 residue, promoting its proteasomal degradation and thus interfering with insulin signaling in macrophages (47, 116).

Elevated circulating levels of glucose induce *de novo* synthesis of DAG, which as aforementioned is PKC activator. Apart from phosphorylation of IRS and direct implication with insulin signaling, DAG can also interfere indirectly via NADPH oxidase activation and ROS production. Increased levels of ROS induce NF- κ B activation pathway and production of pro-inflammatory cytokines (117). Increased glucose concentration results in advanced glycation end products (AGEs), which are

non-enzymatically formed glycated proteins or lipids that are recognized by receptor of AGEs (RAGE). AGE-RAGE interaction leads to activation of IKK and NF- κ B translocation into the nucleus for the expression of pro-inflammatory genes (118). Increased glucose levels can also be funneled through the hexosamine pathway and cause an increase flux and synthesis of UDP-GlcNAc (119). As a response to prolonged insulin signaling during obesity, OGT (O-GlcNAc transferase) can O-GlcNAcylate and modify post-transcriptionally Ser/Thr residues of key molecules of insulin signaling pathway, namely AKT, PDK1 and FOXO and therefore dampen insulin sensitivity (120). O-GlcNAcylation can also increase IKK complex kinase activity and consequently promotes NF- κ B activity. However, studies show that O-GlcNAcylation may have negative regulation on NF- κ B, reducing pro-inflammatory activity (121).

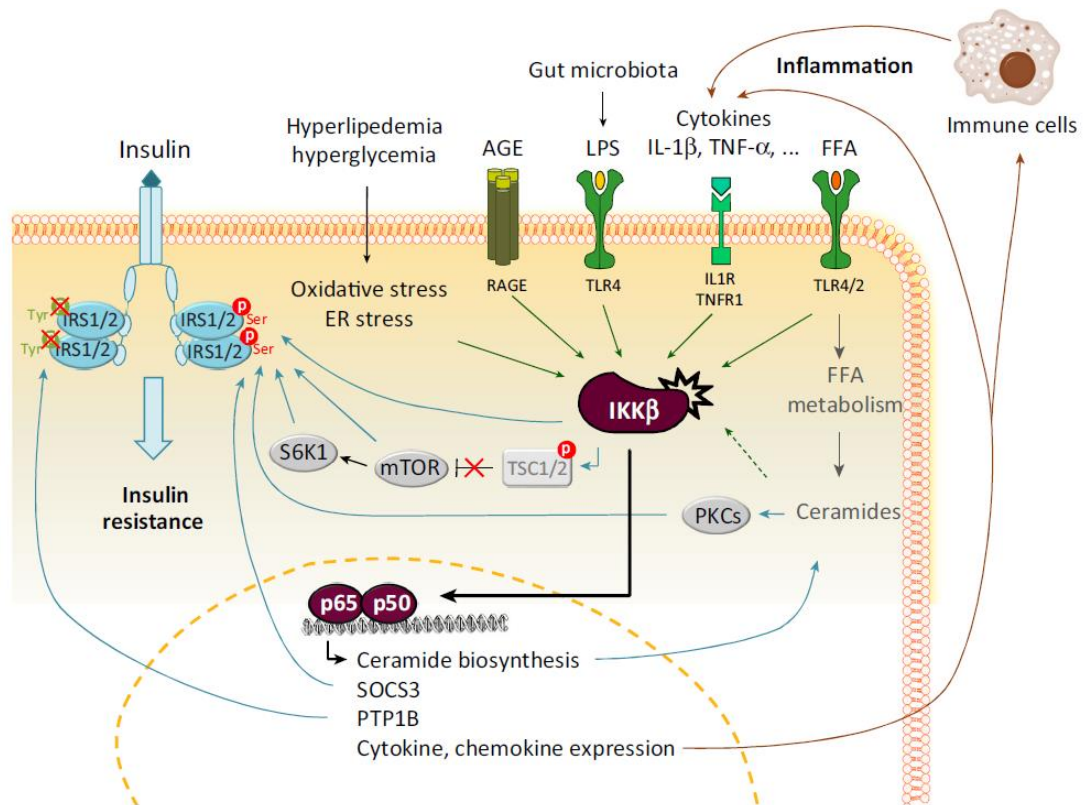


Figure 11: In obesity microbiota-derived LPS, free fatty acids (FFAs), advanced glycation end products (AGEs), inflammatory cytokines, oxidative stress, and endoplasmic reticulum (ER) stress all activate inflammatory signaling pathways that interfere with insulin signaling mostly through serine phosphorylation of IRS and subsequent degradation. (Adapted from Catrysse and van Loo 2017).

Dyslipidemia related to obesity is characterized by increased levels of LDL and triglycerides and low levels of HDL. The excess in circulating FFAs results in increased triglyceride and very low density lipoprotein VLDL formation in the liver.

Triglyceride clearance is further impaired due to reduced expression and function of lipoprotein lipase in adipose tissue and skeletal muscle. Cholesteryl ester transport protein then, facilitates exchanges of triglycerides and cholesteryl esters between VLDL and LDL or HDL. Subsequently, hepatic lipase removes triglycerides and phospholipids from LDL resulting in small dense LDL (122, 123). In macrophages VLDL-VLDLR axis has an important role in insulin sensitivity. VLDL treatment of macrophages increases the intracellular levels of ceramides in a VLDLR-dependent manner and stimulates the MAPK and NF- κ B pathways to exert pro-inflammatory responses (124).

Oxidative stress promotes mild or extensive oxidation of LDL and increased glucose levels can induce glycation-linked oxidative modification of lipoproteins. Macrophages recognize and uptake modified LDL via scavenger receptors, including CD36, SR-AI and lectin-like oxidized LDL receptor-1 (LOX-1), responsible for foam cell formation. Binding of oxLDL on scavenger receptor can activate toll-like receptor cooperative signaling, leading to the induction of pro-inflammatory pathways, NLRP3 activation and ER stress (125). Minimally modified LDL can be recognized by LDL receptor but also from TLR4/CD14 and induces activation of PKC via Syk phosphorylation (126). However, some studies suggest that cholesterol load in macrophages correlates with the acquisition of anti-inflammatory properties (127).

Chronic overnutrition results in elevated circulating levels of amino acids and particularly the Branched-chain amino acids (BCAAs) leucine, isoleucine and valine have been associated with obesity and insulin resistance. Amino acids are potential inducers of mTORC1 that mediates feedback inhibition to the PI3K/Akt pathway (104). Finally, cytokines released by activated immune cells interact with their receptors and trigger pro-inflammatory pathways, further contributing to inflammation and impairment of insulin signaling (128).

Activation of pro-inflammatory pathways besides interfering at the signal transduction level of insulin, they also affect the expression of various genes implicated in maintaining insulin sensitivity. NF- κ B and AP-1 can induce the expression of suppressor of cytokine signaling (SOCS) proteins that antagonize IRS binding to the receptor and insulin signal propagation, as well as protein tyrosine phosphatase 1B (PTP1B) that dephosphorylates tyrosine residues in IR and possibly IRS

proteins. In addition, NF- κ B is able to downregulate the expression of molecules that participate in insulin signaling pathway, including GLUT4, AKT and IRS or other genes implicated in fatty acid metabolism and inflammatory responses (111).

Genetic manipulations that disable pro-inflammatory pathway activation specifically in macrophage protect against obesity-induced insulin resistance. Loss of JNK from macrophages results in improved insulin resistance irrespectively of adiposity (129). In addition, myeloid specific deletion of IKK β protects against diet induced insulin resistance (130). Furthermore, deletion of NADPH oxidase 2, which plays an important role in the inflammatory cytokine expression and lysosomal exocytosis in MMe macrophages, shows both improvement and worsening of insulin resistance depending on the duration of high fat feeding. After 8 weeks of high-fat feeding ablation of Nox2 attenuates inflammation and improves glucose tolerance. However 16 weeks after high fat feeding Nox2 deficiency resulted in exacerbation of obesity, a worsening that is due to impaired dead adipocyte clearance through ATM lysosomal exocytosis (131).

The role of metabolism on macrophage activation and the effect of obesity

The metabolic status of macrophages is important for the regulation of their activation and plasticity. Adaptation to the microenviromental signals implies the induction of different metabolic pathways and thus results in metabolic reprogramming. Classical activation of macrophages is associated with increased glycolytic metabolism that produces ATP as energy fuel for their antibacterial functions (Figure 12) (132). Deletion of glucose transporter 1 (Glut1), essential for glucose uptake in macrophages, results in reduced LPS responses and production of pro-inflammatory cytokines (133), in accordance with its overexpression that results in enhanced LPS responses and ROS production (134). In addition, lack of (fatty acid transporter 1) FATP1 results in M1 activation of macrophages, via induction of glycolysis. In mouse models, deletion of FATP1 from macrophages leads to increased susceptibility to diet-induced insulin resistance and adipose tissue inflammation (135). Glycolysis is also important in trained immunity of macrophages and monocytes. Training with β -glucan increased glucose consumption, lactate production and high ratio of nicotinamide adenine dinucleotide (NAD⁺) to its reduced form (NADH) in a mTOR-dependent way (136).

The levels of pentose phosphate pathway (PPP) are also increased in M1 macrophages. PPP is a glucose-consuming route that branches off from glycolysis at glucose 6-phosphate and produces amino acids for protein synthesis, ribose for

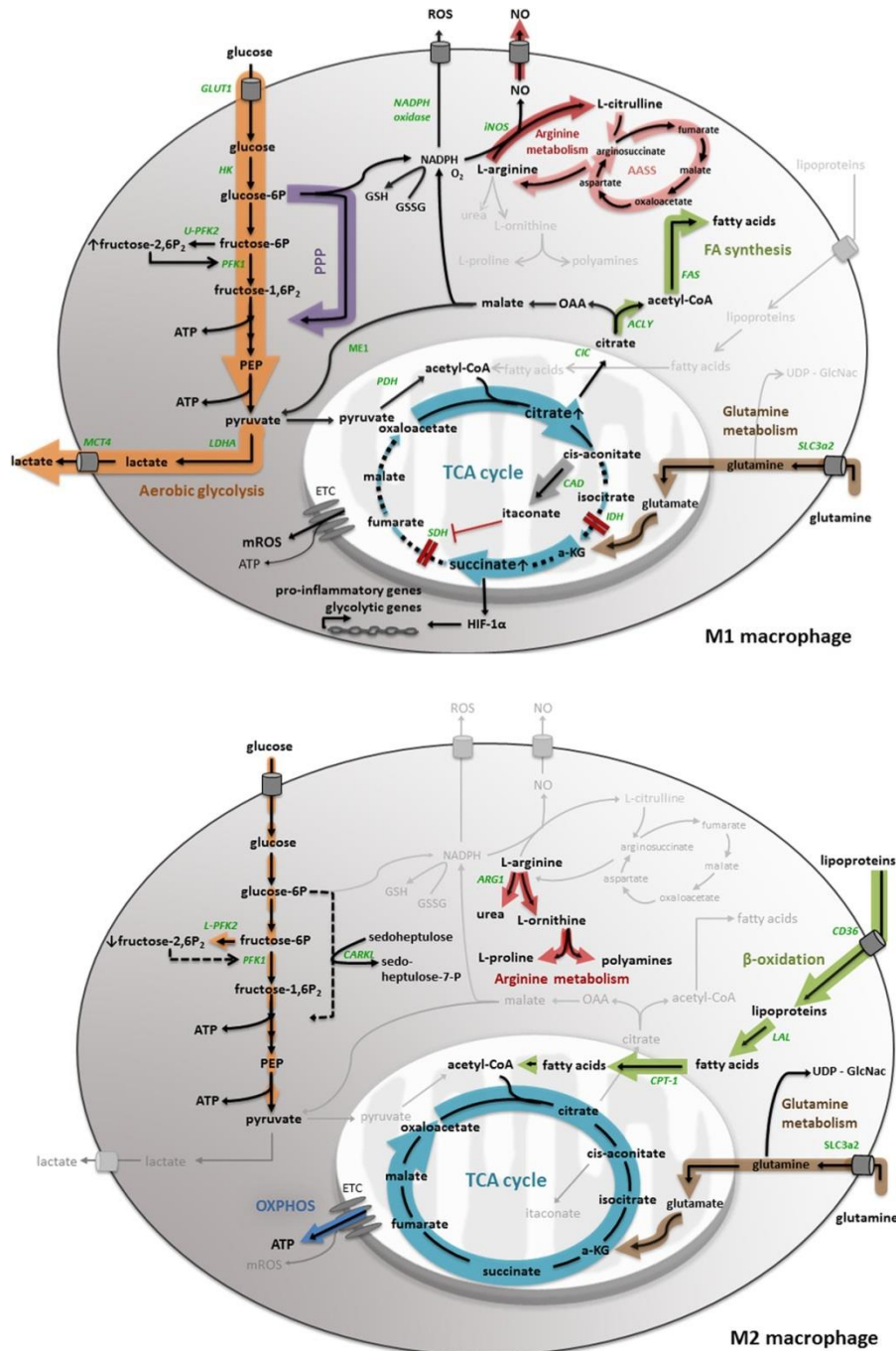


Figure 12: Main metabolic pathways activated in M1 and M2 macrophage polarization. (Adapted from Geeraerts, Bolli et al. 2017).

nucleotides, and NADPH for the production of ROS by NADPH oxidase. Blockage of PPP pathway results in attenuated LPS-induced inflammatory responses, accordingly in M2 type activation of macrophages PPP is suppressed via the sedoheptulose kinase

CARKL (137). During hypercholesterolemia, foam cells suppress PPP resulting in impaired inflammatory responses (101).

Tricarboxylic acid cycle is also fueled by glycolysis, via generation of pyruvate but also as recently found by lactate (138). Accumulation of citrate and subsequent synthesis of acetyl-CoA by ACLY (ATP-Citrate lyase) leads to the formation of fatty acids, lipids and prostaglandins. Acetyl-CoA is converted into malonyl-CoA that is further polymerized by fatty acid synthase to produce fatty acids, like palmitic acid. In addition, three molecules of acetyl-CoA are used to form 3-hydroxy-3-methylglutaryl-coenzyme A (HMG-CoA) that is converted into mevalonate and subsequently leads to cholesterol formation (139). Inhibition of cholesterol synthesis by atorvastatin indicated the important role this pathway in increased cytokine production and epigenetic changes observed in β -glucan induced training of immune cells (140). Citrate is required for fatty acid synthesis pathway that is essential for pro-inflammatory status of macrophages (141). Deletion of fatty acid synthase in macrophages prevents diet-induced insulin resistance and inflammation in mice by changing membrane composition, impairing cholesterol retention and disrupting Rho-GTPase trafficking (137). Upon pro-inflammatory activation of macrophages, glycolysis is induced resulting in production of itaconate via an anaplerotic TCA cycle. Accumulation of citrate leads to the formation of itaconate by IRG1. Itaconate is an anti-inflammatory metabolite and can inhibit succinate dehydrogenase (SDH), thus inhibiting succinate-mediated inflammatory processes in activated macrophages (142). Lack of IRG1 and itaconate results in retained SDH activity and oxidation of succinate, in activated macrophages (143). In addition, the decrease in mitochondrial respiration upon LPS treatment was reversed in the absence of itaconate and its suppressing effect on SDH (or mitochondrial complex II). Finally the production of pro-inflammatory cytokines was increased in macrophages deficient in IRG1. In a model of LPS-induced immune paralysis that mimics the immunosuppression found in sepsis, itaconate-mediated SDH suppression can be relieved by β -glucan training through downregulation of IRG1 expression (144).

Activation of macrophages by LPS leads to increased production of the TCA cycle intermediate succinate. Succinate is essential for the stabilization of hypoxia-inducible factor 1 α (HIF-1 α), a transcription factor responsible for the production of IL-1 β (145). In addition, dimethylallylglycine (DMOG) that is a HIF-1 α activator

mimicked the effect of succinate on IL-1 β . LPS induces both mitochondrial oxidation of succinate via succinate dehydrogenase (SDH) and mitochondrial membrane hyperpolarization that together lead to mitochondrial ROS production (146).

In contrast, IL-4 induced M2 phenotype employs oxidative phosphorylation (OXPHOS) over glycolysis as main ATP source. Treatment of macrophages with compounds that inhibit OXPHOS, like oligomycin and FCCP results in reduced expression of M2 polarization markers. Alternatively activated macrophages also show increased fatty acid oxidation (FAO). During beta-oxidation, carnitine palmitoyltransferase 1 (CPT1) facilitates transmembrane transport of acyl-CoA converted free cytosolic fatty acids. Acyl-CoA is then oxidized producing NADH, one FADH₂ and one molecule of acetyl-CoA per reaction. Malonyl-CoA can regulate FAO through direct inhibition of CPT-1. Fatty acids that fuel FAO derive from lysosomal lipolysis and treatment of macrophages with an inhibitor of lipolysis (orlistat) reduces expression of M2 markers CD206, CD301, PD-L2 and RELM α (147). In accordance, CPT1 overexpressing macrophages treated with palmitate show reduced triglyceride formation, inflammation, ER stress and ROS production (148). However, CPT2 deficient macrophages still have the ability to express M2 markers despite the defective FAO (139). Recent evidence indicates that FAO is important in the activation of NLRP3 inflammasome. Palmitate oxidation via CPT1A and mitochondrial ROS production mediate NLRP3 inflammasome activation, as it is observed after pharmacological inhibition of CPT1A or its activity regulator NOX4. Glycolysis is also induced in alternatively activated macrophages. The Akt/mTORC1 pathway activation upon IL-4 treatment induces glucose metabolism and inhibition of glycolysis with 2-deoxy-D-glucose suppresses the expression of M2 markers, including *Arg1*, *Retnla* and *Mgl2*.

Amino acid metabolism is also important in macrophage activation and function. The amino acid arginine is converted into nitric oxide (NO) by inducible NO synthase (iNOS) in classically activated macrophages, whereas in alternatively activated macrophages it produces urea and ornithine through Arginase 1. Glutamine metabolism promotes M2 polarization of macrophages. Macrophage inhibition of glutamine synthetase the glutamine-synthesizing enzyme from glutamate, results in M2 polarization skewing towards M1-like phenotype (149). Glutamine generates α -ketoglutarate through glutaminolysis and induces FAO and OXPHOS as well as the

expression of M2 markers through Jmjd3 (Jumonji domain-containing 3)-dependent demethylation of H3K27 found in the promoter of these genes (150). Glutamine contributes to UDP-GlcNAc (UDP-N-acetylglucosamine) synthesis via the hexosamine pathway and promotes M2 macrophage polarization through N-glycosylation and thus proper folding and trafficking of important M2 surface markers, namely Relm α , CD206, and CD301. Inhibition of glutamine-UDP-GlcNAc pathway using tunicamycin or glutamine deprivation, results in reduced the expression of these M2 markers (151). UDP-GlcNAc also serves as donor for O-GlcNAcylation that interferes with important signal transduction pathways, like PI3K/Akt and NF- κ B pathways as aforementioned. Glutamine conversion into glutamate fuels TCA cycle and results in the production in fumarate, which is responsible for the enrichment in H3K4me3 that is essential for trained immunity by β -glucan. Fumarate also regulates HIF-1 α degradation (152).

During obesity, ATMs acquire a unique metabolic profile not characteristic for M1-type or M2-type activation displaying increased glycolysis and oxidative phosphorylation. Both extracellular acidification and oxygen consumption were increased in ATMs derived from obese adipose tissue on the contrary to those derived from lean adipose tissue characterized by low bioenergetics. These findings are not in agreement with the switch from M2 towards M1 phenotype that happens during the development of obesity. Antioxidant Mox macrophages are the predominant phenotype found in lean adipose tissue, while during obesity ATMs exhibit characteristics of both M1 and M2 activation and highly activated bioenergetics (99). ATMs in obesity activate a developmental program characterized by increased lysosomal-dependent lipid catabolism, that it is not associated with M1-type activation (153). In metabolically activated adipose tissue macrophages the expression of proteins involved in lipid metabolism like CD36, ABCA1 and PLIN is increased and is probably dependent to the microenvironmental stimuli (131).

The concept of trained immunity as a mechanism of changes in innate immune responses

Trained immunity is a kind of innate immune memory that is developed in response to various environmental stimuli. Adaptive immune cells own a wide variety of antigen specific receptors formed through somatic rearrangement. Upon pathogen invasion

and recognition by a specific receptor, the clone carrying this receptor expands trying to eliminate the infection, but also it forms memory cells that are able to respond immediately after reinfection with the same pathogen.

The innate immune system was thought to respond immediately and with no specificity upon infection. The existence of different pattern recognition receptors (PRRs) that can recognize pathogen-associated molecular patterns (PAMPs) or damage-associated molecular patterns (DAMPs) confers some kind of specificity in these cells. Innate immune cells can also acquire immune memory and induce protection against certain stimuli, through epigenetic modifications and gene expression reprogramming (154).

Immune response to invading pathogen leads to epigenetic modifications and transcriptional and functional reprogramming of the cells. Histone marks are not completely lost after pathogen clearance and this new epigenetic profile results in enhanced responses upon re-stimulation.

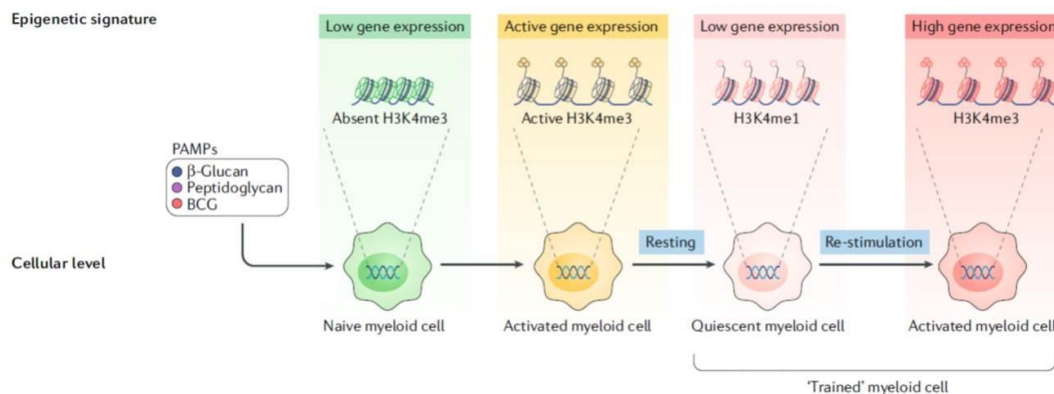


Figure 13: Trained immunity is regulated by epigenetic rewiring of innate immune cells. Bacille Calmette–Guérin (BCG)-induced and β-glucan-induced training are associated with the histone mark H3K4 trimethylation (H3K4me3). Naive cells (green) display a mild response to an insult, however ‘trained’ cells (red) exhibit a strong response to the same stimulus. (Adapted from Mulder, Ochando et al. 2019).

Immune memory induced by LPS treatment is associated with specific chromatin modifications that lead to suppression of genes responsible for inflammatory responses and activation of anti-inflammatory genes, promoting tolerance. In contrast, priming macrophages with bacillus Calmette-Guérin (BCG) or with the *Candida albicans* cell-wall component β-glucan, results in different gene expression and epigenetic marks that lead to increased, instead of suppressed inflammatory responses upon reinfection. Whether trained immunity or tolerance is stimulus-dependent or

dose-dependent is not clear since priming macrophages with low dose LPS can lead to enhanced inflammatory responses during a second infection and in line pre-treatment of monocytes with high dose β -glucan results in suppressed pro-inflammatory cytokine production (Figure 14) (155).

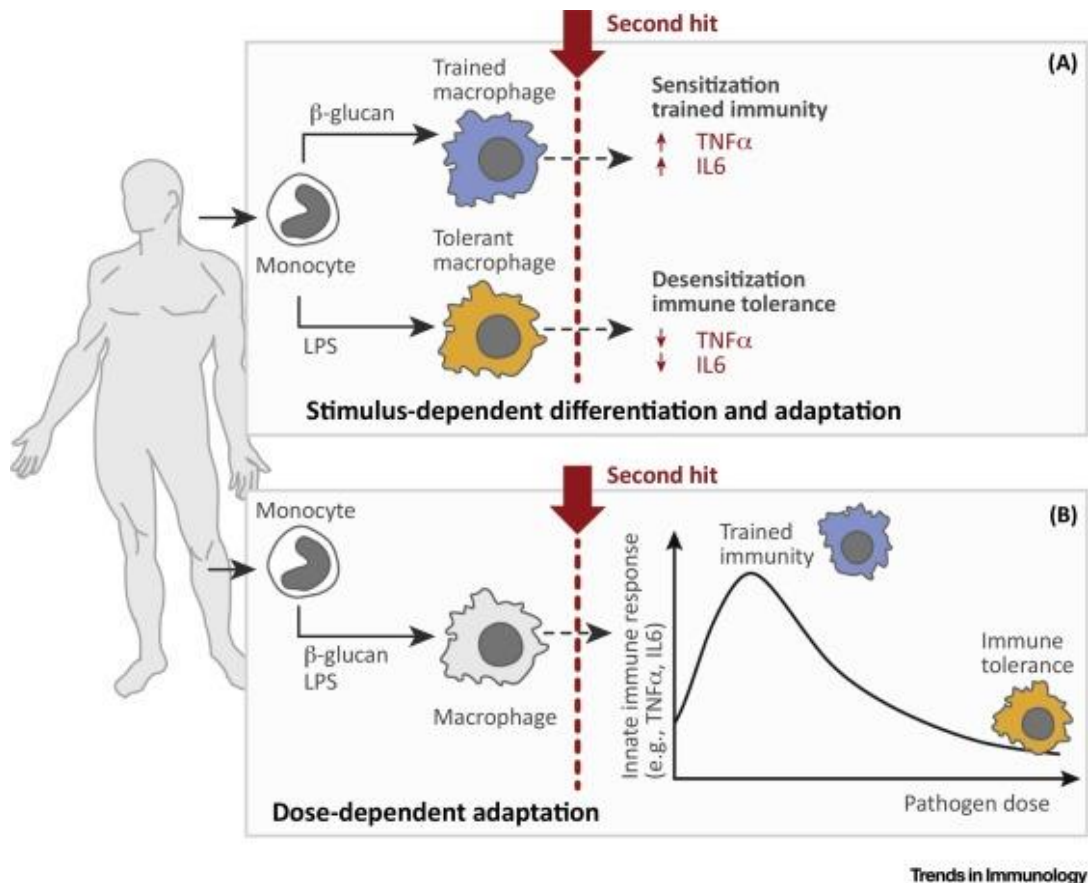


Figure 14: The nature of the pathogen is important for the induction of training or tolerance of macrophages (A). The dose of the pathogen is also important with low doses promoting training and high doses tolerance (B). (Adapted from Bauer, Weis et al. 2018).

As part of the fungal wall, β -glucans are recognized by C-type lectin receptor, Dectin-1 and promotes the activation of Akt/mTOR/HIF-1 α pathway and metabolic shift from OXPHOS towards glycolysis that is important for the formation epigenetic marks, namely H3K4 methylation and H3K27 acetylation (136). Both glycolysis and oxygen consumption are increased in BCG induced training, via Akt/mTOR activation. Inhibition of glycolysis and glutamine metabolism results in changes of histone marks (H3K4me3 and H3K9me3) on the promoters of $\text{TNF}\alpha$ and IL-6 that return to the baseline status (156). The peptidoglycan constituent common in all bacteria is muramyl dipeptide (MDP). BCG and MDP promote training through

activation of the cytoplasmic receptor nucleotide oligomerization domain 2 (NOD2) and induction of epigenetic changes, such as H3K4 that enhances the expression of pro-inflammatory factors (157).

Several metabolites derived from glycolysis and TCA cycle are known co-factors of histone modifying enzymes. The TCA intermediate α -ketoglutarate is an important co-factor of the JmjC and JmjD histone lysine demethylases. It promotes anti-inflammatory phenotype of macrophages and epigenetic modifications in M2 related genes through JmjD3 H3K27 demethylase activity (150).

Increased acetylation of pro-inflammatory genes during training is dependent to histone acetyl transferases that require acetyl-CoA, another intermediate of the TCA cycle can derive from both glycolysis and glytaminolysis. Acetyl-CoA promotes glycolysis through histone acetylation of glycolytic genes, like hexokinase 2, phosphofructokinase and lactate dehydrogenase. Fumarate is derived from glutamine and it mediates training via inhibition of KDM5 histone demethylases, both expression and function and subsequent increase in histone methylation marks on the promoters of genes encoding pro-inflammatory cytokines (152). Melavonate, a metabolite of cholesterol synthesis pathway, can induce training of macrophages through activation of IGF1R and mTOR and subsequent histone modifications, like changes in H3K27ac in inflammatory gene enhancers (158).

Western diet feeding in *Ldlr*^{-/-} mice that are inefficient in cholesterol processing, can induce long-lasting transcriptional and epigenetic modifications in myeloid progenitors along with increased systemic inflammation (159). Training can be triggered by oxidized LDL that is associated with WD and can bind to scavenger receptors like CD36 to enter into the cell. Upon internalization it is released into the cytoplasm where it can form cholesterol crystals, which in turn activate NLRP3 inflammasome (159). Oxidized LDL can induce histone modifications followed by increased pro-inflammatory cytokine production and foam cell formation, via an mTOR dependent pathway (160).

High glucose levels found in obesity and diabetes can induce “hyperglycemic memory”. Hyperglycemia promotes persistent histone marks, like increased H3K4 and reduced H3K9 methylation that result in sustained NF κ B gene activity (161). It is also known that under diabetic conditions, high glucose and AGEs can induce

chromatin remodeling in monocytes. Monocytes from T1D patients show increased acetylation of H3K9 on the promoter of pro-inflammatory TNF α and COX-2 genes (162). Genome wide analysis of histone post-translational modifications in monocytes

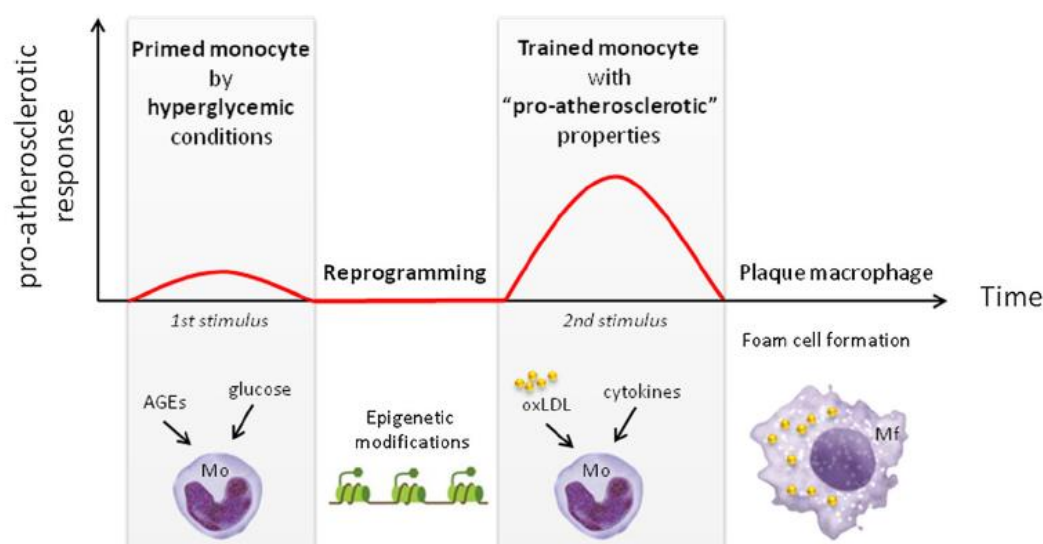


Figure 15: Initial stimulation of monocytes by hyperglycemic conditions (i.e., glucose or AGEs) induces epigenetic reprogramming of monocytes. This trained monocyte exhibit increased response to a second stimulus (e.g., oxLDL or cytokines), a pro-atherosclerotic response associated with increased cytokine secretion and foam cell formation. AGE: advanced glycation end products, Mf: macrophage, Mo: monocytes, oxLDL: oxidized LDL. (Adapted from van Diepen, Thiem et al. 2016).

of untreated versus T1D patients (DCCT/EDIC trial) also revealed H3K9 acetylation as an important epigenetic mark found on the promoter of genes related to inflammatory pathways (163). Hyperglycemia potentially can induce epigenetic changes and training of macrophages that contributes to the development of an activated pro-atherosclerotic phenotype characterized by increased pro-inflammatory response and foam cell formation in response to a second stimulus, like oxLDL and cytokines (Figure 15) (164).

Training and tolerance programs evolved to lead to adaptive states that confer protection to the host in case of infection, since they can modulate inflammatory response in a magnitude that will not damage the tissue or in case of mucosal colonization they will provide tolerance. They can also help for innate immune system maturation and non-specific protection by vaccines. However, they can also result in maladaptive states like post sepsis immune paralysis or hyperinflammation (165). Molecules that inhibit signaling and metabolic pathways that regulate innate immune training could be potentially new drugs to be used in certain inflammatory diseases

with excessive inflammation. For example, metformin or rapamycin that block mTOR, butyrate can act on the inflammasome and suppress inflammation. The butyrate was found to induce an anti-microbial training of macrophages, via mTOR inhibition.

The effect of obesity on sepsis

In 2016, the Third International Consensus taskforce recommended that sepsis be defined as life-threatening organ dysfunction due to a dysregulated host response to infection (166). Sepsis is the primary cause of death from infection, especially if not recognized and treated promptly. The clinical findings of sepsis exhibit great diversity, depending on the site of infection, the kind of the invading organism, the pattern of acute organ injury, the time interval before initiation of treatment and also the host characteristics concerning age, comorbidities, genetics, and immune system. The most common clinical manifestations include fever or hypothermia, tachycardia, tachypnea, hypotension, infection and signs of organ dysfunction(167). The Sequential Organ Failure Assessment (SOFA) Score predicts ICU mortality based on lab results and clinical data as demonstrated in the Table 2. A SOFA score ≥ 2 reflects an overall mortality risk of approximately 10% in a general hospital population with suspected infection (166).

| System | Score | | | | |
|--|---------------------|-------------------|---|---|--|
| | 0 | 1 | 2 | 3 | 4 |
| Respiration | | | | | |
| PaO ₂ /FIO ₂ , mm Hg (kPa) | ≥ 400 (53.3) | <400 (53.3) | <300 (40) | <200 (26.7) with respiratory support | <100 (13.3) with respiratory support |
| Coagulation | | | | | |
| Platelets, $\times 10^3/\mu\text{L}$ | ≥ 150 | <150 | <100 | <50 | <20 |
| Liver | | | | | |
| Bilirubin, mg/dL ($\mu\text{mol/L}$) | <1.2 (20) | 1.2-1.9 (20-32) | 2.0-5.9 (33-101) | 6.0-11.9 (102-204) | >12.0 (204) |
| Cardiovascular | | | | | |
| | MAP ≥ 70 mm Hg | MAP <70 mm Hg | Dopamine <5 or dobutamine (any dose) ^b | Dopamine 5.1-15 or epinephrine ≤ 0.1 or norepinephrine ≤ 0.1 ^b | Dopamine >15 or epinephrine >0.1 or norepinephrine >0.1 ^b |
| Central nervous system | | | | | |
| Glasgow Coma Scale score ^c | 15 | 13-14 | 10-12 | 6-9 | <6 |
| Renal | | | | | |
| Creatinine, mg/dL ($\mu\text{mol/L}$) | <1.2 (110) | 1.2-1.9 (110-170) | 2.0-3.4 (171-299) | 3.5-4.9 (300-440) | >5.0 (440) |
| Urine output, mL/d | | | | <500 | <200 |

Abbreviations: FIO₂, fraction of inspired oxygen; MAP, mean arterial pressure; PaO₂, partial pressure of oxygen.

^a Adapted from Vincent et al.²⁷

^b Catecholamine doses are given as $\mu\text{g/kg/min}$ for at least 1 hour.

^c Glasgow Coma Scale scores range from 3-15; higher score indicates better neurological function.

Table 2: Sequential (Sepsis-Related) Organ Failure Assessment Score

Quick SOFA criteria are used for early recognition of sepsis outside the Internal Care Unit (ICU) and those include a respiratory rate ≥ 22 per minute, altered mentation and systolic blood pressure lower than 100mmHg. If two of these criteria are met organ dysfunction should be suspected, and the classic SOFA score should be determined by ICU specialists (166).

Upon local invasion of a pathogen the innate immune system is activated. Monocytes, tissue resident macrophages, other myeloid cells recognize the pathogen by PRRs and release pro-inflammatory mediators and tissue factor. Increased secretion of inflammatory factors, facilitate the recruitment of other inflammatory cells to the site of infection for elimination of the pathogen. Local vasodilation also occurs due to local imbalance between vasodilators (NO) and vasoconstrictors (168).

Endothelial cells are activated and express adhesion molecules (selectins, ICAM-1/VCAM-1, integrins) that facilitate activated immune cells to adhere and transmigrate across the endothelium to reach the site of infection. During sepsis, the epithelium acquires increased permeability, resulting in increased circulation of inflammatory factors and edema. Coagulation is also activated and slows blood flow to further facilitate the accumulation of immune cells at the site of infection (168).

During sepsis, the local response becomes systemic resulting in diffuse endothelial disruption, vasodilation, vascular permeability and microvascular thrombosis that result eventually in end-organ dysfunction due to hypoperfusion.

Sepsis activates both pro- and anti-inflammatory responses shortly after infection occurs (Figure 16). However, at the initiation of sepsis there is a predominance of hyper-inflammation, the magnitude of which depends on various factors as aforementioned, concerning both the host and the invading microorganism. Usually, the hyper-inflammatory state is followed by hypo-inflammatory state and eventually the patient could recover. An inflammatory response of excessive magnitude due to high virulent microorganism for example, is characterized by robust levels of cytokines, sometimes resulting in a cytokine storm that could lead to organ damage and early death of the septic patient. If the initial hyper-inflammatory state is of low magnitude or even absent, in elderly with various comorbidities, the hypo-inflammatory response that follows can be prolonged and either result to death or recovery. Hypo-inflammation is essential for restoring homeostasis, but if it stays

prolonged or intensive may lead to immunosuppression in the late phase of sepsis. During immunosuppressive state patients may acquire secondary infections that could result to death if not treated properly (169). Though the response seems to be far more complex than this biphasic model with a mix pro- , anti- inflammatory initial responses that lead to immune reprogramming and result in pro- , anti- inflammatory and primed responses (170).

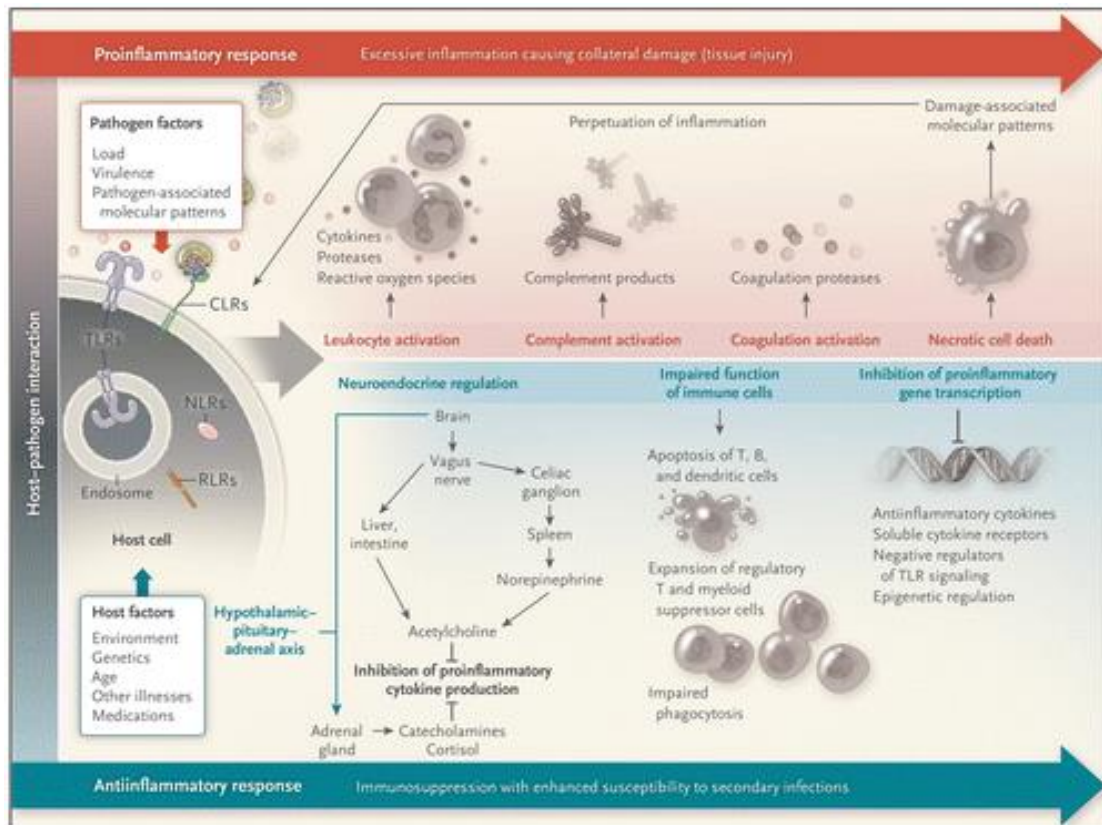


Figure 16: The host responds to sepsis through induction of both proinflammatory and anti-inflammatory immunosuppressive responses. The direction, extent, and duration of these responses are determined by a variety of factors concerning the host (e.g., genetic characteristics, age, coexisting illnesses, and medications) but also the pathogen (e.g., microbial load and virulence).

In the older definition of sepsis, systemic inflammatory response syndrome (SIRS) was used to describe the complex pathophysiologic response to an insult such as infection, trauma, burns, pancreatitis, or a variety of other injuries. SIRS criteria involved 4 clinical manifestations, including temperature, heart rate, respiratory rate, and white blood cell count that once altered they induce inflammatory response. Although the predominance of SIRS criteria versus qSOFA in the predictive validity of mortality needs further investigation, SOFA scoring for in-hospital mortality was superior to that of the SIRS criteria (171).

One of the first organs affected by sepsis is the lung. Alveolar macrophages are antigen-presenting cells found in the pulmonary alveolus in the lung tissue and have an important role in maintaining tissue homeostasis. They are essential for steady state clearance of daily cellular debris but also stand as the guardian of the alveolar–blood interface, serving as the front line of cellular defense against respiratory pathogens. Alveolar macrophages have an important role in the development and progression of acute lung injury.

Acute respiratory distress syndrome (ARDS) is the clinical manifestation of a lung infection (direct lung injury) or an infection of extrapulmonary origin, like an intra-abdominal infection (indirect lung injury). Host immune system is activated against the invading microorganism and results in recruitment of neutrophils and macrophages, release of cytokines and other factors that damage the alveolar-capillary barrier. Loss of integrity of this barrier leads to influx of pulmonary edema fluid and lung injury. Radiographical findings are bilateral infiltrates, patchy or asymmetric,

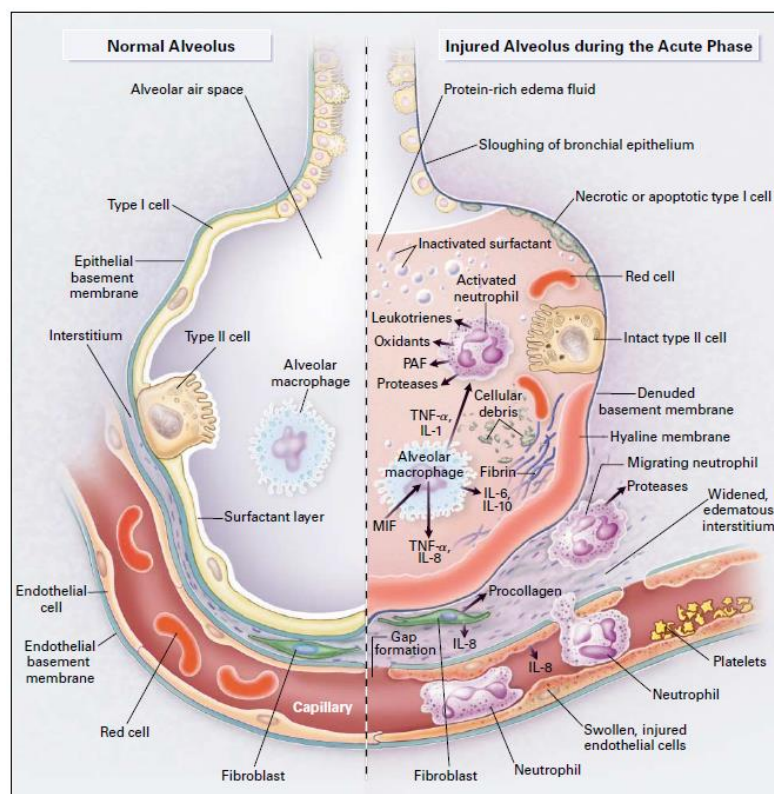


Figure 17: The Normal Alveolus and the Injured Alveolus in the Acute Phase of Acute Lung Injury and the Acute Respiratory Distress Syndrome. Disruption of alveolar capillary barrier leads to exudation of protein rich fluid in the alveolar space and inactivation of surfactant. Alveolar macrophages secrete pro-inflammatory cytokines and neutrophils are recruited to the lung. (Adapted from Ware and Matthay 2000).

due to interstitial and alveolar edema (172).

ARDS can be divided in two phases. The acute phase of ARDS is characterized by the disruption of the alveolar-capillary barrier that leads to endothelial permeability and eventually in exudation of protein rich fluid in the alveolar space. This proteinaceous alveolar exudate (hyaline membrane) can be seen lining alveolar spaces. The production of surfactant, which is a surface-active lipoprotein complex formed by type II alveolar cells to prevent the alveoli from collapsing, is also impaired. Macrophages secrete pro-inflammatory cytokines and neutrophils are recruited to the lung. Increased barrier permeability leads to fluid filled alveoli formation that along with surfactant inactivation, microvascular thrombosis and disorganized repair contribute to impaired function of the lung and hypoxemia (Figure 17). If there is no recovery, sustained inflammation leads to lung fibrosis (173).

Paradoxically, although obesity is associated with increased susceptibility to infection, increased body weight correlate with better prognosis in sepsis. Many observational studies and meta-analyses have shown that obese patients demonstrate lower mortality in sepsis compared to patients with normal body mass indices (174-176). Even morbidly obese septic patients do not associate with increased mortality (176).

There are many pathophysiological mechanisms proposed to explain the “obesity paradox”. First, the most widely believed explanation for the survival benefit of obese septic patients is associated with larger availability of energy reserve that can be consumed during catabolic processes that characterize extreme or prolonged illness. In addition, the enlarged adipose tissue may secrete factors like leptin and soluble tumor necrosis factor-receptor-2 that can affect the inflammatory process underlying sepsis. Another explanation could be the hemodynamic benefit due to increased activation of the renin-angiotensin system during obesity and many other explanations (177). However, the insufficient adjustment for confounding factors, the selection bias, the variability in medical treatment and the misclassification of patients due to inaccurate measurements may lead to false interpretation of the results and inappropriately characterized as proof of causality (177, 178).

Another important reason that could potentially lead to this outcome is the differences in the immune system of obese patients. Obesity is characterized by chronic low grade inflammation that one could hypothesize that the immune system is primed to defend

against infections (179). However, a meta-analysis also shows that although obesity primes the lung for injury due to adipokine imbalance, the inflammatory responses may be altered or attenuated. Lower levels of circulating cytokines were found in obese ARDS patients compared to normal weight patients and mouse models show impaired neutrophil recruitment to the lung (180). In addition, obesity is associated with reduced inflammasome activation and autophagy both necessary for potent antimicrobial defense (181). Subsequently, altered immune responses could be a potential cause for the survival benefit of obese septic patients, though the exact link is still unclear. A better understanding of obesity paradox could lead to the development of new prognostic and therapeutic strategies in sepsis.

Aim of the study

The purpose of this study was to investigate the effect of metabolic factors in the activation and metabolic phenotype of macrophages. Specifically, the aim was to delineate the role of insulin resistance, frequently associated with obesity, on peripheral macrophages. Since macrophages are important mediators of inflammatory responses, we further wanted to investigate their contribution to metabolic inflammation found in obesity. Finally, based to the fact that macrophages are important for the development of acute and sustained inflammatory processes, we will investigate the effect of insulin resistant macrophages on sepsis outcome and on the composition of gut microbiome.

Materials and methods

Diet induced insulin resistance and obesity in mice

For the diet-induced insulin resistant group and the diet-induced obese group 8-week-old male C57BL/6 (WT) mice, were fed a high-fat diet ((HFD; 60% energy from fats, catalog number PF4051/D) or a normal chow diet (ND catalog number 4RF21) (purchased from Mucedola) for 7 days or 10 weeks respectively, according to the protocol (short term HFD or long term HFD).

Primary macrophages isolation and culture

Peritoneal macrophages (TEPMs) were isolated from the peritoneal cavity of C57BL/6 (WT), Akt2^{-/-}, Akt1^{-/-}, LysM^{Cre}Igf1R^{fl/fl} and Igf1R^{fl/fl} mice, injected with 4% thioglycollate 4-5 days before sacrifice. Cells were collected after 2 washes of the peritoneal cavity with cell culture medium. Alveolar macrophages were isolated from mice using the bronchoalveolar lavage fluid (BALF) method. BALF was collected by intratracheal infusion of PBS (DPBS; Life Technologies, Carlsbad, CA) in the lung. After 3-4 washes with 1 ml PBS, cells were collected by centrifugation. 1x10⁵ macrophages per well were seeded in 96-well tissue-culture plates in a volume of 0.2 ml macrophage complete medium. Primary thioglycollate-elicited peritoneal macrophages (TEPMs) and alveolar macrophages were cultured in complete medium (DMEM; Life Technologies, Carlsbad, CA) supplemented with 10% (v/v) FBS, 10 mM L-glutamine, 100 IU/ml penicillin, and 100 mg/ml streptomycin. Escherichia coli-derived LPS (100 ng/ml; Sigma-Aldrich, St. Louis, MO), insulin (100 nM; Humulin R, Eli Lilly and Company), rapamycin (20 nM; Sigma-Aldrich, St. Louis, MO) and 2-deoxy-D-glucose (2.5 mM; Sigma-Aldrich, St. Louis, MO), FCCP (Sigma-Aldrich, St. Louis, MO) were used when indicated.

For Bone Marrow Derived Macrophages (BMDMs), bone marrow was isolated from the legs of Adipoq^{-/-} and WT mice in 1x PBS, 3% FBS, 1% pen/strep. The suspension passed through a BD cell strainer 40um and centrifuged for 5min at 1000rpm. The pellet was resuspended in 2ml erythrocyte lysis buffer and incubated for 5min. Cell culture medium 1640 RPMI GlutaMAX, 10% FBS, 1% pen/strep was added to stop the lysis. Centrifuge for 5min at 1000rpm and the cell pellet was

dissolved in 10ml medium and added in a 10cm cell culture dish. In the medium GM-CSF(10ng/ml) was added for the differentiation of the cells. After 2days and 4 days the medium was changed to fresh differentiation medium. After 7days the cells were differentiated and ready for experiment.

Glucose uptake assay

Cells were cultured in a 96-well plate in a density 10^5 cells/well. Cells were serum starved for 2 h and then glucose starved for 20 min. Insulin was added to the starvation medium for 10 min and then 0,5 uCi/ml (^3H)-2-deoxy-D-glucose (NEN-Perkin Elmer) and 100 uM 2-deoxy-D-glucose were added in each well for 25 min. The cells were washed and lysed in 0.5 M NaOH/0.1% SDS. The uptake of glucose was measured in a beta counter. Alternatively, glucose uptake was measured with a kit from abcam (ab136955) according to the manufacturer's instructions.

Caecal Ligation and Puncture Model of Polymicrobial Sepsis

The Cecal ligation and puncture model is a widely used model of polymicrobial sepsis (182) that can indirectly lead to Acute Lung Injury (ALI). Mice were anesthetized with ketamine (80-100 mg/kg) and xylazine (5-15 mg/kg) injected intra-peritoneally. A midline incision (1.5-2 cm) was made to reach the cecum and exteriorize it. The distal 0.5cm portion of the cecum was ligated with a 4-0 silk ligature suture without

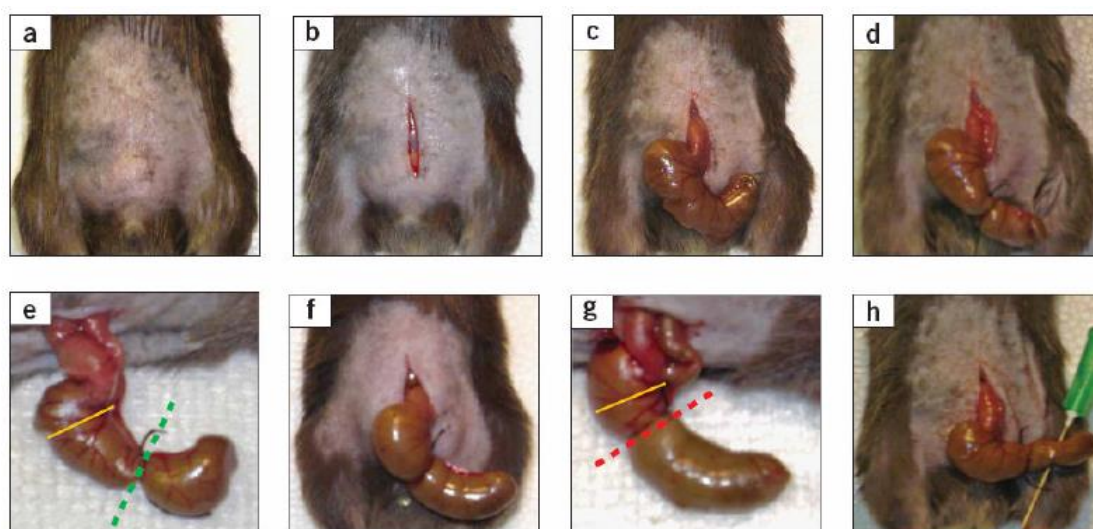


Figure 18: Cecal Ligation and Puncture (CLP) model of polymicrobial sepsis.

interrupting intestinal continuity. The cecum was punctured twice with a 16-gauge needle to become perforated and squeezed softly. The cecum was returned to the abdomen, and the incision was closed in layers with a 2–0 silk suture. After the procedure, the animals were fluid-resuscitated with sterile saline (1 mL) injected s.c. Sham controls were subjected to the same procedures as CLP without ligation and puncture of the cecum.

Bronchoalveolar lavage fluid (BALF) and blood serum collection

BALF was collected by intratracheal infusion of normal saline (30 ml/kg) to the lung. The supernatant was used for measurements of cytokine levels. The alveolar cells were obtained by performing 4 more washes of the alveolar space with 1ml of normal saline and stained for flow cytometry. Blood serum was collected from the right ventricle of the heart using a 1ml syringe. The samples were centrifuged at 5000 rpm for 10 min at 4°C. The serum was collected and used for cytokine levels measurements.

ELISA

Cytokine concentration for TNF α , IL-6 and MIP-2a was determined by ELISA at the indicated time points using ELISA kits (eBioscience and R&D Systems). Briefly, a 96-well plate was coated with 100 uL/well of 1x Capture Antibody in 1x Coating Buffer and left to incubate overnight at 4 °C. The plate was washed three times with Wash Buffer and it was blocked with 200 uL/well of 1x Assay Diluent followed by incubation at room temperature for 1 hour. Next, the plate was washed once with Wash Buffer and the samples as well as the standards (diluted according to manufacturer's protocol) were added (100 uL/well) and left to incubate for 2 hours at room temperature or overnight at 4°C on a rocker. After three washes with Wash Buffer, incubation of 100 uL/well of 1x Detection antibody for 1 hour at room temperature, three washes with Wash Buffer and subsequent incubation of 100 uL/well of 1x Detection enzyme (Avidin-HRP) for 30min at room temperature, 100 uL/well of 1x Tetramethylbenzidine (TMB) Substrate Solution to each well were added and the plate was left to incubate at room temperature for 15 minutes. The

reaction was stopped by adding 50 μ L of Stop Solution to each well and the plate was read at 450 nm and 550 nm at a Model 680 microplate reader. Values at 550 nm were subtracted from those of 450 nm and data were analyzed by Graph Pad Prism 5 software.

Lung histology and lung injury score determination

For histology purposes, lungs were perfused with PBS through the right ventricle. An incision at the left atrium allowed outflow of the blood. Lungs were inflated intratracheally with 10% formalin at 25 cm H₂O pressure, fixed overnight at 4°C, and stored in 70% ethanol before embedding in paraffin. Lung tissue sections of 5 μ m were prepared and further deparaffinized and rehydrated. Sections were stained with H&E and evaluated by a pathologist blinded to the interventions. To perform the histological assessment of lung injury, five independent variables were evaluated - neutrophils in alveolar spaces, neutrophils in the interstitial spaces, hyaline membranes, proteinaceous debris filling the airspaces, and alveolar septal thickening- and weighted according to the relevance ascribed to by the Official American Thoracic Society Workshop Report on Features and Measurements of Experimental Acute Lung Injury in Animals (183). The resulting injury score is a continuous value between 0 and 1.

Glycolysis assay – Extracellular Acidification

Extracellular acidification was measured using glycolysis assay kit (Abcam, Cambridge, U.K) according to the manufacturer's instructions. Briefly, TEPMs were seeded at a density 10^5 cells/well and incubated overnight in CO₂ incubator. Then, CO₂ was purged and medium was replaced with respiration buffer containing glycolysis assay reagent along with different stimulatory compounds. Measurement was performed using time-resolved fluorescence in a Perkin Elmer - VICTOR series X4 microplate reader.

RNA isolation and quantitative PCR

RNA from TEPMs or total lung was isolated using TRIzol reagent (Life Technologies, Carlsbad, CA). One microgram of total RNA was used for cDNA synthesis (TAKARA, Shiga, Japan). The SYBR Green method was followed in the PCR reaction. Primer sequences are shown in Table. Ribosomal protein S9 (RPS9) served as the housekeeping gene. Annealing was carried out at 60°C for 30 s, extension was at 72°C for 30 s, and denaturation at 95°C for 15 s for 40 cycles in a 7500 Fast Real-Time PCR System (Life Technologies/Applied Biosystems). The amplification efficiencies were the same as the one of RPS9 as indicated by the standard curves of amplification, allowing us to use the following formula: fold difference = $2^{-(\Delta CtA - \Delta CtB)}$, where Ct is the cycle threshold.

| Primers for RT-PCR | | |
|--------------------|-----|----------------------------------|
| Ym1 | Fwd | 5'-GCAGAAGCTCTCCAGAAGCAATCCTG-3' |
| | Rev | 5'-ATTGGCCTGTCCTTAGCCCAACTG-3' |
| Fizz1 | Fwd | 5'-GCTGATGGTCCCAGTGAATAC-3' |
| | Rev | 5'-CCAGTAGCAGTCATCCCAGC-3' |
| Arginase-1 | Fwd | 5'-CAGAAGAATGGAAGAGTCAG-3' |
| | Rev | 5'-CAGATATGCAGGGAGTCACC-3' |
| iNOS | Fwd | 5'-TCCTGGAGGAAGTGGGCCGAAG-3' |
| | Rev | 5'-CCTCCACGGGCCCGTACTC-3' |
| IL-12 β | Fwd | 5'-GGAGGGGTGTAACCAGAAAGGTGC-3' |
| | Rev | 5'-CCTGCAGGGAACACATGCCAC-3' |
| HK3 | Fwd | 5'-TGCTGCCCACATACGTGAG-3' |
| | Rev | 5'-GCCTGTCAGTGTTACCCACAA-3' |
| PFKp | Fwd | 5'-CGCCTATCCGAAGTACCTGGA-3' |
| | Rev | 5'-CCCCGTGTAGATTCCCATGC-3' |
| GLUT-1 | Fwd | 5'-AAAGAAGAGGGTCCGCAGAT-3' |
| | Rev | 5'-CTGCCTTCTCGAAGATGCTC-3' |
| InsR | Fwd | 5'-AGAGACTCACTGACCTGATGCG-3' |
| | Rev | 5'-AACGGGACATTCTCCATGTCTT-3' |

| | | |
|--------|-----|----------------------------------|
| Igf1R | Fwd | 5'-AGGAGAAGCCCATGTGTGAGAA-3' |
| | Rev | 5'-GTTGTTCTCGGTGCAGGCTC-3' |
| LDHa | Fwd | 5'-CATTGTCAAGTACAGTCCACACT-3' |
| | Rev | 5'-TTCCAATTACTCGGTTTTTGGGA-3' |
| GLUT-3 | Fwd | 5'-GATCGGCTCTTTCCAGTTTG-3' |
| | Rev | 5'-CAATCATGCCACCAACAGAG-3' |
| RPS9 | Fwd | 5'-GCTAGACGAGAAGGATCCCC-3' |
| | Rev | 5'-CAGGCCAGCTTAAAGACCT-3' |
| Ym1 | Fwd | 5'-GCAGAAGCTCTCCAGAAGCAATCCTG-3' |
| | Rev | 5'-ATTGGCCTGTCCTTAGCCCAACTG-3' |

Measurement of myeloperoxidase (MPO) activity

For MPO determination, 50 mg/ml tissues were homogenized in 50 mmol/l phosphate buffer, pH 6.0, with 0.5% hexadecyltrimethylammonium bromide using mortar and pestle. Samples were frozen and thawed three times and centrifuged for 10 min at 10,000 g, and then supernatants were stored at -20°C until assay. MPO was determined in 96-well plates using a modification of the method described 27. Briefly, 10ul sample was added to 190ul assay buffer (phosphate buffer 50 mM, pH 6.0, containing 0.167 mg/ml o-dianisidine, Sigma Chemical Co) and 0.0005% H₂O₂). Absorbance at 450 nm ($A_{450\text{ nm}}$) was measured in a microtiter reader at 15 min.

Flow Cytometry

Expression of protein levels Arginase1 was determined by flow cytometry cell surface and intracellular staining, as previously described (184). Cells isolated from BALF were incubated with PerCP-Cy5.5 anti-mouse CD11c (Biolegend, San Diego, CA, USA), also cells isolated from peritoneal cavity and from lung after homogenization were incubated with Phycoerythrin anti mouse F4/80 (Biolegend, San Diego, CA, USA) for cell surface staining, fixation and permeabilization (BD Fixation and Permeabilization Solution Kit; BD Biosciences) was performed for intracellular

staining with Mouse monoclonal anti-mouse Arginase1 (BD Biosciences). Allophycocyanin rat anti-mouse IgG1 (Biolegend, San Diego, CA, USA) was used as secondary Ab for Arginase1 staining. The proper isotype controls were used in each case. The flow cytometry events were acquired in a MoFlo Legacy Cell Sorter (Beckman Coulter) and analyzed with Summit Software. Flow cytometry events were gated first based on forward and side scatter and then CD11c+ cells (alveolar macrophages) or F4/80 cells (peritoneal, lung interstitial macrophages) were selected to evaluate the expression of Arginase1. TEPMs were incubated with MitoTracker Red CM-H₂X ROS (Molecular Probes, Invitrogen) in cell culture at a final concentration of 400 nM (Life Technologies) for 20 min at 37 °C, the cells were collected and analyzed with flow cytometry for mitochondrial ROS determination. Mitotracker Green (Molecular Probes, Invitrogen) was used for assessment of mitochondrial biogenesis. TEPMs were isolated and incubated with mitotracker at a final concentration of 200nM for 20min at 37°C then the cells were collected and analyzed using flow cytometry

Western blot analysis

Macrophage protein lysates were resuspended in RIPA buffer containing phosphatase and protease inhibitors (Complete; Roche, Basel, Switzerland). Protein concentration of the samples was determined using BCA kit. Twenty micrograms of protein was electrophoresed on 10% denaturing polyacrylamide gel prior to wet transfer to 0.45 um nitrocellulose membrane (Macherey Nagel, Germany). Briefly, after blocking with 5% BSA PBS (pH 7.4) for an hour at room temperature, the membranes were incubated with rabbit polyclonal anti-mouse p-Akt (Ser473) Ab (Cell Signaling Technology), rabbit polyclonal anti-mouse Akt Ab (Cell Signaling Technology), rabbit polyclonal anti-mouse p-Akt2 (Ser474) Ab (Cell Signaling Technology), rabbit polyclonal anti-mouse Akt2 Ab (Cell Signaling Technology), rabbit polyclonal anti-mouse p-S6(235/236) Ab (Cell Signaling Technology), rabbit polyclonal anti-mouse p-4E-BP1(Thr37/46) Ab (Cell Signaling Technology), rabbit polyclonal anti-mouse iNOS Ab (Abcam, Cambridge, U.K), goat polyclonal anti-mouse Arginase1 (Abcam,Cambridge, U.K), goat polyclonal anti-mouse Fizz1 Ab (Abcam, Cambridge, U.K), rabbit polyclonal anti-mouse IGF-1R Ab (Cell Signaling Technology) or mouse monoclonal anti-mouse beta-actin (Abcam, Cambridge, U.K) at 4°C overnight. The

membranes were then incubated with 40 ng/ml peroxidase-conjugated anti-rabbit, anti-mouse or anti-goat secondary Ab (Santa Cruz Biotechnology), respectively, for 1 h at room temperature, followed by reaction with Chemiluminescent HRP substrate (LumiSensor; GeneScript, USA). Densitometric analysis was performed with the ImageJ program.

Tolerance Test (ITT), Pyruvate Tolerance Test (PTT) and Glucose Tolerance Test (GTT)

For ITT mice were fasted overnight and then injected intraperitoneally with insulin (0.75IU/kg). Glucose measurements were received at time points: 0min, 15min, 30min, 60min and 120min. For PTT mice were fasted overnight and then injected intraperitoneally with 2 g/kg pyruvate. Glucose measurements were received at time points: 0min, 30min, 60min and 120 min. For GTT mice were fasted overnight and then injected intraperitoneally with glucose (1mg/gr). Glucose measurements were received at time points: 0min, 30min, 60min and 120 min.

Phagocytosis assay

Phagocytic capacity of macrophages was measured using Vybrant Phagocytosis Assay Kit (Molecular Probes, Inc) according to the manufacturer's instructions. Briefly, TEPMs were cultured in 96-well plates and incubated with heat-inactivated fluorescein-labeled E.coli (K-12 strain) BioParticles for 2h. Extracellular fluorescence was quenched by trypan blue and phagocytic capacity was quantified by measuring fluorescence intensity of the uptaken particles using a Perkin Elmer - VICTOR series X4 microplate reader.

Statistical Analysis

The results were analyzed using one-way or two-way ANOVA with the Bonferroni multiple comparison posttest. Comparison of nonparametric results between different groups was performed by the Mann–Whitney *U* test, using GraphPad InStat software (GraphPad, San Diego, CA). The *p* values < 0.05 were considered significant. Results are expressed as mean ± SD or as median (5–95 percentiles), as indicated, and are representative of at least three independent experiments.

Results

Macrophages become resistant to insulin and exhibit reduced Akt2 phosphorylation and increased mTORC1 activity

Macrophages harbor all the components of insulin signaling pathway and are responsive to insulin signals through insulin receptor and subsequent phosphorylation of Akt kinase. To determine the effect of insulin resistance in insulin signaling propagation we used thioglycollate-elicited peritoneal macrophages (TEPMs) from mice and treated them with high insulin concentrations for prolonged time, trying to recapitulate hyperinsulinemia found in obesity. TEPMs were isolated and cultured in conditions used to induce insulin resistance in other cell types, like adipocytes, being

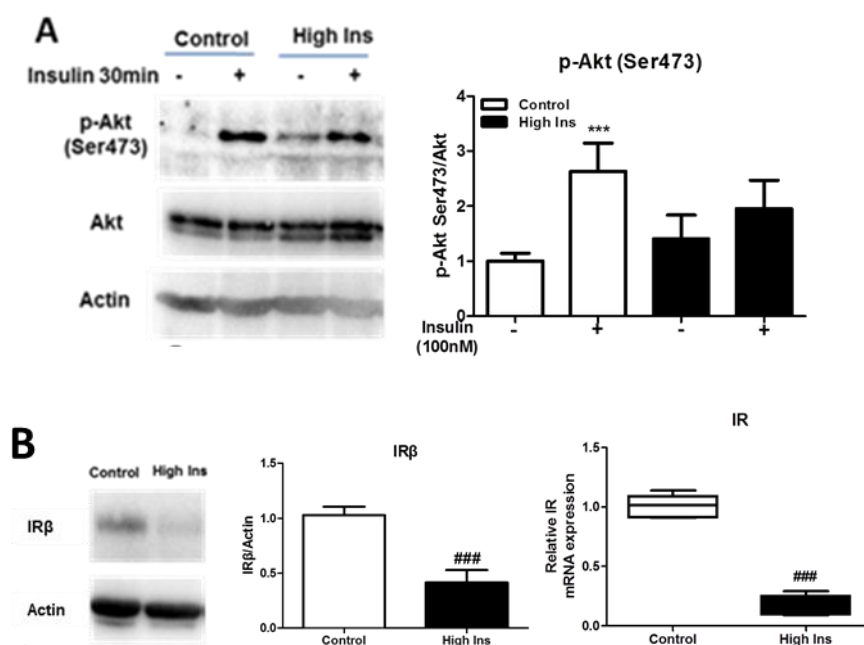


Figure 19: Western blot analysis of p-Akt (Ser473) in non-stimulated (NS) and after 30 min of stimulation with 100 nM insulin for control and macrophages chronically insulin-treated in culture. Summary graph of average phosphorylation of Akt in all conditions (basal and after insulin stimulation) normalized to total Akt. (B) Expression of IR in control and macrophages chronically insulin-treated in culture. Akt1 mediates mTORC1 phosphorylation. All graphs are representative of 3-6 independent experiments and show mean \pm SD. * $p < 0.05$, ** $p < 0.01$, *** $p < 0.001$, insulin stimulation versus no stimulation, # $p < 0.05$, ## $p < 0.01$, ### $p < 0.001$ insulin resistant versus control macrophages.

100nM insulin for 48 hours. To check the insulin sensitivity of these cells we measured the activation status of Akt kinase and the expression levels of insulin receptor β (IR β). Western blot analysis of Akt Ser347 phosphorylation showed a significant reduction in Akt activation in prolonged insulin treated compared to non-insulin treated macrophages after stimulation with 100nM insulin for 30 min. The

levels of IR β in insulin treated macrophages were also significantly downregulated compared to untreated cells (Figure 19).

Furthermore we measured the activation of Akt and IR β levels in macrophages living in a hyperinsulinemic environment *in vivo*. For this purpose we isolated TEPMs from mice fed a high-fat diet for short term (185). These mice acquired insulin resistance and glucose intolerance as indicated by GTT, ITT and PTT, even though the weight gain was only slightly increased (Figure 20).

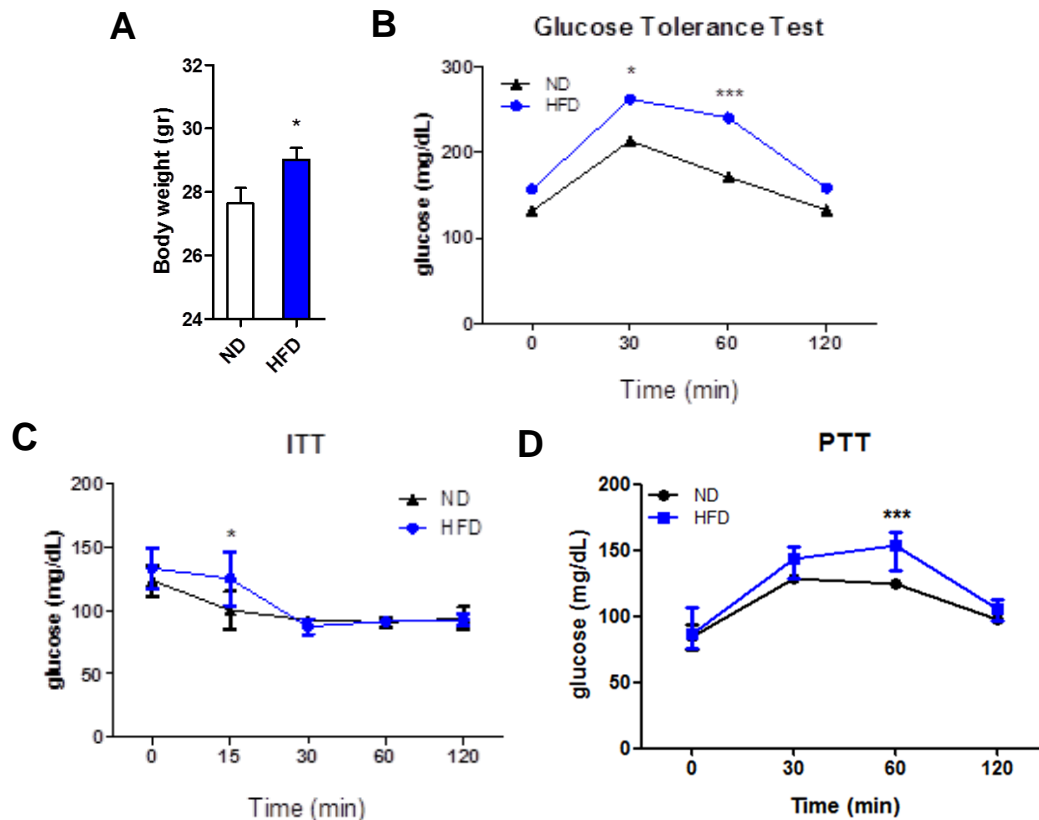


Figure 20: (A) Body weight of mice fed ND or HFD for short-term. (B) Glucose tolerance test – GTT. (C) Insulin tolerance test (ITT) and (D) pyruvate tolerance test in WT (control) and short-term HFD - fed mice ($n = 4-5$ mice/group). Graphs represent mean \pm SD. * $p < 0.05$, ** $p < 0.01$, *** $p < 0.001$, HFD versus control mice

TEPMs from these mice also showed impaired Akt activation following 30 min of 100nM insulin stimulation and the expression levels of IR β were decreased compared to macrophages derived from mice fed a normal diet. The basal levels of Akt phosphorylation were not different in TEPMs derived from HFD fed mice even though IR levels were lower, probably due to IR-independent signals (Figure 21).

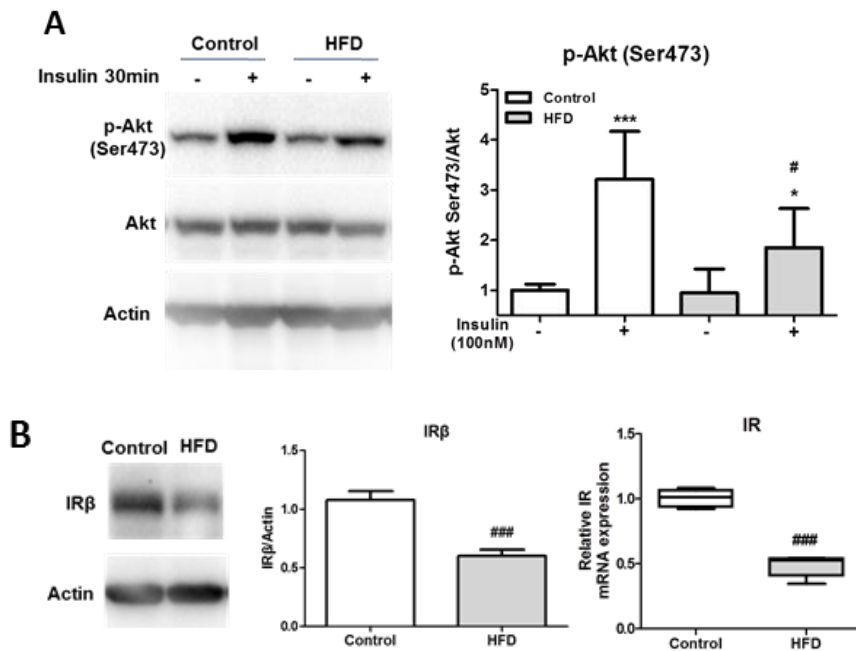


Figure 21: (A) Western blot analysis of p-Akt (Ser473) in non-stimulated (NS) and after 30 min of stimulation with 100 nM insulin for control and macrophages from short term high fat diet fed mice. Summary graph of average phosphorylation of Akt in all conditions (basal and after insulin stimulation) normalized to total Akt. (B) Expression of IR in control and macrophages from short term high fat diet fed mice, measured by real-time PCR and western blot. All graphs are representative of 3-6 independent experiments and show mean \pm SD. * $p < 0.05$, ** $p < 0.01$, *** $p < 0.001$, insulin stimulation versus no stimulation, # $p < 0.05$, ## $p < 0.01$, ### $p < 0.001$ insulin resistant versus control macrophages.

These findings imply that macrophages acquire insulin resistance and we further wanted to check the effect of insulin signaling pathway disruption by genetic ablation of insulin signaling mediators in order to delineate the mechanism responsible for insulin resistance in macrophages.

During obesity and insulin resistance, insulin signaling mediated through Akt/mTOR pathway is impaired. Akt isoforms serve differential functions upon insulin stimulation. Studies suggest that Akt2 is the predominant Akt isoform that mediates insulin signaling, being essential for glucose uptake and homeostasis (186). Lack of Akt2 from mouse models results in hyperinsulinemia, hyperglycemia, insulin resistance and diabetes mellitus-like syndrome (187). We confirmed the insulin resistant phenotype observed in Akt2^{-/-} mice by GTT, ITT and PTT (Figure 23)

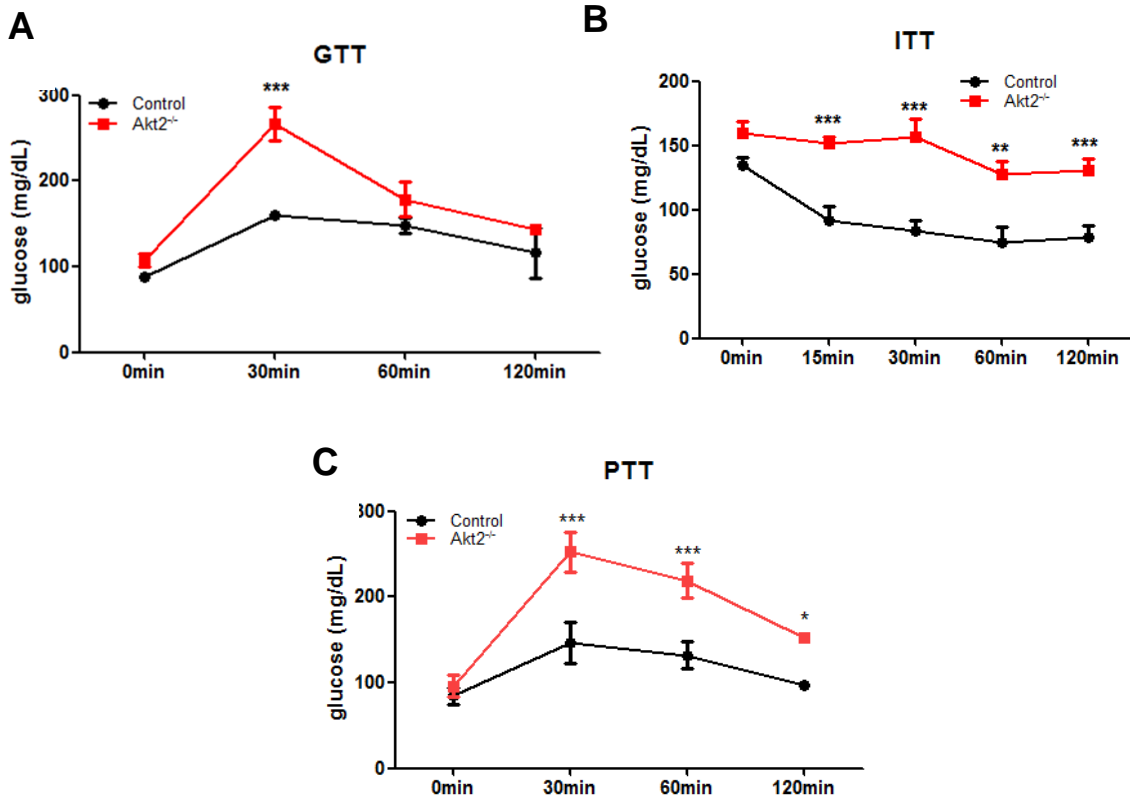


Figure 23: (A) Glucose tolerance test – GTT. (B) Insulin tolerance test (ITT) and (C) pyruvate tolerance test in WT (control), Akt2^{-/-}, (*n* = 4-5mice/group). Graphs represent mean ± SD. **p* < 0.05, ***p* < 0.01, ****p* < 0.001, Akt2^{-/-} versus control mice.

Accordingly, TEMPs isolated from Akt2^{-/-} mice display insulin resistant phenotype as indicated from significantly decreased Akt phosphorylation upon insulin stimulation (Figure 24).

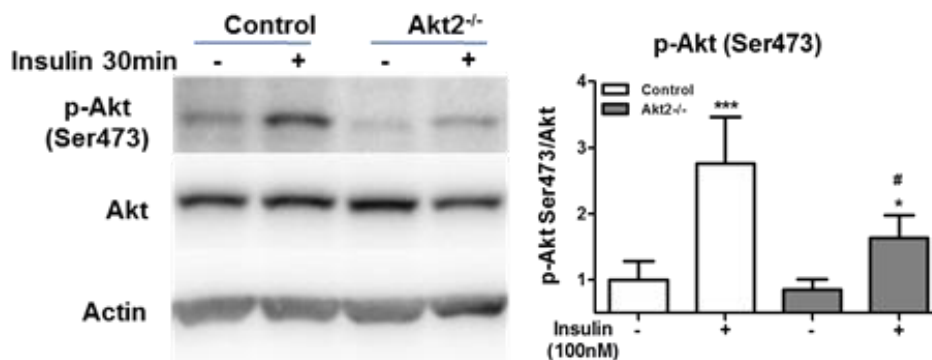


Figure 24: Western blot analysis of p-Akt (Ser473) in non-stimulated (NS) and after 30 min of stimulation with 100 nM insulin for WT (control) and Akt2^{-/-} macrophages. Summary graph of average phosphorylation of Akt in all conditions (basal and after insulin stimulation) normalized to total Akt. Graph is representative of 3-6 independent experiments and show mean ± SD. **p* < 0.05, ***p* < 0.01, ****p* < 0.001, insulin stimulation versus no stimulation, # *p* < 0.05, ## *p* < 0.01, ### *p* < 0.001 insulin resistant versus control macrophages.

Akt2 phosphorylation was also reduced in macrophages derived from HFD fed mice. Akt1 isoform is activated by insulin to induce growth pathways. Measurement of the

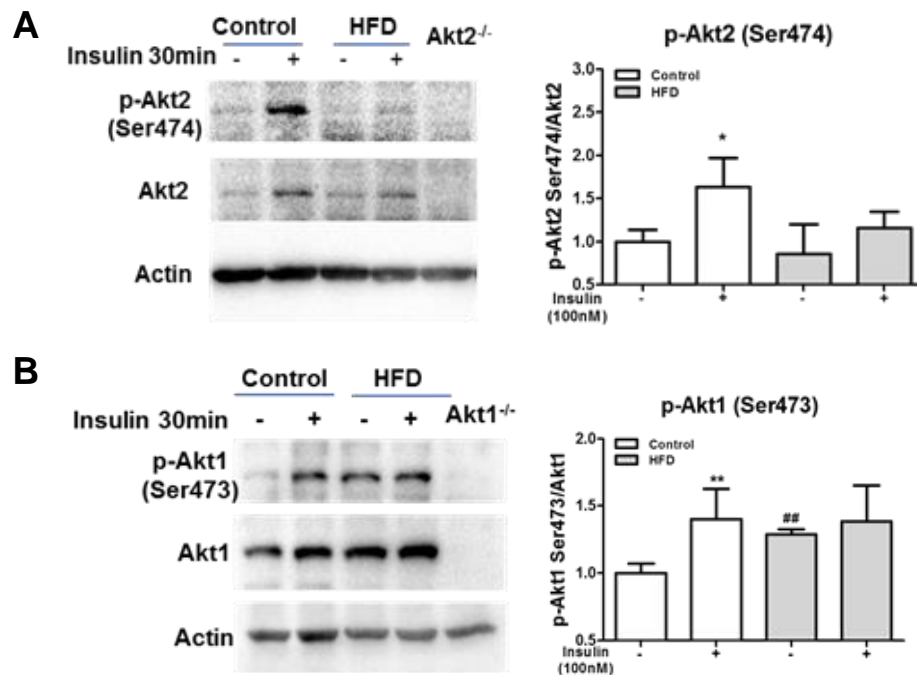


Figure 25: Western blot analysis and summary graph of (A) Akt2 phosphorylation p-Akt2 (Ser474) and (B) Akt1 phosphorylation p-Akt1 (Ser473) in macrophages from control and HFD fed mice before and after 30 min of stimulation with 100 nM insulin. All graphs are representative of 3-6 independent experiments and show mean \pm SD. * $p < 0.05$, ** $p < 0.01$, *** $p < 0.001$, insulin stimulation versus no stimulation, # $p < 0.05$, ## $p < 0.01$, ### $p < 0.001$ insulin resistant versus control macrophages.

Akt1 isoform activity also showed impairment in response to insulin stimulation in HFD macrophages, although the phosphorylation at the basal levels was significantly higher compared to controls (Figure 25). Recent evidence shows that mice having constitutive activation of Akt1 isoform in β -pancreatic cells, display impaired glucose homeostasis and a pre-diabetic phenotype (188).

Activation of Akt kinases results in phosphorylation of mTORC1, which in turn phosphorylates several targets, including p70S6 kinase and 4E-BP1. Prolonged insulin action during obesity leads to the sustained activation of mTORC1 and subsequent feedback inhibition of insulin signaling pathway. The activity of mTORC1 was elevated in macrophages derived from HFD fed insulin resistant mice as well as in macrophages that lack the Akt2 isoform at the basal levels, as evaluated by phosphorylation of mTORC1 targets, ribosomal protein S6 and 4E-BP1, whereas there was only a slight activation after insulin stimulation. Accordingly, the

phosphorylation of these substrates was reduced in Akt1 deficient macrophages both at the basal levels and upon insulin stimulation (Figure 26)

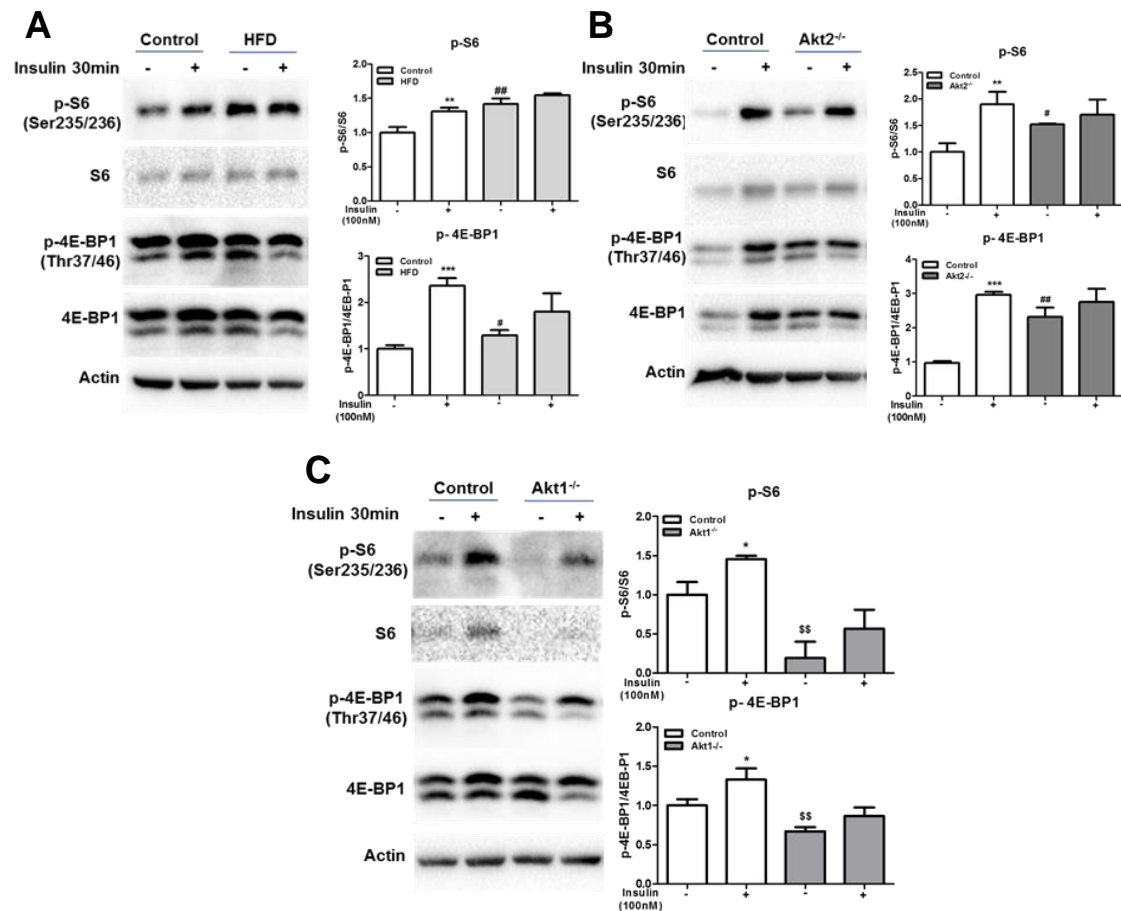


Figure 26: Western blot analysis of p-S6 (Ser235/236) and p-4E-BP1 (Thr37/46) in macrophages from short term high fat diet fed mice (A) from Akt2^{-/-} (B) and from Akt1^{-/-} (C) compared to control before and after 30 min of stimulation with 100 nM insulin. All graphs are representative of 3-6 independent experiments and show mean \pm SD. *p < 0.05, **p < 0.01, ***p < 0.001, insulin stimulation versus no stimulation, #p < 0.05, ##p < 0.01, ###p < 0.001, insulin resistant versus control macrophages, \$\$p < 0.01, Akt1^{-/-} versus control macrophages.

The predominant receptor for insulin is the insulin receptor, which has two isoforms IR α and IR β . IR shares high degree of homology with IGF1R and both insulin and IGF-1 can bind and activate its other receptor with weak affinity. The expression levels of IGF1R were evaluated in insulin resistant macrophages by western blot analysis and real-time PCR and a suppression of its expression was observed in HFD macrophages (Figure 27).

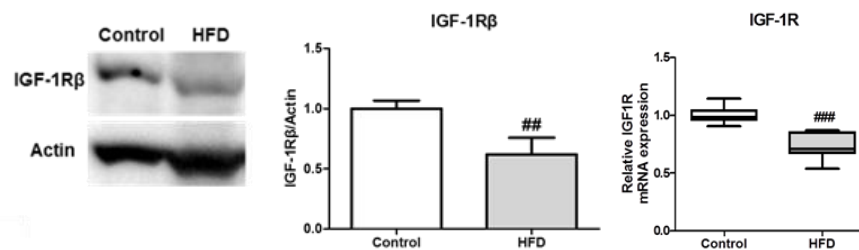


Figure 27: IGF-1R expression in control and macrophages from short term HFD fed mice, measured by real-time PCR and western blot. Graphs are representative of 3-6 independent experiments and show mean \pm SD. Box shows 5–95 percentiles, horizontal line represents median, and whiskers represent minimum and maximum. # $p < 0.05$, ## $p < 0.01$, ### $p < 0.001$ insulin resistant versus control macrophages,

The mechanism that induces insulin resistance in macrophages is not clear. In order to delineate the contribution of IR and IGF1R in insulin resistance we isolated TEMPs from WT mice, we treated them with different concentrations of insulin starting from 0.01nM until 100nM and measured the activation of Akt2 and IR levels. The effect of insulin on Akt2 activity and IR expression started at 1nM, a concentration that mediates signals via IR (189). Decreased phosphorylation of Akt2 and IR expression was observed at 1nM with a gradual impairment until 100nM, a concentration that insulin mediates its action also through IGF1R (Figure 28).

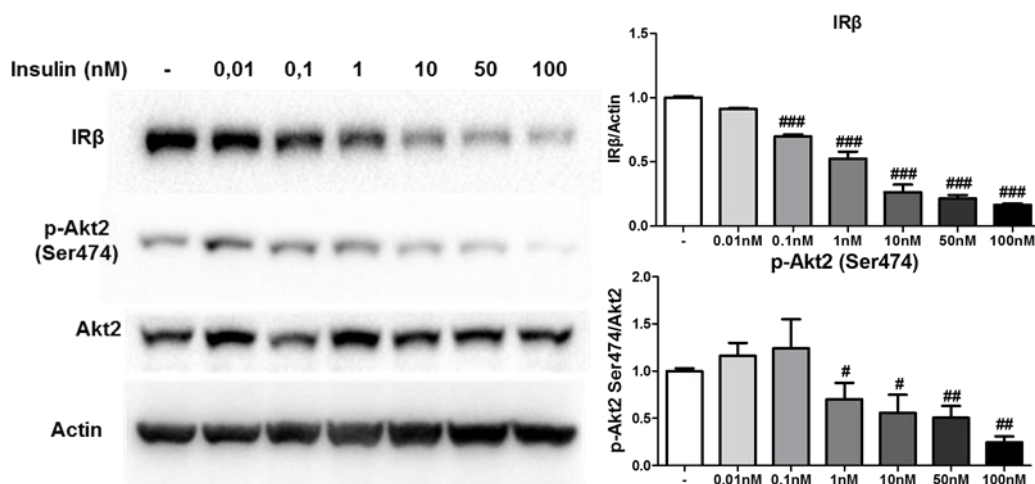


Figure 28: Expression of IR β and phosphorylation of Akt2 in macrophages after long term treatment with different concentrations of insulin. Graphs are representative of 3-6 independent experiments and show mean \pm SD. # $p < 0.05$, ## $p < 0.01$, ### $p < 0.001$ insulin resistant versus control macrophages.

Furthermore, we stimulated HFD macrophages with 2.6 nM IGF-1, a concentration that is able to activate only IGF1R (189) and we observed that in control macrophages the phosphorylation of Akt2 was significantly induced, whereas this activation was abolished in HFD macrophages. These results suggest that both receptors are not able to propagate signals during obesity and contribute to insulin resistance in macrophages (Figure 29).

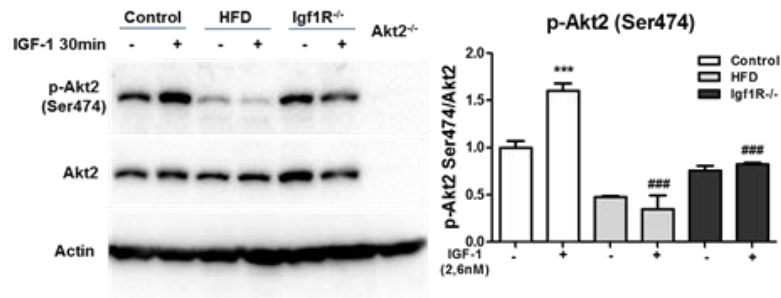


Figure 29: Western blot analysis of Akt2 phosphorylation in control, HFD, Igf1R^{-/-} and Akt2^{-/-} macrophages before and after 30min of stimulation with 2,6 nM IGF-1. All graphs are representative of 3-6 independent experiments and show mean \pm SD. *p < 0.05, **p < 0.01, ***p < 0.001, IGF-1 stimulation versus no stimulation, #p < 0.05, ##p < 0.01, ###p < 0.001, insulin resistant versus control macrophages.

These results are in line with the down-regulation observed in the expression of IGF1R in HFD macrophages, In Akt2 deficient macrophages there was no change in mRNA levels of both receptors, implying that either IR or IGF1R is not responsible for the defect in insulin signaling cascade but the absence of the activation of their downstream target Akt2 is the cause of this effect. We also measured the expression levels of IR in macrophages that lack IGF1R to see if there was a compensatory increase in its expression but no change was observed in the mRNA levels (Figure 30).

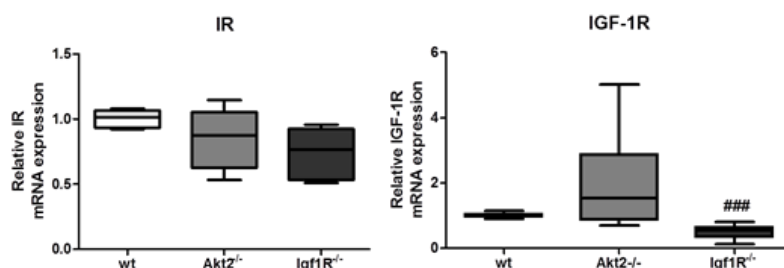


Figure 30: mRNA expression levels of IR and IGF-1R in WT (control), Akt2^{-/-} and Igf1R^{-/-} macrophages. All graphs are representative of 3-6 independent experiments and show mean \pm SD. #p < 0.05, ##p < 0.01, ###p < 0.001, insulin resistant versus control macrophages.

The role of IGF1R in macrophages was recently proven to be important for their activation status (59). To further delineate the role of IGF1R in insulin resistance of macrophages and how its absence could affect insulin signals, we generated mice deficient in IGF1R specifically in macrophages $LysM^{Cre}Igf1R^{fl/fl}$. These mice were glucose tolerant, with normal response to insulin, glucose and pyruvate tolerance test (Figure 31).

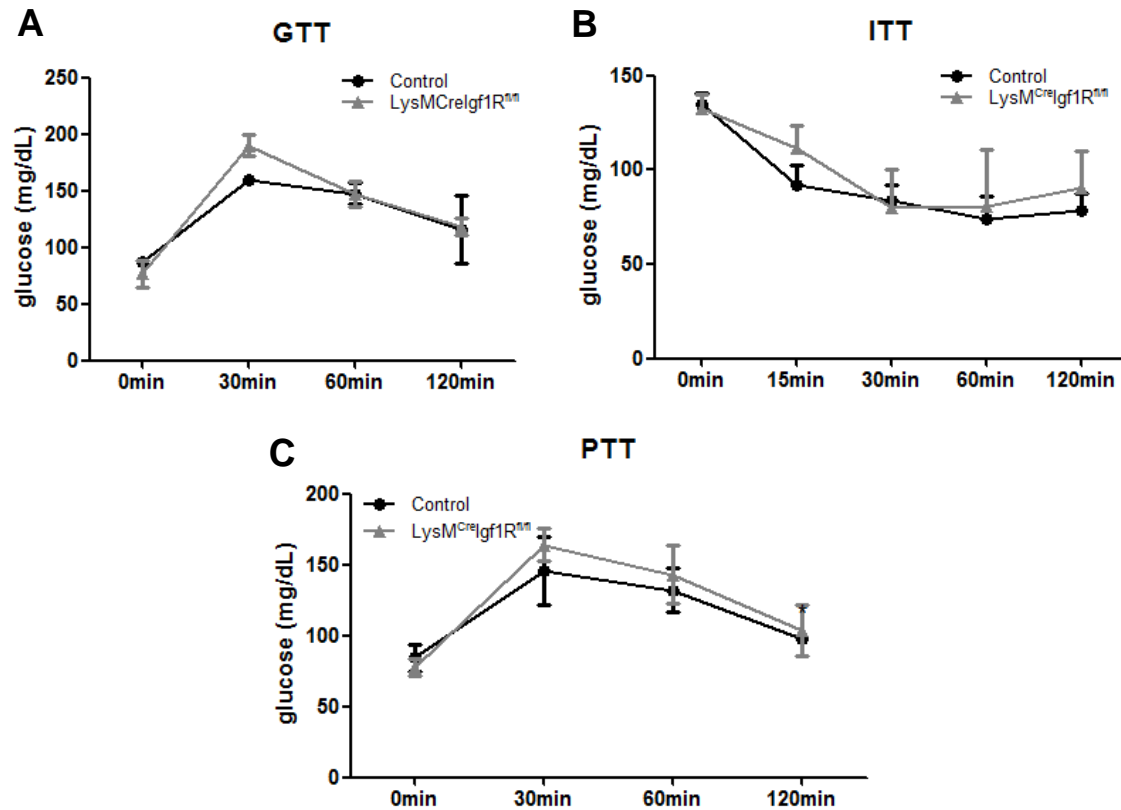


Figure 31: (A) Glucose tolerance test – GTT. (B) Insulin tolerance test (ITT) and (C) pyruvate tolerance test in WT (control), $Igf1R^{-/-}$, ($n = 4-5$ mice/group). Graphs represent mean \pm SD.

In the absence of IGF1R, macrophages displayed insulin resistance as indicated by the activation status of Akt upon insulin stimulation. Western blot analysis of Akt phosphorylation at Ser473 showed a significantly lower activation of Akt after insulin stimulation compared to control macrophages (Figure 32).

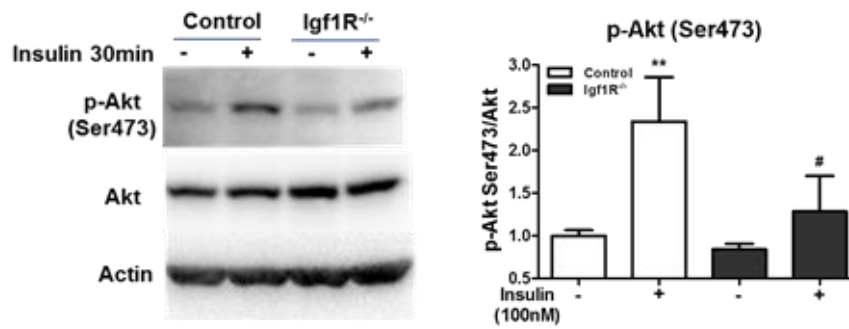


Figure 32: Western blot analysis and summary graph of Akt phosphorylation p-Akt (Ser473) in macrophages from control and Igf1R^{-/-} mice before and after 30 min of stimulation with 100 nM insulin. All graphs are representative of 3-6 independent experiments and show mean ± SD. * $p < 0.05$, ** $p < 0.01$, *** $p < 0.001$, insulin stimulation versus no stimulation, # $p < 0.05$, # $p < 0.01$, ### $p < 0.001$ insulin resistant versus control macrophages.

To determine whether IGF1R mediates its signals through Akt2 isoform and subsequently mTORC1 like IR, we isolated macrophages from LysM^{Cre}Igf1R^{fl/fl} mice,

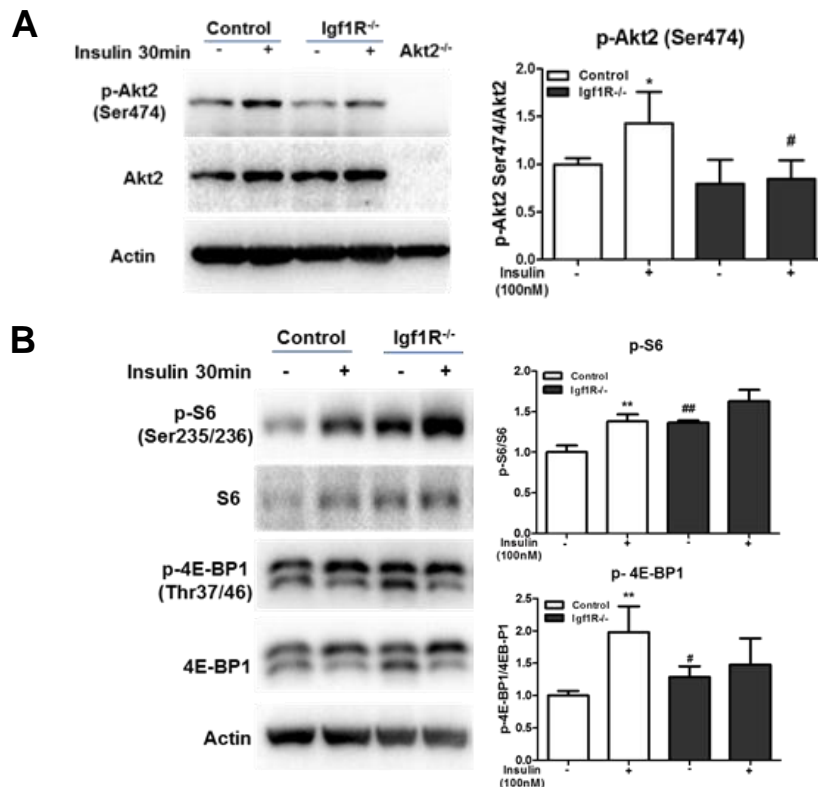


Figure 33: Evaluation of Akt2 phosphorylation (A) and mTORC1 pathway activation (B) by western blot analysis in control and Igf1R^{-/-} macrophages under basal conditions and after 30 min of stimulation with 100 nM insulin. All graphs are representative of 3-6 independent experiments and show mean ± SD. * $p < 0.05$, ** $p < 0.01$, *** $p < 0.001$, insulin stimulation versus no stimulation, # $p < 0.05$, ## $p < 0.01$, ### $p < 0.001$ insulin resistant versus control macrophages.

stimulated them in culture with 100nM insulin and then we measured phosphorylation levels of Akt2 and mTORC1 targets, S6 and 4E-BP1. Western blot analysis showed that the increase in Akt2 Ser474 phosphorylation as well as the phosphorylation of S6 and 4E-BP1 upon insulin stimulation found in control macrophages was abolished in macrophages that lack IGF1R, implying that IGF1R signals through the Akt2/mTORC1 pathway (Figure 33). In addition, we observed an increased activity of mTORC1 at the basal levels in IGF1R^{-/-} macrophages, as was also found in Akt2^{-/-} and HFD macrophages.

Since Akt2 activation is not affected in insulin resistant macrophages, namely HFD and IGF1R^{-/-} macrophages we wanted to check the activation of Akt1 isoform. We found that the phosphorylation of Akt1 at Ser473 was significantly increased in TEMPs from Akt2^{-/-}, LysM^{Cre}Igf1R^{fl/fl} or HFD-fed mice at the basal levels (Figure 34), indicating an important role of this isoform in insulin resistant macrophages and also could be associated with the elevated mTORC1 activation observed in this condition.

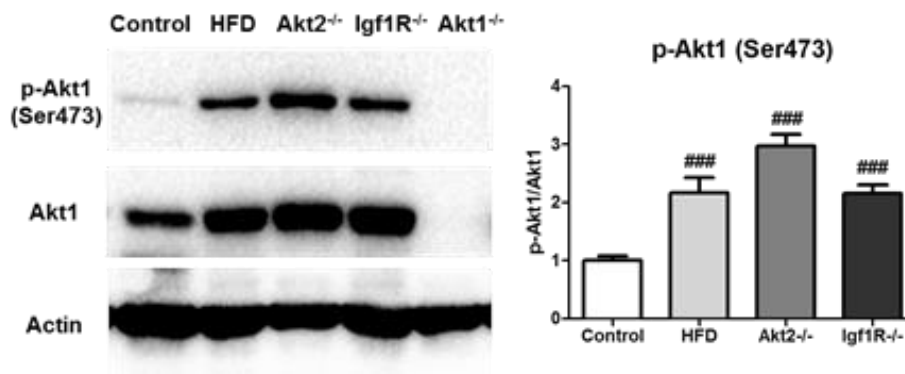


Figure 34: Western blot analysis of p-Akt1 (Ser473), for control, HFD, Akt2^{-/-} Igf1R^{-/-} and Akt1^{-/-} macrophages under basal conditions. Graph is representative of 3-6 independent experiments and shows mean ± SD. ### $p < 0.001$ insulin resistant versus control macrophages.

Insulin resistant macrophages acquire M2-like activation phenotype (M-InsR)

Akt isoforms differentially contribute to the activation status of macrophages. Lack of Akt2 polarizes macrophages towards an anti-inflammatory phenotype (78, 86). Accordingly, in human macrophages pattern-recognition-receptor (PRR) stimulation require Akt2 activation for pro-inflammatory cytokine production and M1 polarization (87). Since Akt2 is implicated in insulin signaling pathway and the lack

of this isoform results in insulin resistance, we further wanted to see how insulin resistant macrophages respond to a pro-inflammatory stimulus. For this reason we

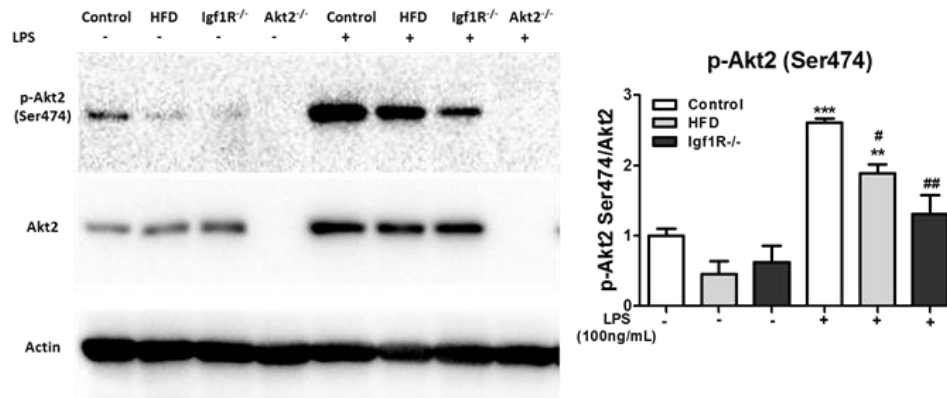


Figure 35: Western blot analysis of p-Akt2 (Ser474) in naive and stimulated with LPS (100 ng/ml) for 6 h, WT (control) and insulin resistant macrophages. Graph is representative of 3-6 independent experiments and shows mean \pm SD. * $p < 0.05$, ** $p < 0.01$, *** $p < 0.001$, LPS-stimulated versus non-stimulated macrophages, # $p < 0.05$, ## $p < 0.01$, ### $p < 0.001$, insulin resistant versus control macrophages.

treated insulin resistant and control macrophages with 100ng/ml LPS for 6 hours *in vitro* and we evaluated the phosphorylation of Akt2 using western blot analysis. We

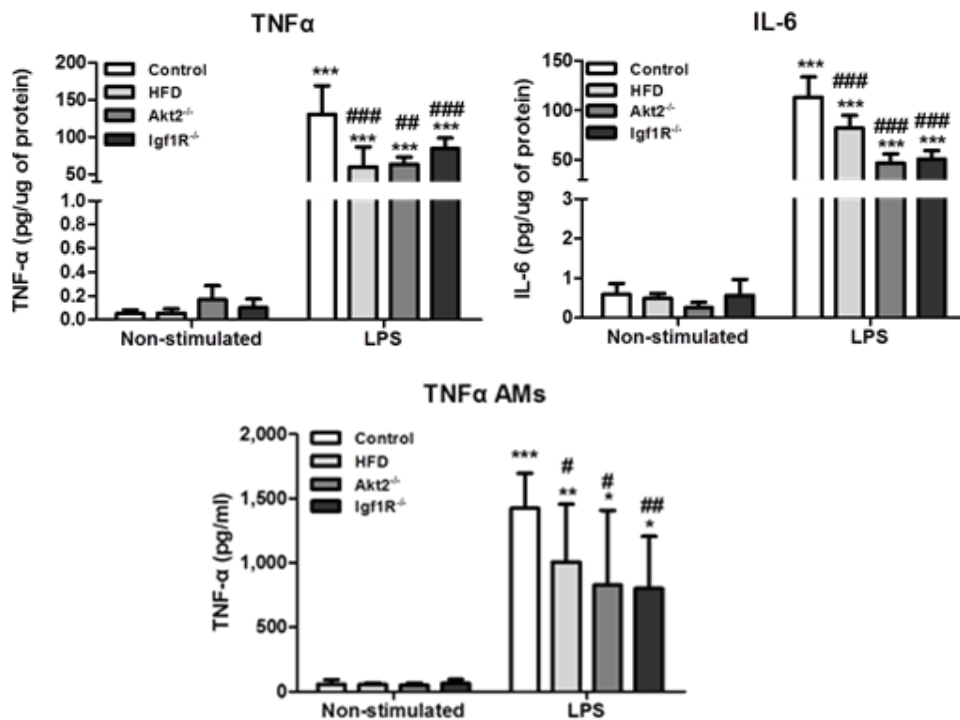


Figure 36: Levels of TNF α and IL-6 secreted in the supernatant of cultures of TEPMs and alveolar macrophages (AMs) of WT (control) and insulin resistant macrophages before (NS) and after 6 h stimulation with LPS. Graphs are representative of 3-6 independent experiments and show mean \pm SD. * $p < 0.05$, ** $p < 0.01$, *** $p < 0.001$, LPS-stimulated versus non-stimulated macrophages, # $p < 0.05$, ## $p < 0.01$, ### $p < 0.001$, insulin resistant versus control macrophages.

found that upon LPS treatment insulin resistant macrophages showed reduced Akt2 activation compared to insulin sensitive control macrophages (Figure 35).

We also measured the secretion of the pro-inflammatory cytokines IL-6 and TNF α and we observed that the production of these cytokines was reduced in LPS-treated

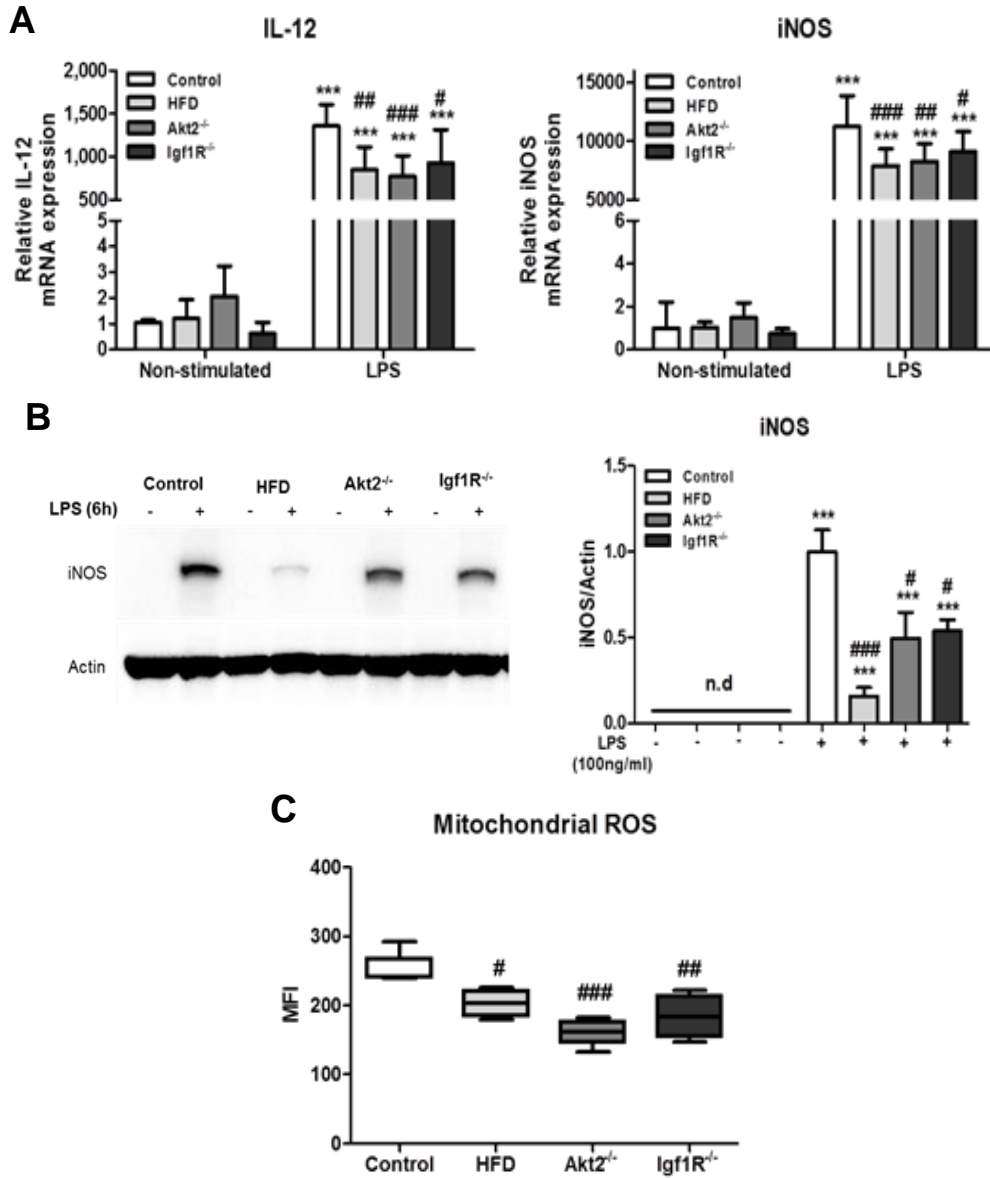


Figure 37: (A) mRNA expression levels of IL-12 and iNOS of WT (control) and insulin resistant macrophages before (NS) and after 6 h stimulation with LPS. (B) Expression levels of iNOS analyzed by western blot in control and insulin resistant macrophages before and after 6 h stimulation with LPS. In (D) ROS production was evaluated by flow cytometry for control and insulin resistant TEPMs 6 h after LPS stimulation. Graphs are representative of 3-6 independent experiments and show mean \pm SD. Box shows 5–95 percentiles, horizontal line represents median, and whiskers represent minimum and maximum. * $p < 0.05$, ** $p < 0.01$, *** $p < 0.001$, LPS-stimulated versus non-stimulated macrophages, # $p < 0.05$, ## $p < 0.01$, ### $p < 0.001$, insulin resistant versus control macrophages. n.d: not detected, MFI: Mean fluorescence intensity of TEPMs.

insulin resistant compared to control macrophages (Figure 36). Besides macrophages derived from the peritoneal cavity, we wanted to check the secretion of pro-inflammatory cytokines from macrophages derived from the alveolar cavity. Alveolar macrophages were treated with LPS *in vitro* and the secretion of TNF α was measured in the supernatant. The results showed again a reduced secretion of TNF α from alveolar macrophages derived from HFD fed mice, Akt2^{-/-} and LysM^{Cre}Igf1R^{fl/fl} mice compared to controls (Figure 36).

We also measured the expression levels of other markers of inflammation, including IL-12 and iNOS. Their mRNA levels were significantly lower in insulin resistant macrophages compared to insulin sensitive control macrophages upon LPS treatment. Western blot analysis also showed that LPS induction of iNOS was not at the same extent in insulin resistant macrophages compared to control macrophages. Finally, we measured mitochondrial ROS that are produced by mitochondria in response to danger signals, like LPS and induce bactericidal activity. Mitochondrial ROS production was also significantly lower in insulin resistant macrophages compared to control macrophages (Figure 37).

The aforementioned findings imply impaired pro-inflammatory responses of insulin resistant macrophages. These findings prompted us to check the expression of anti-inflammatory markers, trying to further characterize the activation status of insulin resistant macrophages. Expression levels of characteristic M2 markers, including Arginase1, Fizz1 and Ym1 were measured and the results showed an up-regulation of these markers in insulin resistant macrophages. Arginase1 and Fizz1 protein levels were also higher in insulin resistant macrophages compared to their controls (Figure 38).

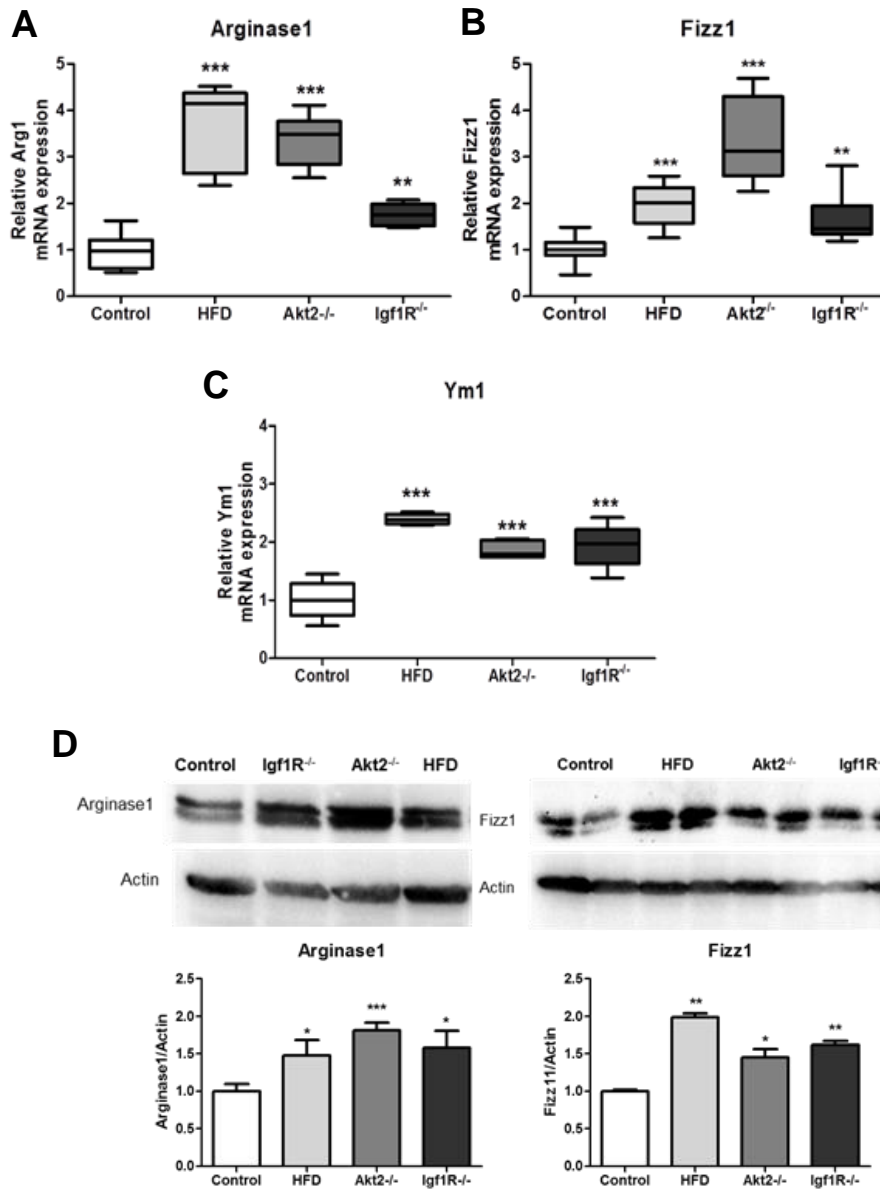


Figure 38: mRNA expression of M2 type macrophage activation arginase 1 (A), Fizz1 (B) and Ym1 (C) in control and insulin resistant macrophages. In (D) Arginase1 and Fizz1 expression was analyzed by western blot in control and insulin resistant macrophages in basal condition. Graphs are representative of 3-6 independent experiments and show mean \pm SD. Box shows 5–95 percentiles, horizontal line represents median, and whiskers represent minimum and maximum. * $p < 0.05$, ** $p < 0.01$, *** $p < 0.001$, insulin resistant versus control macrophages.

Expression levels of Arginase1 were also evaluated in non thioglycollate elicited peritoneal macrophages, alveolar and interstitial lung macrophages. Similarly, the expression of Arginase1 was found to be elevated in macrophages derived from HFD-fed mice, Akt2^{-/-} and LysM^{Cre}Igf1R^{fl/fl} mice compared to control mice (Figure 39). All the aforementioned results indicate that insulin resistant macrophages display an anti-inflammatory, M2-like phenotype (M-InsR).

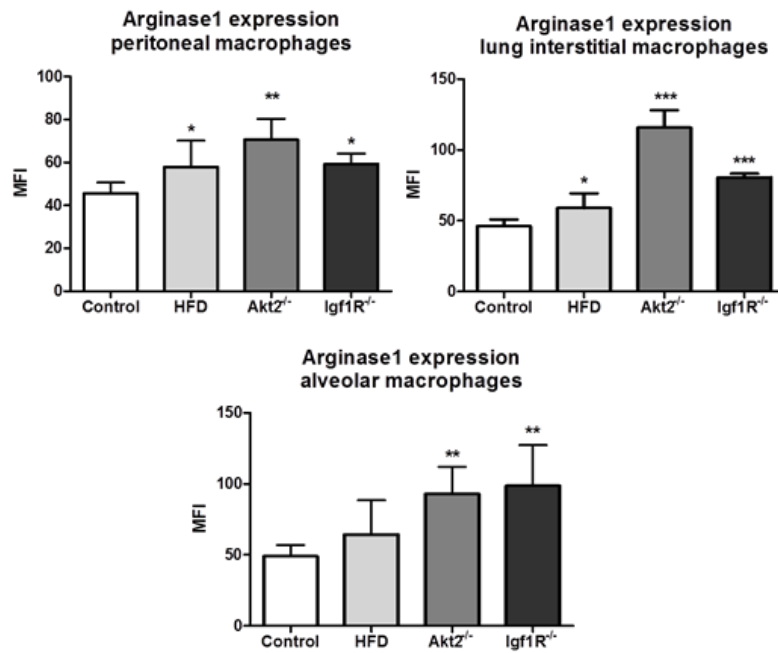


Figure 39: Expression levels of Arginase1 were measured in peritoneal, alveolar and lung interstitial macrophages. Graphs are representative of 3-6 independent experiments and show mean \pm SD. * $p < 0.05$, ** $p < 0.01$, *** $p < 0.001$, insulin resistant versus control macrophages. MFI: Mean fluorescence intensity of F4/80+ for peritoneal and interstitial and CD11c+ cells.

Insulin resistant macrophages exhibit increased glycolysis

To further characterize the transcriptional profile of insulin resistant macrophages we performed RNA-seq analysis. The analysis showed that among the processes mostly affected during insulin resistance was the metabolic process, especially in Akt2 deficient macrophages (Figure 40).

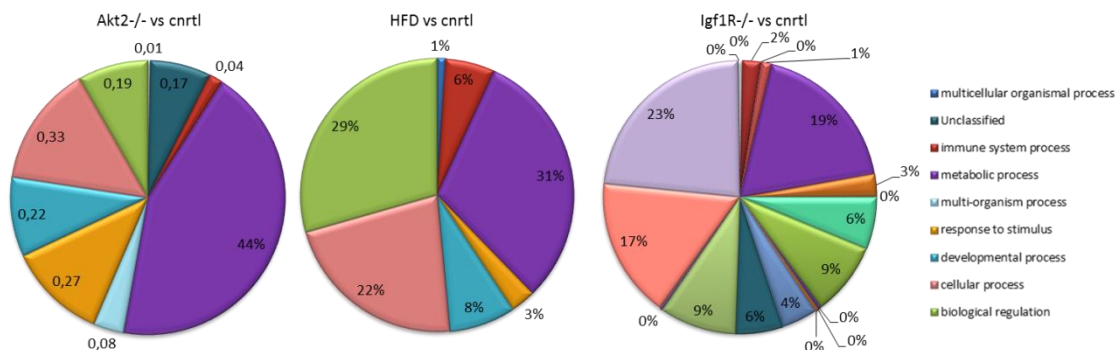


Figure 40: Pie charts from RNA seq analysis showing the processes affected in macrophages from Akt2^{-/-}, HFD, Igf1R^{-/-} versus control macrophages

These findings combined with the fact that the metabolic regulator mTORC1 is activated in insulin resistant macrophages prompted us to further investigate two of the most important energy generating pathways in macrophages, namely glycolysis and OXPHOS.

The pro-inflammatory status of macrophages is characterized by increased rates of glycolysis (Figure 41). However, glycolysis is also important for the anti-inflammatory phenotype of macrophages. We assessed the glycolytic rate of insulin resistant macrophages by measuring extracellular acidification rate and the concentration of lactate the end-product of glycolysis in the culture medium of macrophages. We found that insulin resistant macrophages had increased ECAR at the basal levels compared to insulin sensitive control macrophages. In addition, although insulin stimulation caused only slightly but significant increase in glycolytic rate in control macrophages, this raise was abolished in HFD, Akt2^{-/-} and Igf1R^{-/-} macrophages. The concentration of lactate was also elevated during insulin resistance (Figure 42).

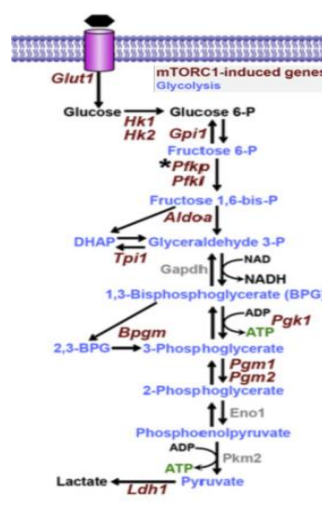


Figure 41: Glycolytic pathway and mTORC1 induced genes.

Activation of mTORC1 drives the expression of glycolytic genes and regulates glucose uptake. Thus, we wanted to check the expression of metabolic enzymes participating in glycolysis. The conversion of glucose to glucose-6-phosphate, the first step of glycolysis, is catalyzed by hexokinase. The mRNA levels of *hexokinase 3* (Hk3) were significantly elevated in insulin resistant macrophages. Similarly, the expression levels of other enzymes that catalyze downstream steps of glycolysis, like *phosphofruktokinase* (Pfkp) and *lactate dehydrogenase* (LDHa), was significantly higher in macrophages derived from HFD-fed, Akt2^{-/-} and Igf1R^{-/-} mice (Figure 43).

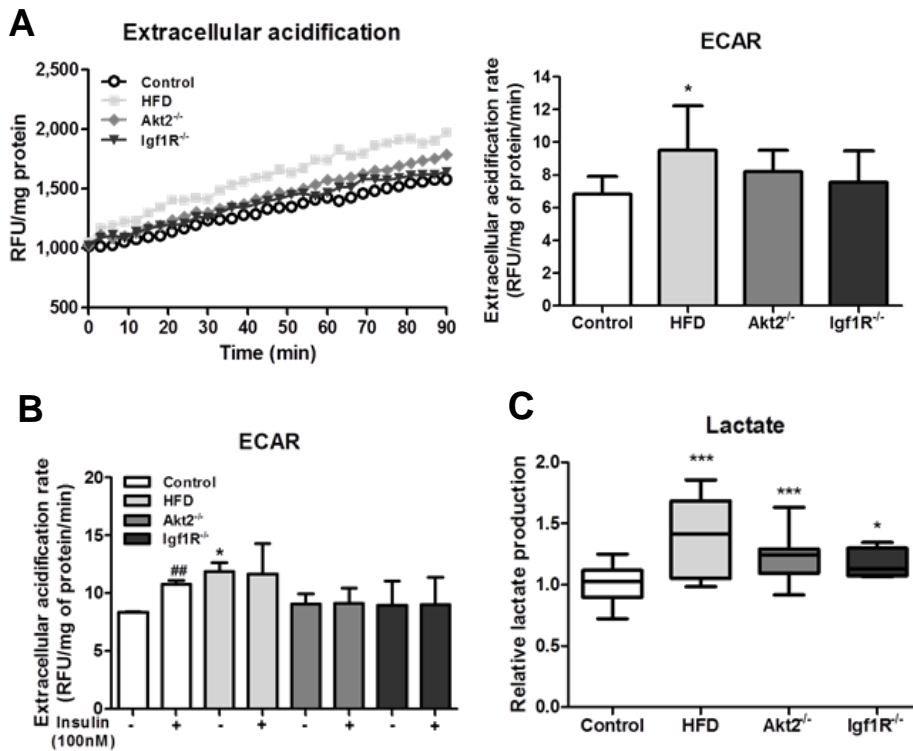


Figure 42: (A) Extracellular acidification of WT (control) and insulin resistant macrophages. (B) ECAR of control and insulin resistant macrophages with or without 100 nM insulin stimulation for 12 h and (C) lactate concentration released in the supernatant of non-stimulated cell cultures. Results are representative of 3-6 independent experiments. Box shows 5–95 percentiles, horizontal line represents median, and whiskers represent minimum and maximum. * $p < 0.05$, ** $p < 0.01$, *** $p < 0.001$, insulin resistant versus control macrophages, ## $p < 0.01$, insulin stimulated versus non-stimulated macrophages.

Then, we wanted to evaluate the glucose uptake ability of insulin resistant macrophages. We checked the mRNA levels of Glut1 and Glut3 that are the main glucose transporters in macrophages (190). We observed an increase in the expression of both transporters, in accordance with elevated basal glucose uptake in insulin resistant macrophages (Figure 44).

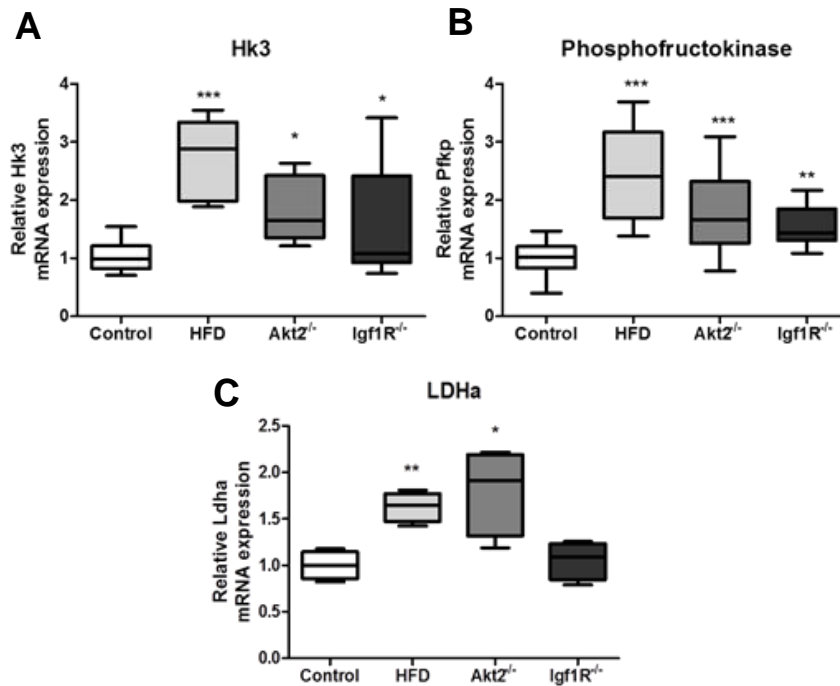


Figure 43: mRNA expression levels of genes involved in glycolysis (A) hexokinase 3, (B) phosphofruktokinase, (C) lactate dehydrogenase. Results are representative of 3-6 independent experiments. Box shows 5–95 percentiles, horizontal line represents median, and whiskers represent minimum and maximum. * $p < 0.05$, ** $p < 0.01$, *** $p < 0.001$, insulin resistant versus control macrophages.

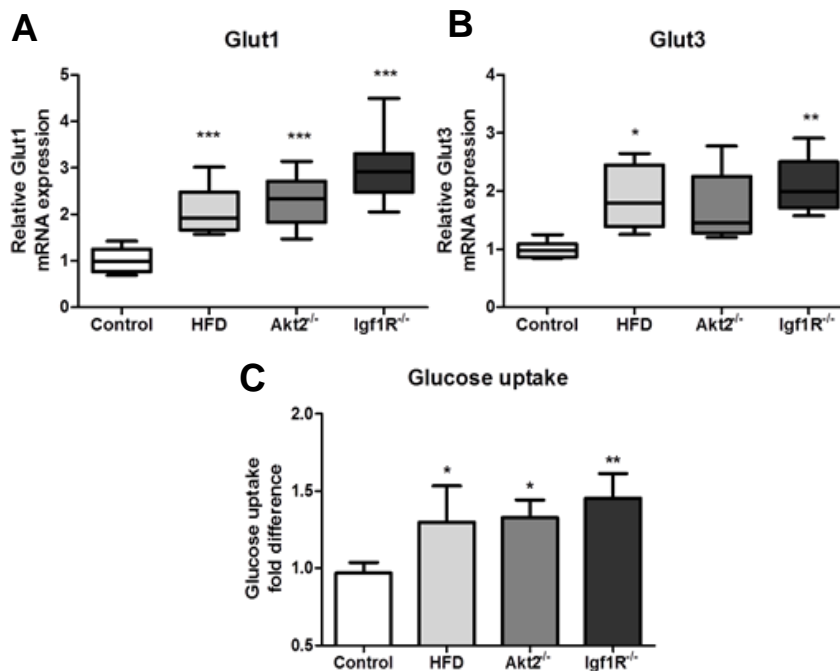


Figure 44: mRNA expression levels of glucose transporters Glut1 (A) and Glut3 (B). (C) Basal levels of glucose uptake in WT (control) and insulin resistant macrophages. Results are representative of 3-6 independent experiments. Box shows 5–95 percentiles, horizontal line represents median, and whiskers represent minimum and maximum. * $p < 0.05$, ** $p < 0.01$, *** $p < 0.001$, insulin resistant versus control macrophages.

We also measured the expression of glycolytic genes after LPS stimulation and we

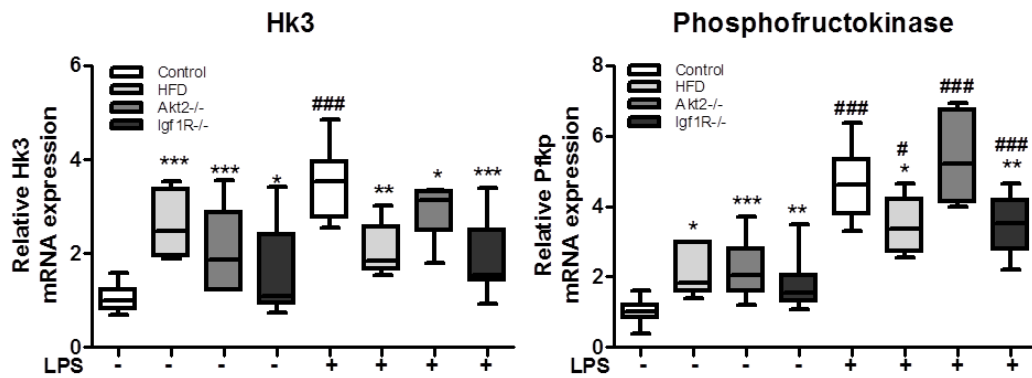


Figure 45: mRNA expression levels of genes involved in glycolysis hexokinase 3 and phosphofruktokinase. Results are representative of 3-6 independent experiments. Box shows 5–95 percentiles, horizontal line represents median, and whiskers represent minimum and maximum. * $p < 0.05$, ** $p < 0.01$, *** $p < 0.001$, insulin resistant versus control macrophages, # $p < 0.05$, ### $p < 0.001$, LPS stimulated versus non-stimulated macrophages.

found that the expression of Hk3 was reduced in all models of insulin resistant macrophages compared to control and Pfkp was also reduced in HFD and Igf1R^{-/-} macrophages compared to control macrophages, that could explain the reduction in

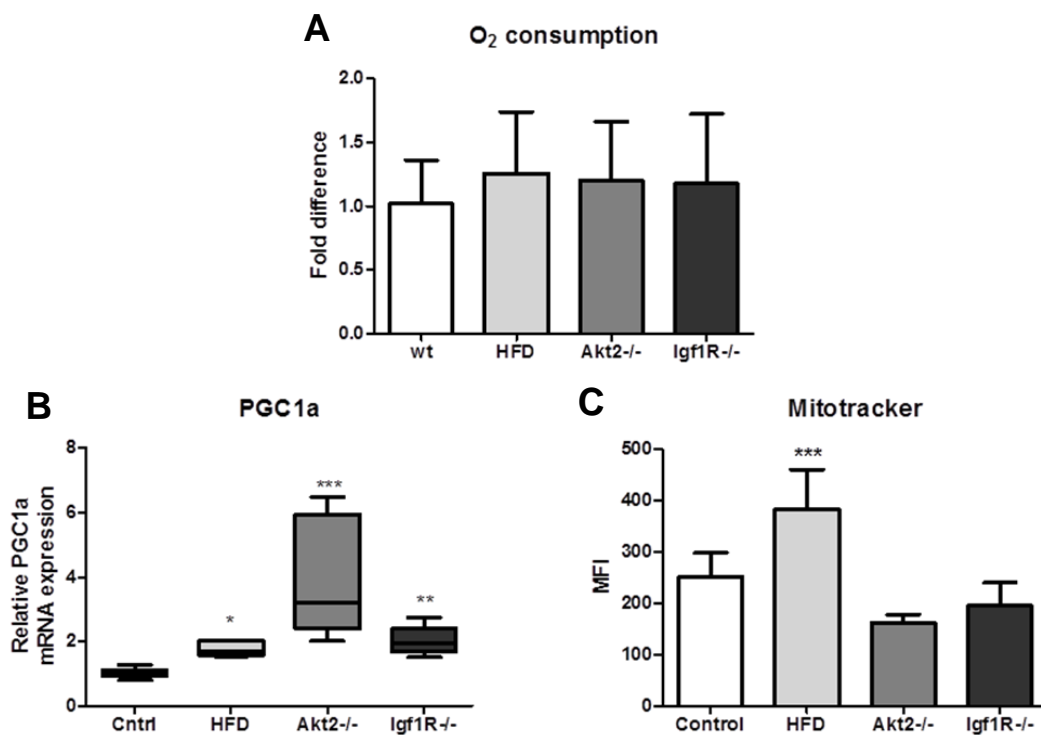


Figure 46: (A) Oxygen consumption difference, mRNA expression levels of PGC1 α (B) and mitochondrial biogenesis levels measured by mitotracker fluorescence (C) in WT (control), HFD, Akt2^{-/-} and Igf1R^{-/-} macrophages. Results are representative of 3-6 independent experiments. Box shows 5–95 percentiles, horizontal line represents median, and whiskers represent minimum and maximum. * $p < 0.05$, ** $p < 0.01$, *** $p < 0.001$, insulin resistant versus control macrophages.

cytokine production after LPS stimulation (Figure 45).

Subsequently we checked the OXPHOS pathway activation, by measuring oxygen consumption rate (OCR). We found that there was no change in OCR between insulin resistant and non-insulin resistant cells. In addition, we measured the expression of PGC1 α and mitotracker levels to evaluate mitochondrial biogenesis. There was a significantly elevated expression of PGC1 α in insulin resistant macrophages. However, this increase is not reflected on mitotracker levels measured by flow cytometry, as we observed an increase only in HFD macrophages (Figure 46).

mTORC1 and glycolysis control M2-like phenotype in insulin resistant macrophages

In order to delineate the role of glycolysis in the activation status of insulin resistant macrophages, we treated insulin resistant TEMPs with 2-deoxy-D-glucose to block glycolysis and we measured the expression of the M2 markers, namely Arginase1 and Fizz1. The results showed that the inhibition of glycolysis abolished the increase observed in the expression of these two markers in insulin resistant macrophages. Inhibition of mTORC1 with rapamycin also suppressed the expression of Arginase1 and Fizz1 in HFD, Akt2^{-/-} and Igf1R^{-/-} macrophages (Figure 47).

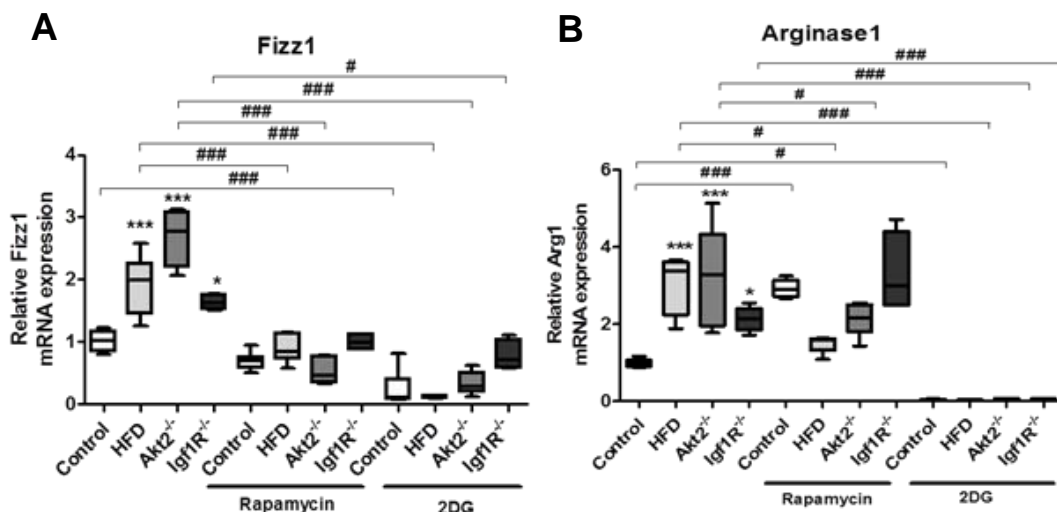


Figure 47: mRNA expression of M2 polarization markers Fizz1 (A) and Arginase1 (B) in naive, following 24 h of 20 nM rapamycin treatment or following 24 h of 2,5 mM 2DG treatment of WT (control) and insulin resistant macrophages. Results are representative of 3-6 independent experiments. Box shows 5–95 percentiles, horizontal line represents median, and whiskers represent minimum and maximum. * $p < 0.05$, ** $p < 0.01$, *** $p < 0.001$, insulin resistant versus control macrophages. # $p < 0.05$, ## $p < 0.01$, ### $p < 0.001$ treated versus non-treated macrophages.

As mentioned earlier mTORC1 regulates glycolysis and the expression of glycolytic enzymes. To determine whether the observed increase in glycolysis in insulin resistant macrophages is mTORC1 dependent we treated TEMP's with rapamycin and we measured the expression of glycolytic genes, including Glut1, Hk3 and LDH. We found that the increase in glycolysis was abolished in insulin resistant macrophages after rapamycin and 2-DG treatment, implying an mTORC1-dependent metabolic reprogramming of insulin resistant macrophages (Figure 48).

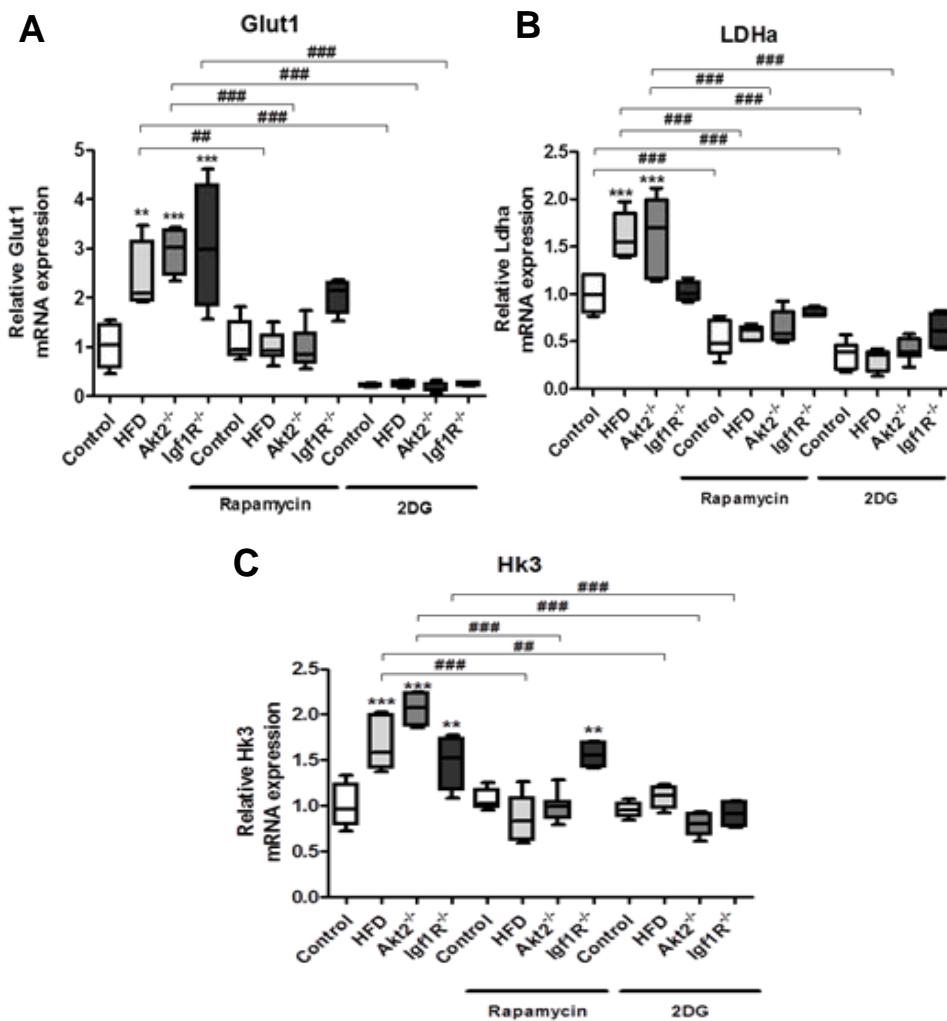


Figure 48: mRNA expression levels of Glut1 (A), LDHa (B) and Hexokinase 3 (C) in naïve, and following treatment for 24 h with 20 nM rapamycin or 2DG of control and insulin resistant macrophages. Results are representative of 3-6 independent experiments. Box shows 5–95 percentiles, horizontal line represents median, and whiskers represent minimum and maximum. * $p < 0.05$, ** $p < 0.01$, *** $p < 0.001$, insulin resistant versus control macrophages. # $p < 0.05$, ## $p < 0.01$, ### $p < 0.001$ treated versus non-treated macrophages.

Since loss of Akt1 leads to impaired mTORC1 activation we acquired the levels of glycolysis in Akt1 deficient macrophages. In line with the aforementioned results, Akt1^{-/-} macrophages exhibited reduced glycolysis as evaluated by ECAR, LDH expression and glucose uptake (Figure 49).

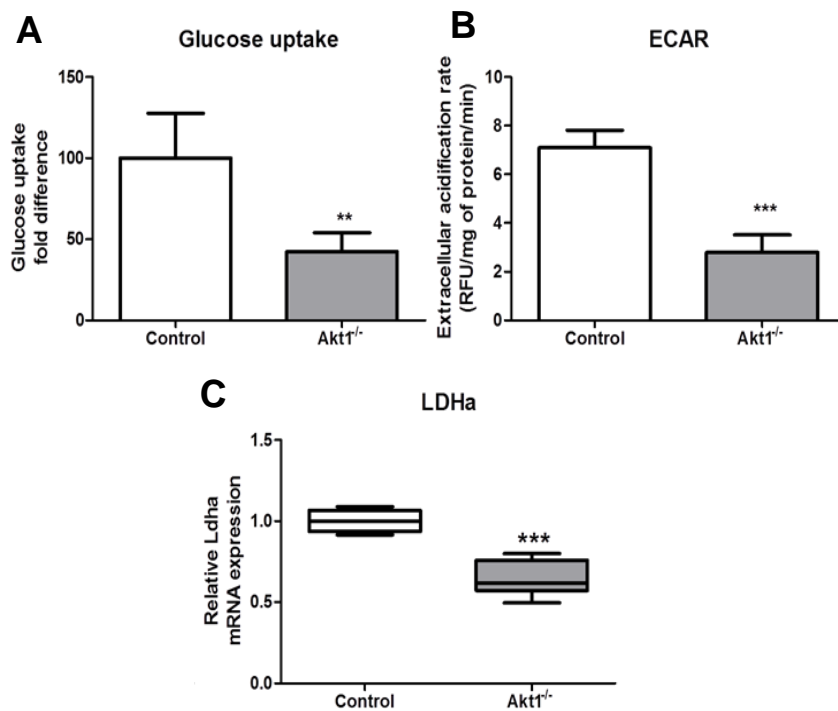


Figure 49: (A) Fold difference of glucose uptake in WT (control) and Akt1^{-/-} macrophages at the basal levels. (B) Extracellular acidification rate of control and Akt1^{-/-} macrophages. (C) mRNA expression levels of LDHa in control and Akt1^{-/-} macrophages. Results are representative of 3-6 independent experiments. Box shows 5-95 percentiles, horizontal line represents median, and whiskers represent minimum and maximum. **p < 0.01, ***p < 0.001, Akt1^{-/-} versus control macrophages.

Obesity and insulin resistance in macrophages is associated with reduced lung injury in polymicrobial sepsis

A common cause of morbidity and mortality in sepsis is injury and dysfunction of multiple organs. Among these, the lungs are the most susceptible tissue to sepsis-induced organ failure. Although obesity is associated with inflammation and increased risk of infection, obese patients with sepsis in the intensive care unit (ICU) do not

have worse outcome or even show increased survival from sepsis (191, 192). Macrophages are central mediators of sepsis and lung injury. To determine the role of insulin resistant macrophages in the development of sepsis-induced systemic

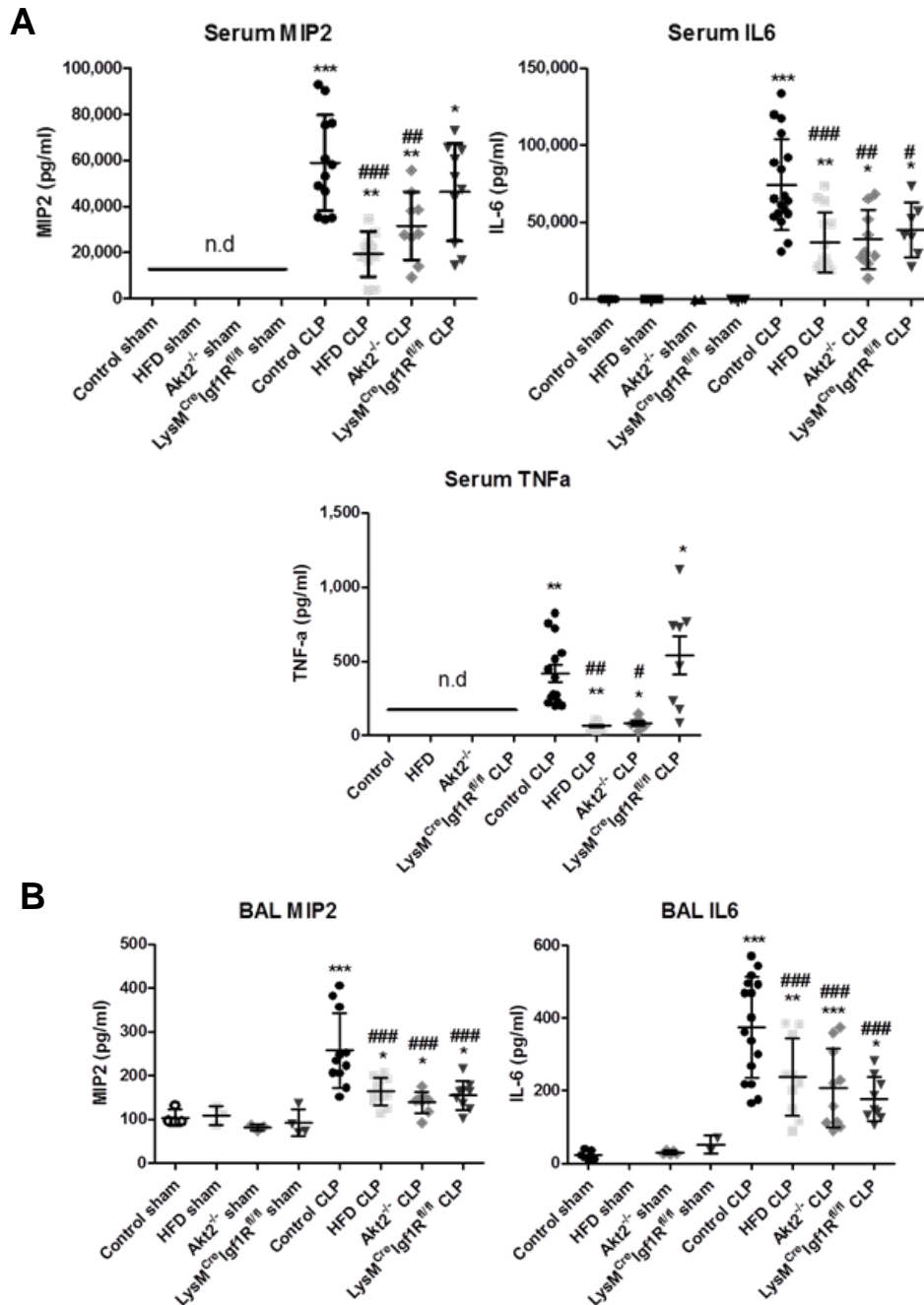


Figure 50: (A) Levels of the pro-inflammatory factors MIP-2 α , IL-6, and TNF α in the serum of control, HFD-induced obese, Akt2^{-/-} and LysM^{Cre}Igf1R^{fl/fl} mice (all bearing insulin resistant macrophages) after 6 h of CLP or sham operation. (B) Levels of MIP-2 α and IL-6 in the bronchoalveolar lavage of control and mice bearing insulin resistant macrophages after 6h of CLP or sham operation. Graphs represent mean \pm SD. * $p < 0.05$, ** $p < 0.01$, *** $p < 0.001$, sham versus CLP operated mice, # $p < 0.05$, ## $p < 0.01$, ### $p < 0.001$, control mice versus mice bearing insulin resistant macrophages after CLP operation. n.d: not detected

inflammation and lung injury, we used an in vivo model of polymicrobial sepsis and lung injury induced by Cecal Ligation and Puncture (CLP). CLP operation was performed in obese mice, Akt2^{-/-} mice and LysM^{Cre}Igf1R^{fl/fl} mice and control mice

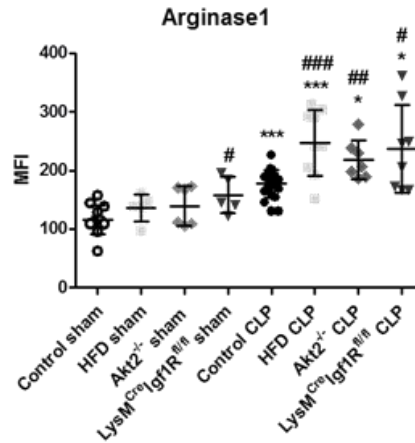


Figure 51: Arginase1 protein levels in alveolar macrophages isolated from control, HFD, Akt2^{-/-} and LysM^{Cre}Igf1R^{fl/fl} mice were assessed by flow cytometry 6 h after CLP or sham operation (n = 5-10 mice/group). Graphs represent mean ± SD. **p* < 0.05, ***p* < 0.01, ****p* < 0.001, sham versus CLP operated mice, #*p* < 0.05, ##*p* < 0.01, ###*p* < 0.001, control mice versus mice bearing insulin resistant macrophages after CLP operation. MFI: Mean fluorescence intensity of CD11c+ cells.

and after 6 hours we evaluated the systemic inflammatory response as well as the pulmonary inflammatory response and injury.

Levels of pro-inflammatory cytokines MIP-2, IL-6 and TNF α were measured in the serum and in the bronchoalveolar lavage (BAL) fluid of CLP and sham operated mice

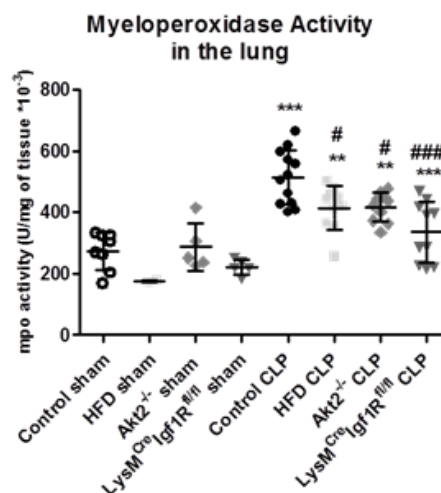


Figure 52: Myeloperoxidase activity measurement in lung lysates as an indication of tissue injury in sham and CLP operated mice. Graphs represent mean ± SD. **p* < 0.05, ***p* < 0.01, ****p* < 0.001, sham versus CLP operated mice, #*p* < 0.05, ##*p* < 0.01, ###*p* < 0.001, control mice versus mice bearing insulin resistant macrophages after CLP operation.

and the results showed that the secretion of pro-inflammatory cytokines was significantly lower in mice bearing insulin resistant macrophages compared to control mice (Figure 50). However, reduction in MIP-2 and TNF α was not significant in LysM^{Cre}Igf1R^{fl/fl} mice.

We also measured the expression of Arginase1 in alveolar macrophages and we found that Arginase1 was induced after CLP and this increase was even higher in alveolar macrophages from mice bearing insulin resistant macrophages (Figure 51).

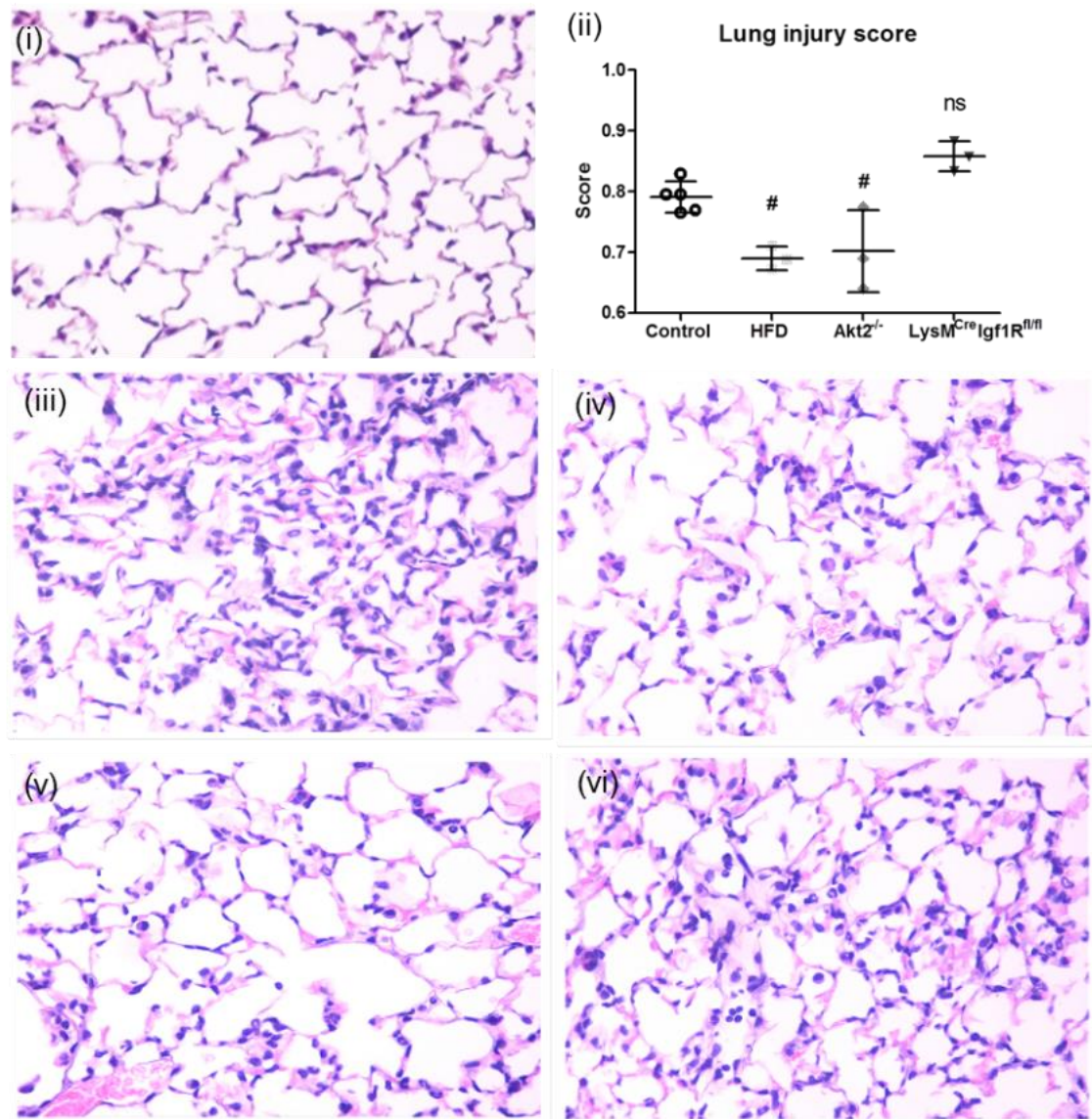


Figure 53: Histological analysis of lung tissue sections of control (iii), HFD (iv), Akt2^{-/-}(v), LysMCreIgf1Rfl/fl (vi) mice after CLP operation (H&E stain). Lung injury score (ii) compared to sham operated mice (i). Graphs represent mean \pm SD. #p < 0.05, control mice versus mice bearing insulin resistant macrophages after CLP operation.

Subsequently, we evaluated the sepsis-induced lung injury by measuring MPO activity and histological examination. MPO activity was significantly reduced in mice bearing insulin resistant macrophages compared to control mice after CLP operation (Figure 52).

Histological examination of the lungs from CLP operated mice also showed a significant decrease in the lung injury of obese mice and Akt2^{-/-} mice. However, there was no difference in the injury score between LysM^{Cre}Igf1R^{fl/fl} and control mice, indicating probably the contribution of other cells in the amelioration observed in the other mouse models (Figure 53).

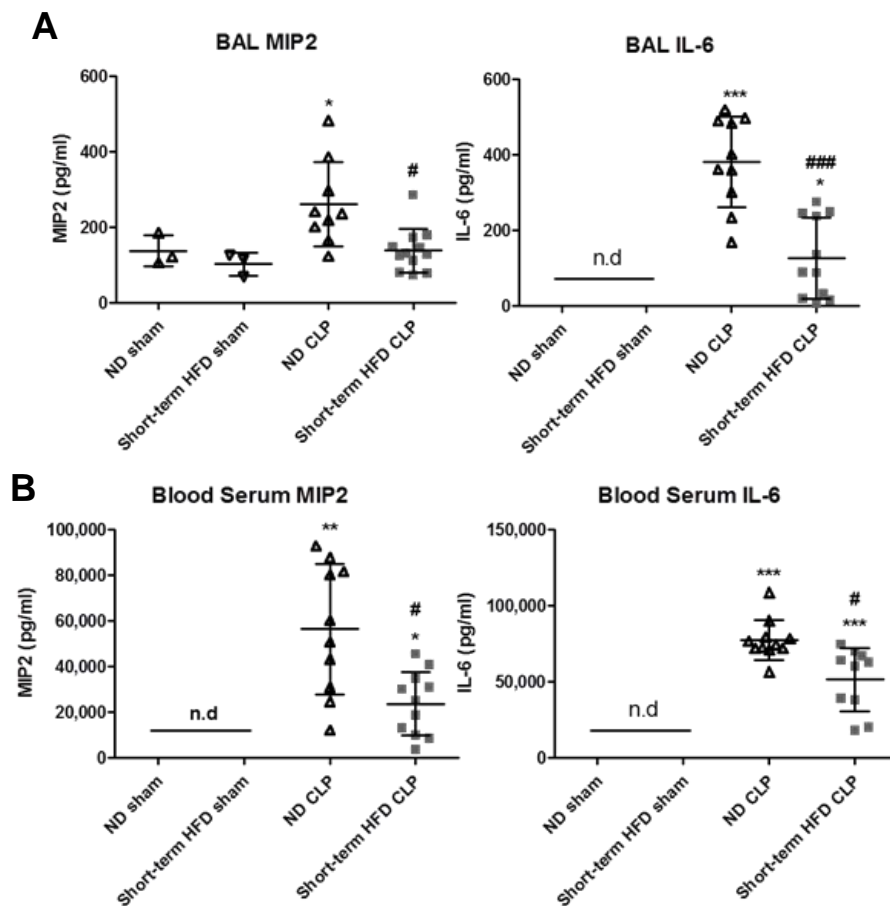


Figure 54: MIP2a and IL-6 cytokine levels in BAL (A) and serum (B) of sham and CLP operated mice (n = 5-10mice/group). Results are representative of 3-6 independent experiments. Graphs represent mean \pm SD. * $p < 0.05$, ** $p < 0.01$, *** $p < 0.001$, sham versus CLP operated mice, # $p < 0.05$, ### $p < 0.001$ short-term HFD fed mice versus ND fed mice after CLP operation, n.d: not detected.

In order to discriminate whether obesity or insulin resistance have different effect on sepsis-induced inflammation we induced polymicrobial sepsis in diet induced insulin resistant mice. The results acquired were similar to those found for diet-induced obese mice. The levels of MIP-2 and IL-6 in BAL and serum were reduced in short-term HFD fed mice compared to ND controls (Figure 54).

Histological evaluation also showed reduced lung injury in insulin resistant compared to control mice (Figure 55). These results imply that the reduced inflammation and lung injury was due to insulin resistance, instead of obesity.

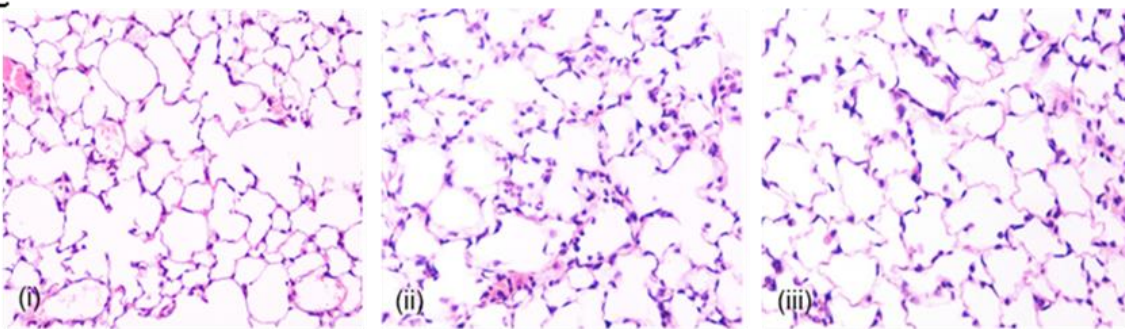


Figure 55: Histological analysis of lung tissue sections (H&E stain) of sham (i) and CLP (ii), (iii) operated mice. ND fed mice subjected to CLP procedure (ii) displayed several foci of interstitial and intra-alveolar neutrophilic infiltrations, capillary congestion and proteinaceous debris in the alveoli, while short term HFD fed mice subjected to CLP procedure (iii) displayed only occasional interstitial and intra-alveolar neutrophilic infiltrates, mild septal thickening and sparse intra-alveolar proteinaceous debris.

Further, we wanted to examine if this decrease in systemic and pulmonary inflammation leads in increased survival. We found that the survival was not improved in mice bearing insulin resistant macrophages (Figure 56).

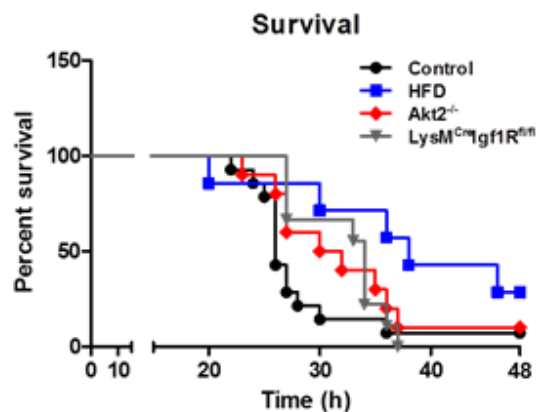


Figure 56: Survival curve of control, HFD-induced obese, Akt2^{-/-} and LysM^{Cre}Igf1R^{fl/fl} mice (all bearing insulin resistant macrophages) subjected to CLP operation (n = 5-10 mice/group).

In order to explain this increased mortality despite the reduced inflammation we measured the bacterial clearance in mice after CLP operation. We found that the

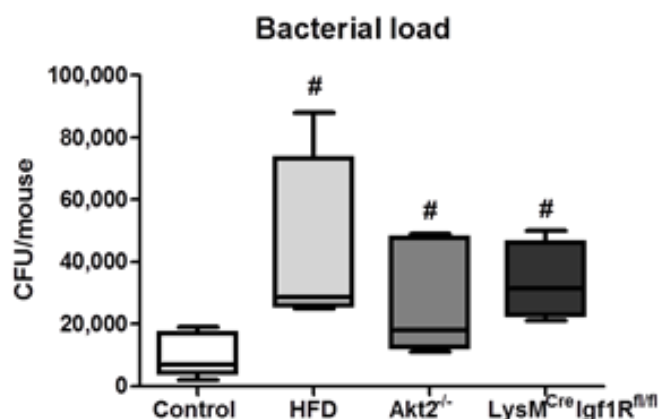


Figure 57: Bacterial load in the peritoneal lavage of all groups of mice subjected to CLP operation for 6 h (n = 5-10 mice/group). Graphs represent mean \pm SD. # $p < 0.05$, control mice versus mice bearing insulin resistant macrophages after CLP operation.

bacterial load in the peritoneal lavage of mice bearing insulin resistant macrophages was increased compared to the control mice (Figure 57).

Then, we checked the phagocytic capacity as it could be the cause of the reduced bacterial clearance observed in insulin resistance, but we found that phagocytosis was not impaired in insulin resistant macrophages, except from the case of Akt2^{-/-} macrophages (Figure 58). This implies that bacterial clearance is not affected at the

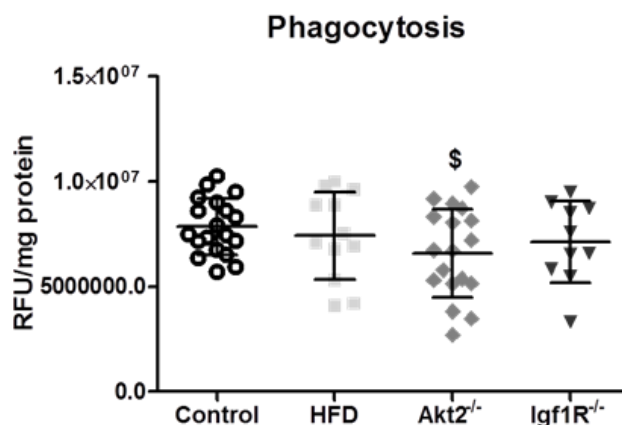


Figure 58: Phagocytic capacity of control and insulin resistant macrophages. Results are representative of 3-6 independent experiments. Graphs represent mean \pm SD. \$ $p < 0.05$, insulin resistant versus control macrophages.

level of phagocytosis but downstream in this process, like phagolysosomal fusion that is known to be controlled by mTOR (193) and could be defective during insulin resistance.

Insulin resistant macrophages shape gut microbiome

We finally wanted to see how insulin resistant macrophages affect sustained responses such as those regulating the gut microbiome. Diet and the immune system shape the intestinal microflora. In order to see the contribution of insulin resistant macrophages in the formation of gut microbiota, we isolated and identified the species that constitute the gut microbiome in obese, *Akt2*^{-/-} and *LysM*^{Cre}*Igf1R*^{fl/fl} mice. We found significant changes in all mouse strains. Specifically, we found a significant increase in the concentration of the phyla *Firmicutes* and a proportional decrease in *Bacteroidetes* in all mice bearing insulin resistant macrophages, even in *LysM*^{Cre}*Igf1R*^{fl/fl} mice implying that insulin resistant macrophages can select and shape microbial composition of the gut irrespective of the diet (Figure 59).

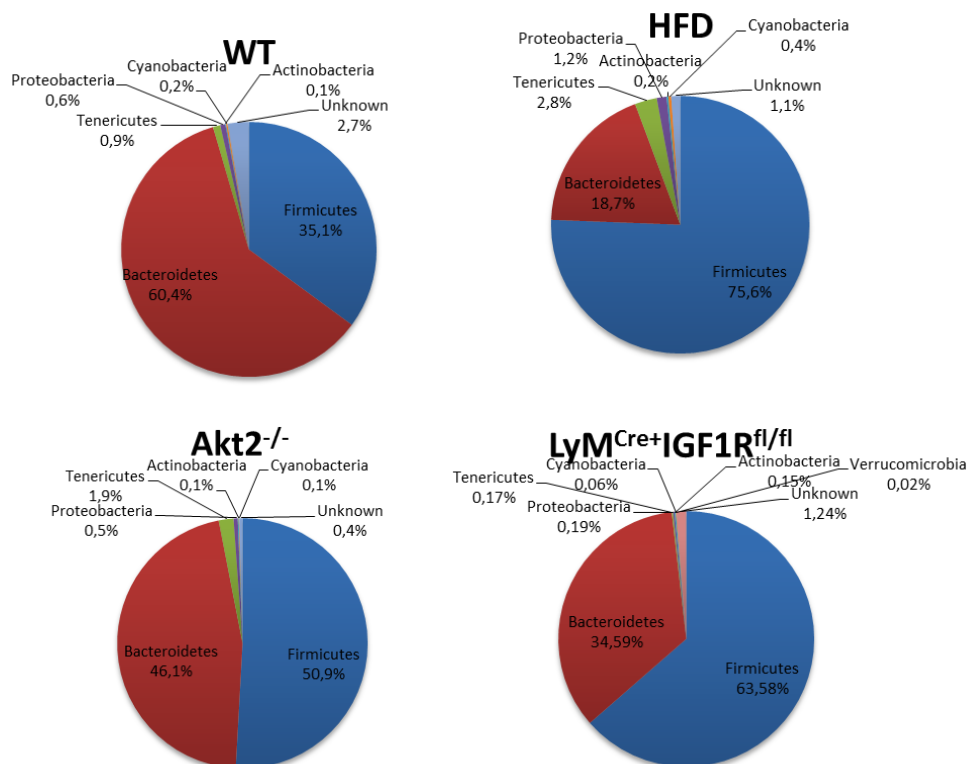


Figure 59: Taxonomic analysis of the gut microbiota from control (WT), *Akt2*^{-/-}, *LysM*^{Cre}*Igf1R*^{fl/fl} and HFD fed obese mice. Pie charts represent the relative abundance of bacterial phyla.

Intestine contains the major pool of resident macrophages. Intestinal macrophages are necessary to maintain gut homeostasis, by remaining tolerant to the commensal bacteria while being responsive against potential pathogenic stimuli. We isolated intestinal macrophages and measured the expression of Arginase1 and we found that

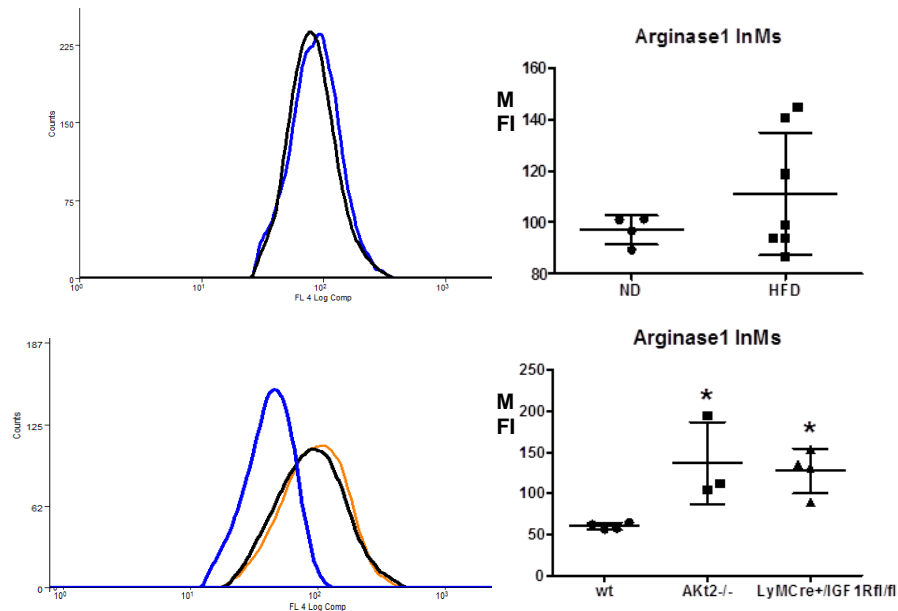


Figure 60: Arginase1 protein levels in intestinal macrophages (InMs) isolated from control (wt/ND), HFD, Akt2^{-/-} and LysM^{Cre}Igf1R^{fl/fl} mice were assessed by flow cytometry. Graphs represent mean \pm SD. * $p < 0.05$, control mice versus mice bearing insulin resistant macrophages. MFI: Mean fluorescence intensity of F4/80⁺ cells.

it is increased in macrophages derived from all obese, Akt2^{-/-} and LysM^{Cre}Igf1R^{fl/fl} mice (Figure 60).

Lack of adiponectin results in a pro-inflammatory macrophage phenotype and abolishes the effect of high fat diet on inflammatory responses.

Adiponectin is released from the lean adipose tissue and is associated with anti-inflammatory macrophage phenotype (194, 195). However, it also induces TNF α and IL-6 and promotes tolerance that could be responsible for its anti-inflammatory effects (196). During obesity adiponectin levels are decreased resulting in an inflamed adipose tissue. Mice that lack adiponectin show accentuated diet induced obesity (197) and are known to exhibit insulin resistance (198). We wanted to investigate the effect of the absence of adiponectin on the macrophage polarization and how high fat diet affects this activation. For this purpose we isolated bone marrow derived macrophages (BMDMs) from mice that lack adiponectin and we measured iNOS and Arginase 1 at the basal levels using flow cytometry. We found that the expression of

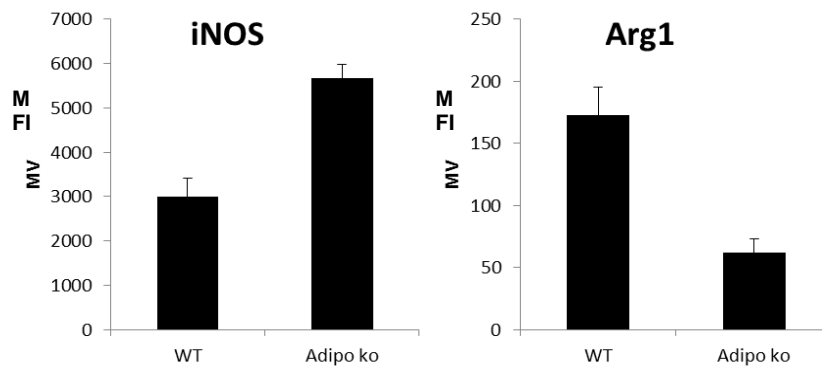


Figure 61: Arginase1 and iNOS protein levels in peritoneal macrophages isolated from control (wt) and Adipoq^{-/-} mice were assessed by flow cytometry. Graphs represent mean ± SD. MFI: Mean fluorescence intensity of F4/80+ cells.

iNOS was elevated, while the expression of Arginase 1 was down regulated as expected (Figure 61)

Then we isolated BMDMs from control and adiponectin knockout mice fed a normal diet and a high fat diet for short term and treated them with LPS. Subsequently, we measured the expression of TNFα and IL-6 and we found that although the expression of both cytokines was reduced after LPS treatment in control (wt) mice after high fat diet feeding this decrease was abolished in macrophages derived from Adipoq^{-/-} mice (Figure 62). Further experiments will delineate the role of adiponectin in macrophage polarization during obesity.

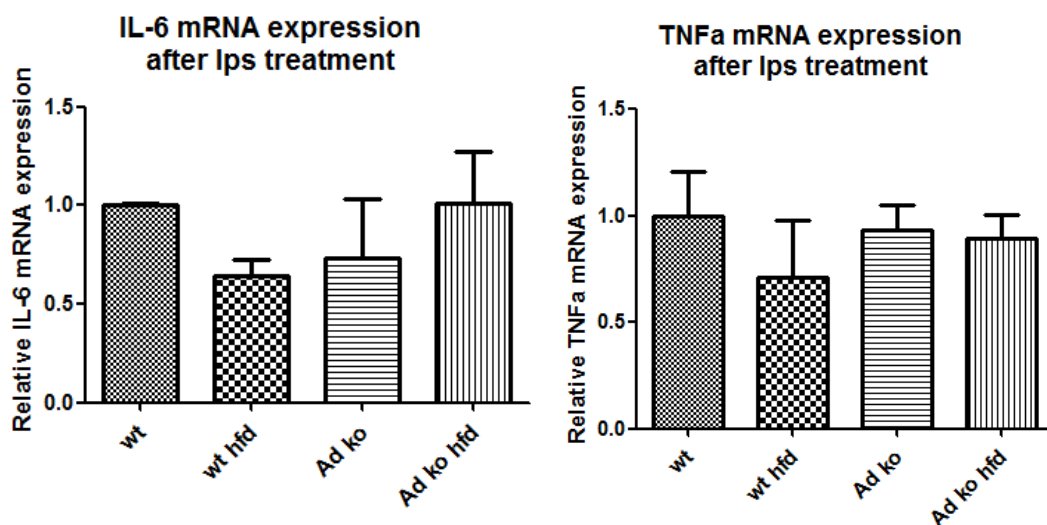


Figure 62: mRNA expression levels of IL-6 and TNFα in BMDMs isolated from control (wt) and Adipoq^{-/-} mice fed normal or high fat diet. Graphs represent mean ± SD.

Discussion

Obesity and the associated metabolic syndrome have been linked to chronic inflammation in various tissues and an increased susceptibility to infection. The innate immune system has an essential role in the development of obesity and obesity-related pathologies. In the present thesis, the effect of insulin resistance on innate immune system has been investigated. Macrophages important mediators of inflammation obtained an M-InsR phenotype characterized by a unique metabolic and activation status. In addition, the role of M-InsR polarized macrophages *in vivo* in a model of polymicrobial sepsis has been investigated.

In the present study we demonstrated that macrophages have a functional insulin signaling pathway that can be disrupted when they are chronically exposed to high insulin levels both *in vivo* and *in vitro*. Impaired insulin signaling was also observed in the absence of Akt2 kinase or IGF1R. Insulin resistance in macrophages resulted in increased glycolytic metabolism and an M2-like activation phenotype (termed M-InsR). M-InsR phenotype was associated with reduced responsiveness to LPS *in vitro*, as well as reduced inflammatory response to polymicrobial sepsis *in vivo*. Insulin resistant macrophages display increased mTORC1 activity that leads to enhanced glycolytic metabolism and expression of M2 polarization markers.

Among the Akt isoforms, Akt2 is the predominant isoform that primarily mediates insulin signaling (186, 199). Previous work of our group has shown that deletion of Akt2 results an anti-inflammatory phenotype mediated by increased C/EBP β (13) expression and subsequent transcription of M2-type target genes (200-202). Furthermore, mTOR is an important regulator of C/EBP β at the post-transcriptional level, providing a potential mechanism through which the insulin/Akt/mTORC1 pathway up-regulates the expression of M2 markers.

We used three models to study the effect of insulin resistance in macrophages. Mice fed high fat diet for short term developed insulin resistance and glucose intolerance and their macrophages displayed impaired insulin signaling, though this defect is dependent on the environmental stimuli. Akt2 deficient mice spontaneously develop a diabetes-like syndrome and insulin resistance (187). Macrophages derived from these mice also acquire this metabolic defect. Akt2 is activated downstream of IGF1R that

can also mediate insulin signaling. Macrophages from LysMCreIgf1R^{fl/fl} mice also acquire insulin resistance. Thus, macrophages that lack Akt2 and Igf1R provide important cell-autonomous models for the study of insulin resistance independent of diet.

All three insulin resistance models, HFD, Akt2^{-/-} and Igf1R^{-/-} macrophages showed a significant change in the expression of genes that take part in the metabolic process. Accordingly, increased basal glycolysis was observed in insulin resistant macrophages. However, no subsequent induction in glycolytic process upon insulin stimulation was observed. The increase in glycolytic metabolism at the basal levels can be partly explained by the increased basal expression of glucose transporters Glut1 and Glut3 and the elevated glucose uptake. The expression of Hexokinase 3, Phosphofructokinase and Lactate Dehydrogenase important enzymes of the glycolytic process was also up-regulated at the basal levels. Glycolysis is essential for optimal IL-4 induced M2-type polarization of macrophages (203). IL-4 activates PI3K/Akt and mTORC2 pathway to promote IRF4-dependent metabolic reprogramming to support M2 activation (203) but the Akt isoform responsible for this altered metabolism was not described. Accordingly, M2 polarization upon parasitic helminth infection, also dependent on IL-4, required mTORC2 activation (204). Our results indicated no change in oxygen consumption and mitochondrial biogenesis in insulin resistant macrophages, thus oxidative metabolism was not affected. In addition, glycolytic metabolism is reduced in insulin resistant macrophages upon LPS stimulation that could explain the reduced cytokine production. However, further investigation concerning oxidative metabolism and other metabolic pathways needs to be done.

We observed that insulin resistant macrophages displayed increased basal mTORC1 activity and reduced activation of Akt2 isoform in response to insulin stimulation. IL-4 promotes the activation of Akt/mTORC1 pathway and subsequent Acly-mediated increased production of Acetyl-CoA metabolite that leads to histone acetylation and induction of a subset of M2 markers (205). Inhibition of Akt activity by pan-Akt inhibitor resulted in decreased expression of *Arg1*, *Retnla*, and *Mgl2* (205), which were also found to be up-regulated in insulin resistant state. Our study could provide evidence of an Akt isoform-dependent expression of these M2 markers. Akt2 deletion was not implicated in Akt1 activation, but on the contrary increased activation of this

isoform at the basal levels was observed. These results suggest that Akt1 isoform positively regulates M2 polarization genes while Akt2 opposes this effect. In agreement with this hypothesis, previous work of our group found that deletion of Akt1 promotes M1 polarization (206).

In the present study, we found that insulin resistant macrophages acquire increased mTORC1 activation that is important for their activation towards an M2-like phenotype. Inhibition of mTORC1 activity by rapamycin reversed the up-regulation of Arginase1 and Fizz1 observed in insulin resistant macrophages. In addition, the increase in glycolytic gene expression was also dependent on mTORC1 activation. Thus, mTORC1 is also an important mediator of the unique phenotype of insulin resistant macrophages, downstream of Akt.

Insulin resistance apart from obesity and obesity-related complications is also associated with several pathologic conditions. Cancer, a condition that harbors M2-like macrophages, namely TAMs (Tumor Associated Macrophages) to support tumor growth is also associated with insulin resistance (207). Critically ill patients in the Intensive Care Unit often develop hyperglycemia and hyperinsulinemia, indicating insulin resistance. The effect of insulin resistance on the phenotype of peripheral macrophages in response to acute inflammatory responses is poorly investigated. Obesity is associated with increased risk of bacterial infection accompanied with reduced inflammatory responses (208), but also it promotes tumorigenesis through TAMs induction (209), conditions both harboring M2-like macrophages (210).

Paradoxically, many clinical studies and meta-analyses have shown that obese patients demonstrate lower short-term mortality in sepsis compared to patients with normal body mass indices (191, 192). Examining the “obesity paradox” and understanding the mechanism through which obesity improves survival in sepsis would inform prognostic and therapeutic strategies. Obesity is associated with increased risk of developing insulin resistance, a condition characterized by low grade systemic inflammation (211). On the other hand, septic patients develop insulin resistance, probably due to various stimuli that can induce pro-inflammatory pathways and suppress insulin signaling. Insulin treatment in the ICU is recommended in septic patients in order to maintain glucose levels into a normal range (212) and to reduce infections (213).

In our study, insulin resistance in macrophages results in reduced systemic and pulmonary inflammatory responses but at the same time it reduces bactericidal capacity of macrophages resulting in increased bacterial load in the context of polymicrobial sepsis. These results could partially explain the effect of obesity and insulin resistance in sepsis. The outcome for obese septic patients is better since they exhibit reduced inflammation in response to sepsis but also they are protected from bacteria, controlled by the provided antibiotics.

In the gut an increase in *Firmicutes* that are more potent to harvest energy was observed in all mice bearing insulin resistant macrophages, even in $LysM^{Cre}Igf1R^{fl/fl}$. Intestinal metabolites are very important in maintaining insulin sensitivity, for example butyrate is decreased in obesity and oral supplementation with this metabolite protects against obesity and associated insulin resistance (45).

Overall, this study describes a kind of innate immune memory in peripheral macrophages characterized by a novel M2-like phenotype, which is under the control of Akt1/mTORC1 signals and glycolytic metabolism (Figure 62). This phenotype may explain changes in macrophage responses and development of related pathologic conditions that occur in obesity and type 2 diabetes.

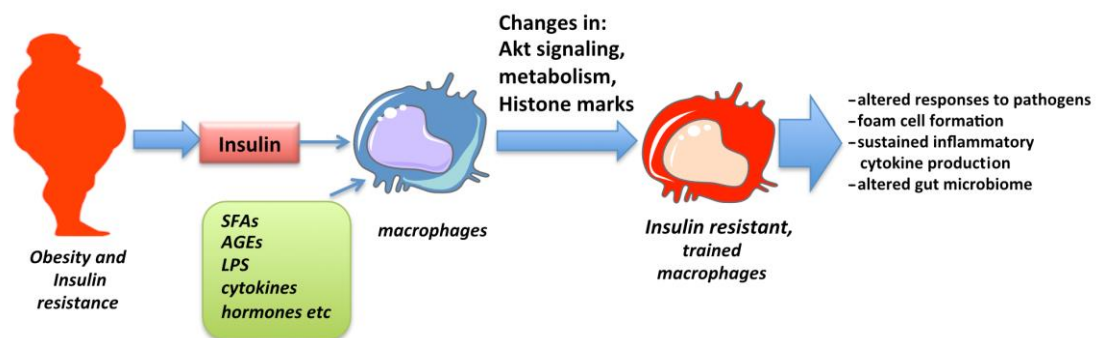


Figure 62: Obesity and insulin resistance promote the development of innate immune memory in macrophages. Chronic exposure of macrophages to high insulin levels, Saturated Fatty Acids (SFAs), adipokines, inflammatory cytokines and low levels of endotoxin, all associated with obesity, results in changes in Akt signaling, cell metabolism and histone marks that eventually lead to epigenetic modifications in inflammatory genes affecting macrophage responses that are described as innate immune memory. (Adapted from Ieronymaki, Daskalaki et al. 2019)

Future directions

A number of recent studies have provided evidence that myeloid cells of the macrophage lineage can undergo training following exposure to PAMPs and that this can confer a type of immunological memory on these cells (214, 215) (216). In addition, western diet reprograms and confers memory in myeloid cells through NLRP3 (217). Hyperglycemia and oxLDL during obesity trigger macrophage training that result in histone modifications and expression of genes related to inflammatory responses. Macrophage metabolism is also important for training of macrophages. Many training factors redirect metabolism towards glycolysis that is essential for the formation of epigenetic marks on specific genes.

In the present study insulin resistance in macrophages activates Akt1/mTORC1 pathway and results in increased glycolytic capacity. Probably this activation could lead to epigenetic changes that result in the activation and inactivation of specific genes that result to the M-InsR macrophage phenotype. Further study on insulin resistant macrophages could reveal changes on histone marks on the promoters of macrophage polarization genes. In addition, we could investigate the role of Akt dependent histone demethylases PHF2 and PHF8, which are also implicated in macrophage polarization as well as Jmjd3 (218).

Insulin could create memory in macrophages that could be Akt isoform-dependent. Inhibition of mTORC1 through rapamycin abolished the M2-like skewing of macrophages probably interfering with epigenetic gene regulation. Having in mind the importance of the innate immune system in the development obesity and T2D, targeting macrophages could potentially improve insulin resistance and related pathologies. Oral supplementation with butyrate decreases training of peripheral macrophages by oxLDL in obese humans with metabolic syndrome (46). Butyrate can also promote epigenetic modifications that down-regulate glycolysis and mTORC1 activation and lead to an antimicrobial phenotype (219). Oral supplementation with butyrate or macrophage specific blockage of immune memory could be used in mouse models of obesity to check the development of insulin resistance and metabolic inflammation. Therapeutic interventions could employ immunomodulatory agents to block this kind of memory and reverse insulin resistance and M2-like activation status in macrophages.

References

1. (WHO) WHO. 2000. Technical report series 894: Obesity: Preventing and managing the global epidemic.. . *Geneva: World Health Organization* ISBN 92-4-120894-5.
2. de Koning L, Merchant AT, Pogue J, Anand SS. 2007. Waist circumference and waist-to-hip ratio as predictors of cardiovascular events: meta-regression analysis of prospective studies. *Eur Heart J* 28: 850-6
3. Cao Q, Yu S, Xiong W, Li Y, Li H, Li J, Li F. 2018. Waist-hip ratio as a predictor of myocardial infarction risk: A systematic review and meta-analysis. *Medicine (Baltimore)* 97: e11639
4. Megnien JL, Denarie N, Cocaul M, Simon A, Levenson J. 1999. Predictive value of waist-to-hip ratio on cardiovascular risk events. *Int J Obes Relat Metab Disord* 23: 90-7
5. Catrysse L, van Loo G. 2017. Inflammation and the Metabolic Syndrome: The Tissue-Specific Functions of NF- κ B. *Trends in Cell Biology* 27: 417-29
6. Abdelaal M, le Roux CW, Docherty NG. 2017. Morbidity and mortality associated with obesity. *Annals of translational medicine* 5: 161-
7. Calay ES, Hotamisligil GS. 2013. Turning off the inflammatory, but not the metabolic, flames. *Nature Medicine* 19: 265
8. Clària J, González-Pérez A, López-Vicario C, Rius B, Titos E. 2011. New Insights into the Role of Macrophages in Adipose Tissue Inflammation and Fatty Liver Disease: Modulation by Endogenous Omega-3 Fatty Acid-Derived Lipid Mediators. *Frontiers in Immunology* 2
9. Murray PJ. 2017. Macrophage Polarization. *Annual Review of Physiology* 79: 541-66
10. Murray Peter J, Allen Judith E, Biswas Subhra K, Fisher Edward A, Gilroy Derek W, Goerdt S, Gordon S, Hamilton John A, Ivashkiv Lionel B, Lawrence T, Locati M, Mantovani A, Martinez Fernando O, Mege J-L, Mosser David M, Natoli G, Saeij Jeroen P, Schultze Joachim L, Shirey Kari A, Sica A, Suttles J, Udalova I, van Ginderachter Jo A, Vogel Stefanie N, Wynn Thomas A. 2014. Macrophage Activation and Polarization: Nomenclature and Experimental Guidelines. *Immunity* 41: 14-20

11. Lawrence T, Natoli G. 2011. Transcriptional regulation of macrophage polarization: enabling diversity with identity. *Nature Reviews Immunology* 11: 750
12. Lu YC, Yeh WC, Ohashi PS. 2008. LPS/TLR4 signal transduction pathway. *Cytokine* 42: 145-51
13. Lyroni K, Patsalos A, Daskalaki MG, Doxaki C, Soennichsen B, Helms M, Liapis I, Zacharioudaki V, Kampranis SC, Tsatsanis C. 2017. Epigenetic and Transcriptional Regulation of IRAK-M Expression in Macrophages. *The Journal of Immunology* 198: 1297
14. Biswas Subhra K, Mantovani A. 2012. Orchestration of Metabolism by Macrophages. *Cell Metabolism* 15: 432-7
15. Reilly SM, Saltiel AR. 2017. Adapting to obesity with adipose tissue inflammation. *Nat Rev Endocrinol* 13: 633-43
16. Lee YS, Li P, Huh JY, Hwang IJ, Lu M, Kim JI, Ham M, Talukdar S, Chen A, Lu WJ, Bandyopadhyay GK, Schwendener R, Olefsky J, Kim JB. 2011. Inflammation Is Necessary for Long-Term but Not Short-Term High-Fat Diet-Induced Insulin Resistance. *Diabetes* 60: 2474
17. Stolarczyk E. 2017. Adipose tissue inflammation in obesity: a metabolic or immune response? *Curr Opin Pharmacol* 37: 35-40
18. Achari AE, Jain SK. 2017. Adiponectin, a Therapeutic Target for Obesity, Diabetes, and Endothelial Dysfunction. *International journal of molecular sciences* 18: 1321
19. Zacharioudaki V, Androulidaki A, Arranz A, Vrentzos G, Margioris AN, Tsatsanis C. 2009. Adiponectin promotes endotoxin tolerance in macrophages by inducing IRAK-M expression. *J Immunol* 182: 6444-51
20. Jeon S-M. 2016. Regulation and function of AMPK in physiology and diseases. *Experimental & Molecular Medicine* 48: e245
21. Ruderman NB, Carling D, Prentki M, Cacicedo JM. 2013. AMPK, insulin resistance, and the metabolic syndrome. *The Journal of clinical investigation* 123: 2764-72
22. Francisco V, Pino J, Campos-Cabaleiro V, Ruiz-Fernández C, Mera A, Gonzalez-Gay MA, Gómez R, Gualillo O. 2018. Obesity, Fat Mass and Immune System: Role for Leptin. *Frontiers in Physiology* 9
23. Vegiopoulos A, Rohm M, Herzig S. 2017. Adipose tissue: between the extremes. 36: 1999-2017

24. Park HK, Kwak MK, Kim HJ, Ahima RS. 2017. Linking resistin, inflammation, and cardiometabolic diseases. *The Korean journal of internal medicine* 32: 239-47
25. Dasari R, Raghunath V. 2018. Obesity and Type II diabetes mellitus: Is resistin the link? *Journal of Diabetes and Endocrine Practice* 1: 1-8
26. Lee YS, Wollam J, Olefsky JM. 2018. An Integrated View of Immunometabolism. *Cell* 172: 22-40
27. Lauterbach MAR, Wunderlich FT. 2017. Macrophage function in obesity-induced inflammation and insulin resistance. *Pflugers Archiv : European journal of physiology* 469: 385-96
28. Quail DF, Dannenberg AJ. 2019. The obese adipose tissue microenvironment in cancer development and progression. *Nature Reviews Endocrinology* 15: 139-54
29. Lackey DE, Olefsky JM. 2016. Regulation of metabolism by the innate immune system. *Nat Rev Endocrinol* 12: 15-28
30. Kratz M, Coats BR, Hisert KB, Hagman D, Mutskov V, Peris E, Schoenfelt KQ, Kuzma JN, Larson I, Billing PS, Landerholm RW, Crouthamel M, Gozal D, Hwang S, Singh PK, Becker L. 2014. Metabolic dysfunction drives a mechanistically distinct proinflammatory phenotype in adipose tissue macrophages. *Cell metabolism* 20: 614-25
31. Stoger JL, Gijbels MJ, van der Velden S, Manca M, van der Loos CM, Biessen EA, Daemen MJ, Lutgens E, de Winther MP. 2012. Distribution of macrophage polarization markers in human atherosclerosis. *Atherosclerosis* 225: 461-8
32. McArdle M, Finucane O, Connaughton R, McMorrow A, Roche H. 2013. Mechanisms of Obesity-Induced Inflammation and Insulin Resistance: Insights into the Emerging Role of Nutritional Strategies. *Frontiers in Endocrinology* 4
33. Morgantini C, Jager J, Li X, Levi L, Azzimato V, Sulen A, Barreby E, Xu C, Tencerova M, Näslund E, Kumar C, Verdeguer F, Straniero S, Hulthenby K, Björkström NK, Ellis E, Rydén M, Kutter C, Hurrell T, Lauschke VM, Boucher J, Tomčala A, Krejčová G, Bajgar A, Aouadi M. 2019. Liver macrophages regulate systemic metabolism through non-inflammatory factors. *Nature Metabolism* 1: 445-59
34. O'Brien PD, Hinder LM, Callaghan BC, Feldman EL. 2017. Neurological consequences of obesity. *Lancet Neurol* 16: 465-77
35. Torres-Fuentes C, Schellekens H, Dinan TG, Cryan JF. 2017. The microbiota-gut-brain axis in obesity. *Lancet Gastroenterol Hepatol* 2: 747-56

36. Chelakkot C, Ghim J, Ryu SH. 2018. Mechanisms regulating intestinal barrier integrity and its pathological implications. *Experimental & Molecular Medicine* 50: 103
37. Belizrio JE, Faintuch J, Garay-Malpartida M. 2018. Gut Microbiome Dysbiosis and Immunometabolism: New Frontiers for Treatment of Metabolic Diseases. *Mediators of Inflammation* 2018: 12
38. Ríos-Covián D, Ruas-Madiedo P, Margolles A, Gueimonde M, de Los Reyes-Gavilán CG, Salazar N. 2016. Intestinal Short Chain Fatty Acids and their Link with Diet and Human Health. *Frontiers in microbiology* 7: 185-
39. Vital M, Karch A, Pieper DH. 2017. Colonic Butyrate-Producing Communities in Humans: an Overview Using Omics Data. *mSystems* 2: e00130-17
40. Cani PD, de Vos WM. 2017. Next-Generation Beneficial Microbes: The Case of *Akkermansia muciniphila*. *Frontiers in Microbiology* 8
41. Kho ZY, Lal SK. 2018. The Human Gut Microbiome - A Potential Controller of Wellness and Disease. *Frontiers in microbiology* 9: 1835-
42. Dewulf EM, Cani PD, Neyrinck AM, Possemiers S, Van Holle A, Muccioli GG, Deldicque L, Bindels LB, Pachikian BD, Sohet FM, Mignolet E, Francaux M, Larondelle Y, Delzenne NM. 2011. Inulin-type fructans with prebiotic properties counteract GPR43 overexpression and PPARgamma-related adipogenesis in the white adipose tissue of high-fat diet-fed mice. *J Nutr Biochem* 22: 712-22
43. Neyrinck AM, Hiel S, Bouzin C, Campayo VG, Cani PD, Bindels LB, Delzenne NM. 2018. Wheat-derived arabinoxylan oligosaccharides with bifidogenic properties abolishes metabolic disorders induced by western diet in mice. *Nutrition & diabetes* 8: 15-
44. Neyrinck AM, Possemiers S, Druart C, Van de Wiele T, De Backer F, Cani PD, Larondelle Y, Delzenne NM. 2011. Prebiotic effects of wheat arabinoxylan related to the increase in bifidobacteria, Roseburia and Bacteroides/Prevotella in diet-induced obese mice. *PLoS One* 6: e20944
45. Liu H, Wang J, He T, Becker S, Zhang G, Li D, Ma X. 2018. Butyrate: A Double-Edged Sword for Health? *Advances in Nutrition* 9: 21-9
46. Cleophas MCP, Ratter JM, Bekkering S, Quintin J, Schraa K, Stroes ES, Netea MG, Joosten LAB. 2019. Effects of oral butyrate supplementation on inflammatory potential of circulating peripheral blood mononuclear cells in healthy and obese males. *Scientific reports* 9: 775-

47. Ieronymaki E, Daskalaki MG, Lyroni K, Tsatsanis C. 2019. Insulin Signaling and Insulin Resistance Facilitate Trained Immunity in Macrophages Through Metabolic and Epigenetic Changes. *Frontiers in Immunology* 10
48. Vergadi E, Ieronymaki E, Lyroni K, Vaporidi K, Tsatsanis C. 2017. Akt Signaling Pathway in Macrophage Activation and M1/M2 Polarization. 198: 1006-14
49. Jean S, Kiger AA. 2014. Classes of phosphoinositide 3-kinases at a glance. *Journal of cell science* 127: 923-8
50. Chen C-Y, Chen J, He L, Stiles BL. 2018. PTEN: Tumor Suppressor and Metabolic Regulator. *Frontiers in Endocrinology* 9
51. Manning BD, Toker A. 2017. AKT/PKB Signaling: Navigating the Network. *Cell* 169: 381-405
52. Laplante M, Sabatini DM. 2012. mTOR signaling in growth control and disease. *Cell* 149: 274-93
53. Saxton RA, Sabatini DM. 2017. mTOR Signaling in Growth, Metabolism, and Disease. *Cell* 168: 960-76
54. Costa Rosa LF, Safi DA, Cury Y, Curi R. 1996. The effect of insulin on macrophage metabolism and function. *Cell Biochem Funct* 14: 33-42
55. Renier G, Clement I, Desfaits AC, Lambert A. 1996. Direct stimulatory effect of insulin-like growth factor-I on monocyte and macrophage tumor necrosis factor-alpha production. *Endocrinology* 137: 4611-8
56. Kratz M, Coats BR, Hisert KB, Hagman D, Mutskov V, Peris E, Schoenfeld KQ, Kuzma JN, Larson I, Billing PS, Landerholm RW, Crouthamel M, Gozal D, Hwang S, Singh PK, Becker L. 2014. Metabolic dysfunction drives a mechanistically distinct proinflammatory phenotype in adipose tissue macrophages. *Cell Metab* 20: 614-25
57. Senokuchi T, Liang CP, Seimon TA, Han S, Matsumoto M, Banks AS, Paik JH, DePinho RA, Accili D, Tabas I, Tall AR. 2008. Forkhead transcription factors (FoxOs) promote apoptosis of insulin-resistant macrophages during cholesterol-induced endoplasmic reticulum stress. *Diabetes* 57: 2967-76
58. Mauer J, Chaurasia B, Plum L, Quast T, Hampel B, Bluher M, Kolanus W, Kahn CR, Bruning JC. 2010. Myeloid cell-restricted insulin receptor deficiency protects against obesity-induced inflammation and systemic insulin resistance. *PLoS Genet* 6: e1000938

59. Spadaro O, Camell CD, Bosurgi L, Nguyen KY, Youm Y-H, Rothlin CV, Dixit VD. 2017. IGF1 Shapes Macrophage Activation in Response to Immunometabolic Challenge. *Cell Reports* 19: 225-34
60. Higashi Y, Sukhanov S, Shai SY, Danchuk S, Tang R, Snarski P, Li Z, Lobelle-Rich P, Wang M, Wang D, Yu H, Korthuis R, Delafontaine P. 2016. Insulin-Like Growth Factor-1 Receptor Deficiency in Macrophages Accelerates Atherosclerosis and Induces an Unstable Plaque Phenotype in Apolipoprotein E-Deficient Mice. *Circulation* 133: 2263-78
61. Knuever J, Willenborg S, Ding X, Akyuz MD, Partridge L, Niessen CM, Bruning JC, Eming SA. 2015. Myeloid Cell-Restricted Insulin/IGF-1 Receptor Deficiency Protects against Skin Inflammation. *J Immunol* 195: 5296-308
62. Rached M-T, Millership SJ, Pedroni SMA, Choudhury AI, Costa ASH, Hardy DG, Glegola JA, Irvine EE, Selman C, Woodberry MC, Yadav VK, Khadayate S, Vidal-Puig A, Virtue S, Frezza C, Withers DJ. 2019. Deletion of myeloid IRS2 enhances adipose tissue sympathetic nerve function and limits obesity. *Molecular Metabolism* 20: 38-50
63. Kubota T, Inoue M, Kubota N, Takamoto I, Mineyama T, Iwayama K, Tokuyama K, Moroi M, Ueki K, Yamauchi T, Kadowaki T. 2018. Downregulation of macrophage *Irs2* by hyperinsulinemia impairs IL-4-induced M2a-subtype macrophage activation in obesity. *Nature Communications* 9: 4863
64. Dasgupta P, Dorsey NJ, Li J, Qi X, Smith EP, Yamaji-Kegan K, Keegan AD. 2016. The adaptor protein insulin receptor substrate 2 inhibits alternative macrophage activation and allergic lung inflammation. *Sci Signal* 9: ra63
65. Luyendyk JP, Schabbauer GA, Tencati M, Holscher T, Pawlinski R, Mackman N. 2008. Genetic analysis of the role of the PI3K-Akt pathway in lipopolysaccharide-induced cytokine and tissue factor gene expression in monocytes/macrophages. *J Immunol* 180: 4218-26
66. Guha M, Mackman N. 2002. The phosphatidylinositol 3-kinase-Akt pathway limits lipopolysaccharide activation of signaling pathways and expression of inflammatory mediators in human monocytic cells. *J Biol Chem* 277: 32124-32
67. Beharka AA, Crowther JE, McCormack FX, Denning GM, Lees J, Tibesar E, Schlesinger LS. 2005. Pulmonary surfactant protein A activates a phosphatidylinositol 3-kinase/calcium signal transduction pathway in human macrophages: participation in the up-regulation of mannose receptor activity. *J Immunol* 175: 2227-36

68. Lee JS, Nauseef WM, Moeenrezakhanlou A, Sly LM, Noubir S, Leidal KG, Schlomann JM, Krystal G, Reiner NE. 2007. Monocyte p110alpha phosphatidylinositol 3-kinase regulates phagocytosis, the phagocyte oxidase, and cytokine production. *J Leukoc Biol* 81: 1548-61
69. Sakai K, Suzuki H, Oda H, Akaike T, Azuma Y, Murakami T, Sugi K, Ito T, Ichinose H, Koyasu S, Shirai M. 2006. Phosphoinositide 3-kinase in nitric oxide synthesis in macrophage: critical dimerization of inducible nitric-oxide synthase. *J Biol Chem* 281: 17736-42
70. Konrad S, Ali SR, Wiege K, Syed SN, Engling L, Piekorz RP, Hirsch E, Nürnberg B, Schmidt RE, Gessner JE. 2008. Phosphoinositide 3-kinases gamma and delta, linkers of coordinate C5a receptor-Fc gamma receptor activation and immune complex-induced inflammation. *The Journal of biological chemistry* 283: 33296-303
71. Lee PY, Yang CH, Kao MC, Su NY, Tsai PS, Huang CJ. 2015. Phosphoinositide 3-kinase beta, phosphoinositide 3-kinase delta, and phosphoinositide 3-kinase gamma mediate the anti-inflammatory effects of magnesium sulfate. *J Surg Res* 197: 390-7
72. Wang TY, Su NY, Shih PC, Tsai PS, Huang CJ. 2014. Anti-inflammation effects of naloxone involve phosphoinositide 3-kinase delta and gamma. *J Surg Res* 192: 599-606
73. Sahin E, Haubenwallner S, Kuttke M, Kollmann I, Halfmann A, Dohnal AM, Chen L, Cheng P, Hoesel B, Einwallner E, Brunner J, Kral JB, Schrottmair WC, Thell K, Saferding V, Blüml S, Schabbauer G. 2014. Correction: Macrophage PTEN Regulates Expression and Secretion of Arginase I Modulating Innate and Adaptive Immune Responses. *The Journal of Immunology* 193: 5350
74. Sly LM, Ho V, Antignano F, Ruschmann J, Hamilton M, Lam V, Rauh MJ, Krystal G. 2007. The role of SHIP in macrophages. *Front Biosci* 12: 2836-48
75. Chaurasia B, Mauer J, Koch L, Goldau J, Kock AS, Bruning JC. 2010. Phosphoinositide-dependent kinase 1 provides negative feedback inhibition to Toll-like receptor-mediated NF-kappaB activation in macrophages. *Mol Cell Biol* 30: 4354-66
76. Tan Z, Xie N, Cui H, Moellering DR, Abraham E, Thannickal VJ, Liu G. 2015. Pyruvate dehydrogenase kinase 1 participates in macrophage polarization via regulating glucose metabolism. *J Immunol* 194: 6082-9

77. Androulidaki A, Iliopoulos D, Arranz A, Doxaki C, Schworer S, Zacharioudaki V, Margioris AN, Tsihchlis PN, Tsatsanis C. 2009. The kinase Akt1 controls macrophage response to lipopolysaccharide by regulating microRNAs. *Immunity* 31: 220-31
78. Arranz A, Doxaki C, Vergadi E, Martinez de la Torre Y, Vaporidi K, Lagoudaki ED, Ieronymaki E, Androulidaki A, Venihaki M, Margioris AN, Stathopoulos EN, Tsihchlis PN, Tsatsanis C. 2012. Akt1 and Akt2 protein kinases differentially contribute to macrophage polarization. *Proc Natl Acad Sci U S A* 109: 9517-22
79. Kuijl C, Savage ND, Marsman M, Tuin AW, Janssen L, Egan DA, Ketema M, van den Nieuwendijk R, van den Eeden SJ, Geluk A, Poot A, van der Marel G, Beijersbergen RL, Overkleeft H, Ottenhoff TH, Neefjes J. 2007. Intracellular bacterial growth is controlled by a kinase network around PKB/AKT1. *Nature* 450: 725-30
80. Xu F, Kang Y, Zhang H, Piao Z, Yin H, Diao R, Xia J, Shi L. 2013. Akt1-mediated regulation of macrophage polarization in a murine model of *Staphylococcus aureus* pulmonary infection. *J Infect Dis* 208: 528-38
81. Li R, Tan S, Yu M, Jundt MC, Zhang S, Wu M. 2015. Annexin A2 Regulates Autophagy in *Pseudomonas aeruginosa* Infection through the Akt1-mTOR-ULK1/2 Signaling Pathway. *Journal of immunology (Baltimore, Md. : 1950)* 195: 3901-11
82. Larson-Casey JL, Deshane JS, Ryan AJ, Thannickal VJ, Carter AB. 2016. Macrophage Akt1 Kinase-Mediated Mitophagy Modulates Apoptosis Resistance and Pulmonary Fibrosis. *Immunity* 44: 582-96
83. Arranz A, Androulidaki A, Zacharioudaki V, Martinez C, Margioris AN, Gomariz RP, Tsatsanis C. 2008. Vasoactive intestinal peptide suppresses toll-like receptor 4 expression in macrophages via Akt1 reducing their responsiveness to lipopolysaccharide. *Mol Immunol* 45: 2970-80
84. Fernandez-Hernando C, Ackah E, Yu J, Suarez Y, Murata T, Iwakiri Y, Prendergast J, Miao RQ, Birnbaum MJ, Sessa WC. 2007. Loss of Akt1 leads to severe atherosclerosis and occlusive coronary artery disease. *Cell Metab* 6: 446-57
85. Babaev VR, Hebron KE, Wiese CB, Toth CL, Ding L, Zhang Y, May JM, Fazio S, Vickers KC, Linton MF. 2014. Macrophage deficiency of Akt2 reduces atherosclerosis in *Ldlr* null mice. *J Lipid Res* 55: 2296-308
86. Vergadi E, Vaporidi K, Theodorakis EE, Doxaki C, Lagoudaki E, Ieronymaki E, Alexaki VI, Helms M, Kondili E, Soennichsen B, Stathopoulos EN, Margioris AN, Georgopoulos D, Tsatsanis C. 2014. Akt2 deficiency protects from acute lung injury

via alternative macrophage activation and miR-146a induction in mice. *J Immunol* 192: 394-406

87. Hedl M, Yan J, Abraham C. 2016. IRF5 and IRF5 Disease-Risk Variants Increase Glycolysis and Human M1 Macrophage Polarization by Regulating Proximal Signaling and Akt2 Activation. *Cell Rep* 16: 2442-55

88. Jiang H, Westerterp M, Wang C, Zhu Y, Ai D. 2014. Macrophage mTORC1 disruption reduces inflammation and insulin resistance in obese mice. *Diabetologia* 57: 2393-404

89. Zhu L, Yang T, Li L, Sun L, Hou Y, Hu X, Zhang L, Tian H, Zhao Q, Peng J, Zhang H, Wang R, Yang Z, Zhang L, Zhao Y. 2014. TSC1 controls macrophage polarization to prevent inflammatory disease. *Nat Commun* 5: 4696

90. Byles V, Covarrubias AJ, Ben-Sahra I, Lamming DW, Sabatini DM, Manning BD, Horng T. 2013. The TSC-mTOR pathway regulates macrophage polarization. *Nat Commun* 4: 2834

91. Fang C, Yu J, Luo Y, Chen S, Wang W, Zhao C, Sun Z, Wu W, Guo W, Han Z, Hu X, Liao F, Feng X. 2015. Tsc1 is a Critical Regulator of Macrophage Survival and Function. *Cellular Physiology and Biochemistry* 36: 1406-18

92. Paschoal VA, Belchior T, Amano MT, Burgos-Silva M, Peixoto AS, Magdalon J, Vieira TS, Andrade ML, Moreno MF, Chimin P, Camara NO, Festuccia WT. 2018. Constitutive Activation of the Nutrient Sensor mTORC1 in Myeloid Cells Induced by Tsc1 Deletion Protects Mice from Diet-Induced Obesity. *Mol Nutr Food Res* 62: e1800283

93. Linke M, Pham HT, Katholnig K, Schnoller T, Miller A, Demel F, Schutz B, Rosner M, Kovacic B, Sukhbaatar N, Niederreiter B, Bluml S. 2017. Chronic signaling via the metabolic checkpoint kinase mTORC1 induces macrophage granuloma formation and marks sarcoidosis progression. 18: 293-302

94. Weichhart T, Haidinger M, Katholnig K, Kopecky C, Poglitsch M, Lassnig C, Rosner M, Zlabinger GJ, Hengstschlager M, Muller M, Horl WH, Saemann MD. 2011. Inhibition of mTOR blocks the anti-inflammatory effects of glucocorticoids in myeloid immune cells. *Blood* 117: 4273-83

95. Festuccia WT, Pouliot P, Bakan I, Sabatini DM, Laplante M. 2014. Myeloid-specific Rictor deletion induces M1 macrophage polarization and potentiates in vivo pro-inflammatory response to lipopolysaccharide. *PLoS One* 9: e95432

96. Shrivastava R, Asif M, Singh V, Dubey P, Ahmad Malik S, Lone M-UD, Tewari BN, Baghel KS, Pal S, Nagar GK, Chattopadhyay N, Bhadauria S. 2019. M2 polarization of macrophages by Oncostatin M in hypoxic tumor microenvironment is mediated by mTORC2 and promotes tumor growth and metastasis. *Cytokine* 118: 130-43
97. Hallowell RW, Collins SL, Craig JM, Zhang Y, Oh M, Illei PB, Chan-Li Y, Vigeland CL, Mitzner W, Scott AL, Powell JD, Horton MR. 2017. mTORC2 signalling regulates M2 macrophage differentiation in response to helminth infection and adaptive thermogenesis. *Nature Communications* 8: 14208
98. Babaev VR, Huang J, Ding L, Zhang Y, May JM, Linton MF. 2018. Loss of Rictor in Monocyte/Macrophages Suppresses Their Proliferation and Viability Reducing Atherosclerosis in LDLR Null Mice. *Front Immunol* 9: 215
99. Serbulea V, Upchurch CM, Schappe MS, Voigt P, DeWeese DE, Desai BN, Meher AK, Leitinger N. 2018. Macrophage phenotype and bioenergetics are controlled by oxidized phospholipids identified in lean and obese adipose tissue. *Proceedings of the National Academy of Sciences* 115: E6254
100. Kadl A, Meher AK, Sharma PR, Lee MY, Doran AC, Johnstone SR, Elliott MR, Gruber F, Han J, Chen W, Kensler T, Ravichandran KS, Isakson BE, Wamhoff BR, Leitinger N. 2010. Identification of a novel macrophage phenotype that develops in response to atherogenic phospholipids via Nrf2. *Circ Res* 107: 737-46
101. Baardman J, Verberk SGS, Prange KHM, van Weeghel M, van der Velden S, Ryan DG, Wüst RCI, Neele AE, Speijer D, Denis SW, Witte ME, Houtkooper RH, O'Neill LA, Knatko EV, Dinkova-Kostova AT, Lutgens E, de Winther MPJ, Van den Bossche J. 2018. A Defective Pentose Phosphate Pathway Reduces Inflammatory Macrophage Responses during Hypercholesterolemia. *Cell Reports* 25: 2044-52.e5
102. Kim K, Shim D, Lee Jun S, Zaitsev K, Williams Jesse W, Kim K-W, Jang M-Y, Seok Jang H, Yun Tae J, Lee Seung H, Yoon Won K, Prat A, Seidah Nabil G, Choi J, Lee S-P, Yoon S-H, Nam Jin W, Seong Je K, Oh Goo T, Randolph Gwendalyn J, Artyomov Maxim N, Cheong C, Choi J-H. 2018. Transcriptome Analysis Reveals Nonfoamy Rather Than Foamy Plaque Macrophages Are Proinflammatory in Atherosclerotic Murine Models. *Circulation Research* 123: 1127-42
103. Albracht-Schulte K, Kalupahana NS, Ramalingam L, Wang S, Rahman SM, Robert-McComb J, Moustaid-Moussa N. 2018. Omega-3 fatty acids in obesity and metabolic syndrome: a mechanistic update. *J Nutr Biochem* 58: 1-16

104. Yang Q, Vijayakumar A, Kahn BB. 2018. Metabolites as regulators of insulin sensitivity and metabolism. *Nat Rev Mol Cell Biol* 19: 654-72
105. Innes JK, Calder PC. 2018. Omega-6 fatty acids and inflammation. *Prostaglandins Leukot Essent Fatty Acids* 132: 41-8
106. Kawasaki N, Asada R, Saito A, Kanemoto S, Imaizumi K. 2012. Obesity-induced endoplasmic reticulum stress causes chronic inflammation in adipose tissue. *Sci Rep* 2: 799
107. Shan B, Wang X, Wu Y, Xu C, Xia Z, Dai J, Shao M, Zhao F, He S, Yang L, Zhang M, Nan F, Li J, Liu J, Liu J, Jia W, Qiu Y, Song B, Han JJ, Rui L, Duan SZ, Liu Y. 2017. The metabolic ER stress sensor IRE1alpha suppresses alternative activation of macrophages and impairs energy expenditure in obesity. *Nat Immunol* 18: 519-29
108. Ly LD, Xu S, Choi S-K, Ha C-M, Thoudam T, Cha S-K, Wiederkehr A, Wollheim CB, Lee I-K, Park K-S. 2017. Oxidative stress and calcium dysregulation by palmitate in type 2 diabetes. *Experimental & molecular medicine* 49: e291-e
109. Robblee MM, Kim CC, Porter Abate J, Valdearcos M, Sandlund KL, Shenoy MK, Volmer R, Iwawaki T, Koliwad SK. 2016. Saturated Fatty Acids Engage an IRE1alpha-Dependent Pathway to Activate the NLRP3 Inflammasome in Myeloid Cells. *Cell Rep* 14: 2611-23
110. Lyons CL, Roche HM. 2018. Nutritional Modulation of AMPK-Impact upon Metabolic-Inflammation. *International journal of molecular sciences* 19: 3092
111. Catrysse L, van Loo G. 2017. Inflammation and the Metabolic Syndrome: The Tissue-Specific Functions of NF-kappaB. *Trends Cell Biol* 27: 417-29
112. Schubert KM, Scheid MP, Duronio V. 2000. Ceramide inhibits protein kinase B/Akt by promoting dephosphorylation of serine 473. *J Biol Chem* 275: 13330-5
113. Fox TE, Houck KL, O'Neill SM, Nagarajan M, Stover TC, Pomianowski PT, Unal O, Yun JK, Naides SJ, Kester M. 2007. Ceramide recruits and activates protein kinase C zeta (PKC zeta) within structured membrane microdomains. *J Biol Chem* 282: 12450-7
114. Konner AC, Bruning JC. 2011. Toll-like receptors: linking inflammation to metabolism. *Trends Endocrinol Metab* 22: 16-23
115. Lancaster GI, Langley KG, Berglund NA, Kammoun HL, Reibe S, Estevez E, Weir J, Mellett NA, Pernes G, Conway JRW, Lee MKS, Timpson P, Murphy AJ, Masters SL, Gerondakis S, Bartonicek N, Kaczorowski DC, Dinger ME, Meikle PJ,

- Bond PJ, Febbraio MA. 2018. Evidence that TLR4 Is Not a Receptor for Saturated Fatty Acids but Mediates Lipid-Induced Inflammation by Reprogramming Macrophage Metabolism. *Cell Metab* 27: 1096-110.e5
116. Hartstra AV, Bouter KE, Backhed F, Nieuwdorp M. 2015. Insights into the role of the microbiome in obesity and type 2 diabetes. *Diabetes Care* 38: 159-65
117. Yuan T, Yang T, Chen H, Fu D, Hu Y, Wang J, Yuan Q, Yu H, Xu W, Xie X. 2018. New insights into oxidative stress and inflammation during diabetes mellitus-accelerated atherosclerosis. *Redox biology* 20: 247-60
118. Senatus LM, Schmidt AM. 2017. The AGE-RAGE Axis: Implications for Age-Associated Arterial Diseases. *Frontiers in genetics* 8: 187-
119. Volpe CMO, Villar-Delfino PH, Dos Anjos PMF, Nogueira-Machado JA. 2018. Cellular death, reactive oxygen species (ROS) and diabetic complications. *Cell Death Dis* 9: 119
120. Zhao L, Shah JA, Cai Y, Jin J. 2018. 'O-GlcNAc Code' Mediated Biological Functions of Downstream Proteins. 23
121. Baudoin L, ISSAD T. 2015. O-GlcNAcylation and inflammation: a vast territory to explore. *Frontiers in Endocrinology* 5
122. Bays HE, Toth PP, Kris-Etherton PM, Abate N, Aronne LJ, Brown WV, Gonzalez-Campoy JM, Jones SR, Kumar R, La Forge R, Samuel VT. 2013. Obesity, adiposity, and dyslipidemia: a consensus statement from the National Lipid Association. *J Clin Lipidol* 7: 304-83
123. Jung UJ, Choi MS. 2014. Obesity and its metabolic complications: the role of adipokines and the relationship between obesity, inflammation, insulin resistance, dyslipidemia and nonalcoholic fatty liver disease. *Int J Mol Sci* 15: 6184-223
124. Shin KC, Hwang I, Choe SS, Park J, Ji Y, Kim JI, Lee GY, Choi SH, Ching J, Kovalik J-P, Kim JB. 2017. Macrophage VLDLR mediates obesity-induced insulin resistance with adipose tissue inflammation. *Nature communications* 8: 1087-
125. Lara-Guzman OJ, Gil-Izquierdo A, Medina S, Osorio E, Alvarez-Quintero R, Zuluaga N, Oger C, Galano JM, Durand T, Munoz-Durango K. 2018. Oxidized LDL triggers changes in oxidative stress and inflammatory biomarkers in human macrophages. *Redox Biol* 15: 1-11
126. Levitan I, Volkov S, Subbaiah PV. 2010. Oxidized LDL: diversity, patterns of recognition, and pathophysiology. *Antioxidants & redox signaling* 13: 39-75

127. Jongstra-Bilen J, Zhang CX, Wisnicki T, Li MK, White-Alfred S, Ilaalagan R, Ferri DM, Deonarain A, Wan MH, Hyduk SJ, Cummins CL, Cybulsky MI. 2017. Oxidized Low-Density Lipoprotein Loading of Macrophages Downregulates TLR-Induced Proinflammatory Responses in a Gene-Specific and Temporal Manner through Transcriptional Control. *199*: 2149-57
128. McLaughlin T, Ackerman SE, Shen L, Engleman E. 2017. Role of innate and adaptive immunity in obesity-associated metabolic disease. *J Clin Invest* 127: 5-13
129. Han MS, Jung DY, Morel C, Lakhani SA, Kim JK, Flavell RA, Davis RJ. 2013. JNK expression by macrophages promotes obesity-induced insulin resistance and inflammation. *Science* 339: 218-22
130. Arkan MC, Hevener AL, Greten FR, Maeda S, Li ZW, Long JM, Wynshaw-Boris A, Poli G, Olefsky J, Karin M. 2005. IKK-beta links inflammation to obesity-induced insulin resistance. *Nat Med* 11: 191-8
131. Coats BR, Schoenfelt KQ, Barbosa-Lorenzi VC, Peris E, Cui C, Hoffman A, Zhou G, Fernandez S, Zhai L, Hall BA, Haka AS, Shah AM, Reardon CA, Brady MJ, Rhodes CJ, Maxfield FR, Becker L. 2017. Metabolically Activated Adipose Tissue Macrophages Perform Detrimental and Beneficial Functions during Diet-Induced Obesity. *Cell Rep* 20: 3149-61
132. Geeraerts X, Bolli E, Fendt S-M, Van Ginderachter JA. 2017. Macrophage Metabolism As Therapeutic Target for Cancer, Atherosclerosis, and Obesity. *Frontiers in Immunology* 8
133. Freerman AJ, Zhao L, Pingili AK, Teng B, Cozzo AJ, Fuller AM, Johnson AR, Milner JJ, Lim MF, Galanko JA, Beck MA, Bear JE, Rotty JD, Bezavada L, Smallwood HS, Puchowicz MA, Liu J, Locasale JW, Lee DP, Bennett BJ, Abel ED, Rathmell JC, Makowski L. 2019. Myeloid Slc2a1-Deficient Murine Model Revealed Macrophage Activation and Metabolic Phenotype Are Fueled by GLUT1. *202*: 1265-86
134. Freerman AJ, Johnson AR, Sacks GN, Milner JJ, Kirk EL, Troester MA, Macintyre AN, Goraksha-Hicks P, Rathmell JC, Makowski L. 2014. Metabolic reprogramming of macrophages: glucose transporter 1 (GLUT1)-mediated glucose metabolism drives a proinflammatory phenotype. *J Biol Chem* 289: 7884-96
135. Johnson AR, Qin Y, Cozzo AJ, Freerman AJ, Huang MJ, Zhao L, Sampey BP, Milner JJ, Beck MA, Damania B, Rashid N, Galanko JA, Lee DP, Edin ML, Zeldin DC, Fueger PT, Dietz B, Stahl A, Wu Y, Mohlke KL, Makowski L. 2016.

Metabolic reprogramming through fatty acid transport protein 1 (FATP1) regulates macrophage inflammatory potential and adipose inflammation. *Molecular metabolism* 5: 506-26

136. Cheng S-C, Quintin J, Cramer RA, Shepardson KM, Saeed S, Kumar V, Giamarellos-Bourboulis EJ, Martens JHA, Rao NA, Aghajani A, Manjari GR, Li Y, Ifrim DC, Arts RJW, van der Veer BMJW, Deen PMT, Logie C, O'Neill LA, Willems P, van de Veerdonk FL, van der Meer JWM, Ng A, Joosten LAB, Wijmenga C, Stunnenberg HG, Xavier RJ, Netea MG. 2014. mTOR- and HIF-1 α -mediated aerobic glycolysis as metabolic basis for trained immunity. *Science (New York, N.Y.)* 345: 1250684-

137. Van den Bossche J, O'Neill LA, Menon D. 2017. Macrophage Immunometabolism: Where Are We (Going)? *Trends in Immunology* 38: 395-406

138. Hui S, Ghergurovich JM, Morscher RJ, Jang C, Teng X, Lu W, Esparza LA, Reya T, Le Z, Yanxiang Guo J, White E, Rabinowitz JD. 2017. Glucose feeds the TCA cycle via circulating lactate. *Nature* 551: 115-8

139. Diskin C, Pålsson-McDermott EM. 2018. Metabolic Modulation in Macrophage Effector Function. *Frontiers in immunology* 9: 270-

140. Bekkering S, Arts RJW, Novakovic B, Kourtzelis I, van der Heijden CDCC, Li Y, Popa CD, ter Horst R, van Tuijl J, Netea-Maier RT, van de Veerdonk FL, Chavakis T, Joosten LAB, van der Meer JWM, Stunnenberg H, Riksen NP, Netea MG. 2018. Metabolic Induction of Trained Immunity through the Mevalonate Pathway. *Cell* 172: 135-46.e9

141. Williams NC, O'Neill LAJ. 2018. A Role for the Krebs Cycle Intermediate Citrate in Metabolic Reprogramming in Innate Immunity and Inflammation. *Frontiers in Immunology* 9

142. O'Neill LAJ, Artyomov MN. 2019. Itaconate: the poster child of metabolic reprogramming in macrophage function. *Nature Reviews Immunology* 19: 273-81

143. Lampropoulou V, Sergushichev A, Bambouskova M, Nair S, Vincent EE, Loginicheva E, Cervantes-Barragan L, Ma X, Huang SC, Griss T, Weinheimer CJ, Khader S, Randolph GJ, Pearce EJ, Jones RG, Diwan A, Diamond MS, Artyomov MN. 2016. Itaconate Links Inhibition of Succinate Dehydrogenase with Macrophage Metabolic Remodeling and Regulation of Inflammation. *Cell Metab* 24: 158-66

144. Domínguez-Andrés J, Novakovic B, Li Y, Scicluna BP, Gresnigt MS, Arts RJW, Oosting M, Moorlag SJCFM, Groh LA, Zwaag J, Koch RM, ter Horst R,

Joosten LAB, Wijmenga C, Michelucci A, van der Poll T, Kox M, Pickkers P, Kumar V, Stunnenberg H, Netea MG. 2019. The Itaconate Pathway Is a Central Regulatory Node Linking Innate Immune Tolerance and Trained Immunity. *Cell Metabolism* 29: 211-20.e5

145. Tannahill GM, Curtis AM, Adamik J, Palsson-McDermott EM, McGettrick AF, Goel G, Frezza C, Bernard NJ, Kelly B, Foley NH, Zheng L, Gardet A, Tong Z, Jany SS, Corr SC, Haneklaus M, Caffrey BE, Pierce K, Walmsley S, Beasley FC, Cummins E, Nizet V, Whyte M, Taylor CT, Lin H, Masters SL, Gottlieb E, Kelly VP, Clish C, Auron PE, Xavier RJ, O'Neill LAJ. 2013. Succinate is an inflammatory signal that induces IL-1 β through HIF-1 α . *Nature* 496: 238

146. Mills EL, Kelly B, Logan A, Costa ASH, Varma M, Bryant CE, Tourlomousis P, Dabritz JHM, Gottlieb E, Latorre I, Corr SC, McManus G, Ryan D, Jacobs HT, Szibor M, Xavier RJ, Braun T, Frezza C, Murphy MP, O'Neill LA. 2016. Succinate Dehydrogenase Supports Metabolic Repurposing of Mitochondria to Drive Inflammatory Macrophages. *Cell* 167: 457-70.e13

147. Huang SC-C, Everts B, Ivanova Y, O'Sullivan D, Nascimento M, Smith AM, Beatty W, Love-Gregory L, Lam WY, O'Neill CM, Yan C, Du H, Abumrad NA, Urban JF, Jr., Artyomov MN, Pearce EL, Pearce EJ. 2014. Cell-intrinsic lysosomal lipolysis is essential for alternative activation of macrophages. *Nature immunology* 15: 846-55

148. Malandrino MI, Fucho R, Weber M, Calderon-Dominguez M, Mir JF, Valcarcel L, Escote X, Gomez-Serrano M, Peral B, Salvado L, Fernandez-Veledo S, Casals N, Vazquez-Carrera M, Villarroya F, Vendrell JJ, Serra D, Herrero L. 2015. Enhanced fatty acid oxidation in adipocytes and macrophages reduces lipid-induced triglyceride accumulation and inflammation. *Am J Physiol Endocrinol Metab* 308: E756-69

149. Palmieri EM, Menga A, Martin-Perez R, Quinto A, Riera-Domingo C, De Tullio G, Hooper DC, Lamers WH, Ghesquiere B, McVicar DW, Guarini A, Mazzone M, Castegna A. 2017. Pharmacologic or Genetic Targeting of Glutamine Synthetase Skews Macrophages toward an M1-like Phenotype and Inhibits Tumor Metastasis. *Cell Rep* 20: 1654-66

150. Liu PS, Wang H, Li X, Chao T, Teav T, Christen S, Di Conza G, Cheng WC, Chou CH, Vavakova M, Muret C, Debackere K, Mazzone M, Huang HD, Fendt SM, Ivanisevic J, Ho PC. 2017. alpha-ketoglutarate orchestrates macrophage activation through metabolic and epigenetic reprogramming. *18: 985-94*

151. Jha AK, Huang SC, Sergushichev A, Lampropoulou V, Ivanova Y, Loginicheva E, Chmielewski K, Stewart KM, Ashall J, Everts B, Pearce EJ, Driggers EM, Artyomov MN. 2015. Network integration of parallel metabolic and transcriptional data reveals metabolic modules that regulate macrophage polarization. *Immunity* 42: 419-30
152. Arts RJ, Novakovic B, Ter Horst R, Carvalho A, Bekkering S, Lachmandas E, Rodrigues F, Silvestre R, Cheng SC, Wang SY, Habibi E, Goncalves LG, Mesquita I, Cunha C, van Laarhoven A, van de Veerdonk FL, Williams DL, van der Meer JW, Logie C, O'Neill LA, Dinarello CA, Riksen NP, van Crevel R, Clish C, Notebaart RA, Joosten LA, Stunnenberg HG, Xavier RJ, Netea MG. 2016. Glutaminolysis and Fumarate Accumulation Integrate Immunometabolic and Epigenetic Programs in Trained Immunity. *Cell Metab* 24: 807-19
153. Xu X, Grijalva A, Skowronski A, van Eijk M, Serlie MJ, Ferrante AW, Jr. 2013. Obesity activates a program of lysosomal-dependent lipid metabolism in adipose tissue macrophages independently of classic activation. *Cell metabolism* 18: 816-30
154. Crisan TO, Netea MG, Joosten LA. 2016. Innate immune memory: Implications for host responses to damage-associated molecular patterns. *Eur J Immunol* 46: 817-28
155. Bauer M, Weis S, Netea MG, Wetzker R. 2018. Remembering Pathogen Dose: Long-Term Adaptation in Innate Immunity. *Trends Immunol* 39: 438-45
156. Arts RJW, Carvalho A, La Rocca C, Palma C, Rodrigues F, Silvestre R, Kleinnijenhuis J, Lachmandas E, Goncalves LG, Belinha A, Cunha C, Oosting M, Joosten LAB, Matarese G, van Crevel R, Netea MG. 2016. Immunometabolic Pathways in BCG-Induced Trained Immunity. *Cell Rep* 17: 2562-71
157. Mulder WJM, Ochando J, Joosten LAB, Fayad ZA, Netea MG. 2019. Therapeutic targeting of trained immunity. *Nature Reviews Drug Discovery*
158. Bekkering S, Arts RJW, Novakovic B, Kourtzelis I, van der Heijden C, Li Y, Popa CD, Ter Horst R, van Tuijl J, Netea-Maier RT, van de Veerdonk FL, Chavakis T, Joosten LAB, van der Meer JWM, Stunnenberg H, Riksen NP, Netea MG. 2018. Metabolic Induction of Trained Immunity through the Mevalonate Pathway. *Cell* 172: 135-46.e9
159. Christ A, Gunther P, Lauterbach MAR, Duewell P, Biswas D, Pelka K, Scholz CJ, Oosting M, Haendler K, Bassler K, Klee K, Schulte-Schrepping J, Ulas T,

- Moorlag S, Kumar V, Park MH, Joosten LAB, Groh LA, Riksen NP, Espevik T, Schlitzer A, Li Y, Fitzgerald ML, Netea MG, Schultze JL, Latz E. 2018. Western Diet Triggers NLRP3-Dependent Innate Immune Reprogramming. *Cell* 172: 162-75.e14
160. Sohrabi Y, Lagache SMM, Schnack L, Godfrey R, Kahles F, Bruemmer D, Waltenberger J, Findeisen HM. 2019. mTOR-Dependent Oxidative Stress Regulates oxLDL-Induced Trained Innate Immunity in Human Monocytes. *Frontiers in Immunology* 9
161. Brasacchio D, Okabe J, Tikellis C, Balcerczyk A, George P, Baker EK, Calkin AC, Brownlee M, Cooper ME, El-Osta A. 2009. Hyperglycemia induces a dynamic cooperativity of histone methylase and demethylase enzymes associated with gene-activating epigenetic marks that coexist on the lysine tail. *Diabetes* 58: 1229-36
162. Miao F, Gonzalo IG, Lanting L, Natarajan R. 2004. In vivo chromatin remodeling events leading to inflammatory gene transcription under diabetic conditions. *J Biol Chem* 279: 18091-7
163. Miao F, Chen Z, Genuth S, Paterson A, Zhang L, Wu X, Li SM, Cleary P, Riggs A, Harlan DM, Lorenzi G, Kolterman O, Sun W, Lachin JM, Natarajan R. 2014. Evaluating the role of epigenetic histone modifications in the metabolic memory of type 1 diabetes. *Diabetes* 63: 1748-62
164. van Diepen JA, Thiem K, Stienstra R, Riksen NP, Tack CJ, Netea MG. 2016. Diabetes propels the risk for cardiovascular disease: sweet monocytes becoming aggressive? *Cellular and molecular life sciences : CMLS* 73: 4675-84
165. Netea MG, Joosten LAB, Latz E, Mills KHG, Natoli G, Stunnenberg HG, O'Neill LAJ, Xavier RJ. 2016. Trained immunity: A program of innate immune memory in health and disease. *Science* 352: aaf1098
166. Singer M, Deutschman CS, Seymour CW, Shankar-Hari M, Annane D, Bauer M, Bellomo R, Bernard GR, Chiche J-D, Cooper-Smith CM, Hotchkiss RS, Levy MM, Marshall JC, Martin GS, Opal SM, Rubenfeld GD, van der Poll T, Vincent J-L, Angus DC. 2016. The Third International Consensus Definitions for Sepsis and Septic Shock (Sepsis-3) Consensus Definitions for Sepsis and Septic Shock Consensus Definitions for Sepsis and Septic Shock. *JAMA* 315: 801-10
167. Hotchkiss RS, Karl IE. 2003. The pathophysiology and treatment of sepsis. *N Engl J Med* 348: 138-50
168. Aird WC. 2003. The role of the endothelium in severe sepsis and multiple organ dysfunction syndrome. *Blood* 101: 3765

169. Skrupky LP, Kerby PW, Hotchkiss RS. 2011. Advances in the management of sepsis and the understanding of key immunologic defects. *Anesthesiology* 115: 1349-62
170. Denstaedt SJ, Singer BH, Standiford TJ. 2018. Sepsis and Nosocomial Infection: Patient Characteristics, Mechanisms, and Modulation. *Frontiers in Immunology* 9
171. Marik PE, Taeb AM. 2017. SIRS, qSOFA and new sepsis definition. *Journal of thoracic disease* 9: 943-5
172. Englert JA, Bobba C, Baron RM. 2019. Integrating molecular pathogenesis and clinical translation in sepsis-induced acute respiratory distress syndrome. *JCI Insight* 4
173. Ware LB, Matthay MA. 2000. The acute respiratory distress syndrome. *N Engl J Med* 342: 1334-49
174. Papadimitriou-Olivgeris M, Aretha D, Zotou A, Koutsileou K, Zbouki A, Lefkaditi A, Sklavou C, Marangos M, Fligou F. 2016. The Role of Obesity in Sepsis Outcome among Critically Ill Patients: A Retrospective Cohort Analysis. *BioMed research international* 2016: 5941279-
175. Wang S, Liu X, Chen Q, Liu C, Huang C, Fang X. 2017. The role of increased body mass index in outcomes of sepsis: a systematic review and meta-analysis. *BMC anesthesiology* 17: 118-
176. Pepper DJ, Demirkale CY, Sun J, Rhee C, Fram D, Eichacker P, Klompas M, Suffredini AF, Kadri SS. 2019. Does Obesity Protect Against Death in Sepsis? A Retrospective Cohort Study of 55,038 Adult Patients. *Crit Care Med* 47: 643-50
177. Ng PY, Eikermann M. 2017. The obesity conundrum in sepsis. *BMC anesthesiology* 17: 147-
178. Braun N, Gomes F, Schutz P. 2015. "The obesity paradox" in disease--is the protective effect of obesity true? *Swiss Med Wkly* 145: w14265
179. Gribsholt SB, Pedersen L, Richelsen B, Dekkers O, Thomsen RW. 2018. Body Mass Index of 92,027 patients acutely admitted to general hospitals in Denmark: Associated clinical characteristics and 30-day mortality. *PloS one* 13: e0195853-e
180. Zhi G, Xin W, Ying W, Guohong X, Shuying L. 2016. "Obesity Paradox" in Acute Respiratory Distress Syndrome: Asystematic Review and Meta-Analysis. *PLOS ONE* 11: e0163677

181. Kumar V. 2018. Inflammasomes: Pandora's box for sepsis. *J Inflamm Res* 11: 477-502
182. Rittirsch D, Huber-Lang MS, Flierl MA, Ward PA. 2009. Immunodesign of experimental sepsis by cecal ligation and puncture. *Nat Protoc* 4: 31-6
183. Matute-Bello G, Downey G, Moore BB, Groshong SD, Matthay MA, Slutsky AS, Kuebler WM, Acute Lung Injury in Animals Study G. 2011. An official American Thoracic Society workshop report: features and measurements of experimental acute lung injury in animals. *Am J Respir Cell Mol Biol* 44: 725-38
184. van Rijt LS, Kuipers H, Vos N, Hijdra D, Hoogsteden HC, Lambrecht BN. 2004. A rapid flow cytometric method for determining the cellular composition of bronchoalveolar lavage fluid cells in mouse models of asthma. *J Immunol Methods* 288: 111-21
185. Lo KA, Labadorf A, Kennedy NJ, Han MS, Yap YS, Matthews B, Xin X, Sun L, Davis RJ, Lodish HF, Fraenkel E. 2013. Analysis of in vitro insulin resistance models and their physiological relevance to in vivo diet-induced adipose insulin resistance. *Cell reports* 5: 10.1016/j.celrep.2013.08.039
186. Mitsuuchi Y, Johnson SW, Moonblatt S, Testa JR. 1998. Translocation and activation of AKT2 in response to stimulation by insulin. *J Cell Biochem* 70: 433-41
187. Cho H, Mu J, Kim JK, Thorvaldsen JL, Chu Q, Crenshaw EB, 3rd, Kaestner KH, Bartolomei MS, Shulman GI, Birnbaum MJ. 2001. Insulin resistance and a diabetes mellitus-like syndrome in mice lacking the protein kinase Akt2 (PKB beta). *Science* 292: 1728-31
188. Toya MA-W, Veethika P, Lina PS, Michal MM, Deborah AA. 2016. Prediabetes linked to excess glucagon in transgenic mice with pancreatic active AKT1. *Journal of Endocrinology* 228: 49-59
189. Schumacher R, Mosthaf L, Schlessinger J, Brandenburg D, Ullrich A. 1991. Insulin and insulin-like growth factor-1 binding specificity is determined by distinct regions of their cognate receptors. *J Biol Chem* 266: 19288-95
190. Calder PC, Dimitriadis G, Newsholme P. 2007. Glucose metabolism in lymphoid and inflammatory cells and tissues. *Curr Opin Clin Nutr Metab Care* 10: 531-40
191. Utzolino S, Ditzel CM, Baier PK, Hopt UT, Kaffarnik MF. 2014. The obesity paradox in surgical intensive care patients with peritonitis. *J Crit Care* 29: 887.e1-5

192. Arabi YM, Dara SI, Tamim HM, Rishu AH, Bouchama A, Khedr MK, Feinstein D, Parrillo JE, Wood KE, Keenan SP, Zanotti S, Martinka G, Kumar A, Kumar A. 2013. Clinical characteristics, sepsis interventions and outcomes in the obese patients with septic shock: an international multicenter cohort study. *Crit Care* 17: R72
193. Krajcovic M, Krishna S, Akkari L, Joyce JA, Overholtzer M. 2013. mTOR regulates phagosome and entotic vacuole fission. *Mol Biol Cell* 24: 3736-45
194. Lovren F, Pan Y, Quan A, Szmitko PE, Singh KK, Shukla PC, Gupta M, Chan L, Al-Omran M, Teoh H, Verma S. 2010. Adiponectin primes human monocytes into alternative anti-inflammatory M2 macrophages. *American journal of physiology. Heart and circulatory physiology* 299: H656-H63
195. Ohashi K, Parker JL, Ouchi N, Higuchi A, Vita JA, Gokce N, Pedersen AA, Kalthoff C, Tullin S, Sams A, Summer R, Walsh K. 2010. Adiponectin promotes macrophage polarization toward an anti-inflammatory phenotype. *The Journal of biological chemistry* 285: 6153-60
196. Tsatsanis C, Zacharioudaki V, Androulidaki A, Dermitzaki E, Charalampopoulos I, Minas V, Gravanis A, Margioris AN. 2005. Adiponectin induces TNF-alpha and IL-6 in macrophages and promotes tolerance to itself and other pro-inflammatory stimuli. *Biochem Biophys Res Commun* 335: 1254-63
197. Guo R, Zhang Y, Turdi S, Ren J. 2013. Adiponectin knockout accentuates high fat diet-induced obesity and cardiac dysfunction: role of autophagy. *Biochimica et biophysica acta* 1832: 1136-48
198. Yano W, Kubota N, Itoh S, Kubota T, Awazawa M, Moroi M, Sugi K, Takamoto I, Ogata H, Tokuyama K, Noda T, Terauchi Y, Ueki K, Kadowaki T. 2008. Molecular mechanism of moderate insulin resistance in adiponectin-knockout mice. *Endocr J* 55: 515-22
199. Leavens KF, Easton RM, Shulman GI, Previs SF, Birnbaum MJ. 2009. Akt2 is required for hepatic lipid accumulation in models of insulin resistance. *Cell Metab* 10: 405-18
200. Takiguchi M, Mori M. 1991. In vitro analysis of the rat liver-type arginase promoter. *J Biol Chem* 266: 9186-93
201. Chowdhury S, Gotoh T, Mori M, Takiguchi M. 1996. CCAAT/enhancer-binding protein beta (C/EBP beta) binds and activates while hepatocyte nuclear

factor-4 (HNF-4) does not bind but represses the liver-type arginase promoter. *Eur J Biochem* 236: 500-9

202. Stutz AM, Pickart LA, Trifilieff A, Baumruker T, Prieschl-Strassmayr E, Woisetschlager M. 2003. The Th2 cell cytokines IL-4 and IL-13 regulate found in inflammatory zone 1/resistin-like molecule alpha gene expression by a STAT6 and CCAAT/enhancer-binding protein-dependent mechanism. *J Immunol* 170: 1789-96

203. Huang SC, Smith AM, Everts B, Colonna M, Pearce EL, Schilling JD, Pearce EJ. 2016. Metabolic Reprogramming Mediated by the mTORC2-IRF4 Signaling Axis Is Essential for Macrophage Alternative Activation. *Immunity* 45: 817-30

204. Hallowell RW, Collins SL, Craig JM, Zhang Y, Oh M, Illei PB, Chan-Li Y, Vigeland CL, Mitzner W, Scott AL, Powell JD, Horton MR. 2017. mTORC2 signalling regulates M2 macrophage differentiation in response to helminth infection and adaptive thermogenesis. *Nat Commun* 8: 14208

205. Covarrubias AJ, Aksoylar HI, Yu J, Snyder NW, Worth AJ, Iyer SS, Wang J, Ben-Sahra I, Byles V, Polynne-Stapornkul T, Espinosa EC, Lamming D, Manning BD, Zhang Y, Blair IA, Horng T. 2016. Akt-mTORC1 signaling regulates Acly to integrate metabolic input to control of macrophage activation. *Elife* 5

206. Androulidaki A, Iliopoulos D, Arranz A, Doxaki C, Schworer S, Zacharioudaki V, Margioris AN, Tsihchlis PN, Tsatsanis C. 2009. The kinase Akt1 controls macrophage response to lipopolysaccharide by regulating microRNAs. *Immunity* 31: 220-31

207. Mantovani A, Marchesi F, Malesci A, Laghi L, Allavena P. 2017. Tumour-associated macrophages as treatment targets in oncology. *Nature reviews. Clinical oncology* 14: 399-416

208. Amar S, Zhou Q, Shaik-Dasthagirisahab Y, Leeman S. 2007. Diet-induced obesity in mice causes changes in immune responses and bone loss manifested by bacterial challenge. *Proc Natl Acad Sci U S A* 104: 20466-71

209. Biswas SK, Mantovani A. 2012. Orchestration of metabolism by macrophages. *Cell Metab* 15: 432-7

210. Murray PJ, Allen JE, Biswas SK, Fisher EA, Gilroy DW, Goerdts S, Gordon S, Hamilton JA, Ivashkiv LB, Lawrence T, Locati M, Mantovani A, Martinez FO, Mege JL, Mosser DM, Natoli G, Saeij JP, Schultze JL, Shirey KA, Sica A, Suttles J, Udalova I, van Genderachter JA, Vogel SN, Wynn TA. 2014. Macrophage activation and polarization: nomenclature and experimental guidelines. *Immunity* 41: 14-20

211. Odegaard JI, Chawla A. 2013. Pleiotropic actions of insulin resistance and inflammation in metabolic homeostasis. *Science* 339: 172-7
212. Dellinger RP, Levy MM, Rhodes A, Annane D, Gerlach H, Opal SM, Sevransky JE, Sprung CL, Douglas IS, Jaeschke R, Osborn TM, Nunnally ME, Townsend SR, Reinhart K, Kleinpell RM, Angus DC, Deutschman CS, Machado FR, Rubenfeld GD, Webb S, Beale RJ, Vincent JL, Moreno R. 2013. Surviving Sepsis Campaign: international guidelines for management of severe sepsis and septic shock, 2012. *Intensive Care Med* 39: 165-228
213. Gauglitz GG, Toliver-Kinsky TE, Williams FN, Song J, Cui W, Herndon DN, Jeschke MG. 2010. Insulin increases resistance to burn wound infection-associated sepsis. *Crit Care Med* 38: 202-8
214. Saeed S, Quintin J, Kerstens HH, Rao NA, Aghajani-refah A, Matarese F, Cheng SC, Ratter J, Berentsen K, van der Ent MA, Sharifi N, Janssen-Megens EM, Ter Huurne M, Mandoli A, van Schaik T, Ng A, Burden F, Downes K, Frontini M, Kumar V, Giamarellos-Bourboulis EJ, Ouwehand WH, van der Meer JW, Joosten LA, Wijmenga C, Martens JH, Xavier RJ, Logie C, Netea MG, Stunnenberg HG. 2014. Epigenetic programming of monocyte-to-macrophage differentiation and trained innate immunity. *Science* 345: 1251086
215. Cheng SC, Quintin J, Cramer RA, Shepardson KM, Saeed S, Kumar V, Giamarellos-Bourboulis EJ, Martens JH, Rao NA, Aghajani-refah A, Manjeri GR, Li Y, Ifrim DC, Arts RJ, van der Veer BM, Deen PM, Logie C, O'Neill LA, Willems P, van de Veerdonk FL, van der Meer JW, Ng A, Joosten LA, Wijmenga C, Stunnenberg HG, Xavier RJ, Netea MG. 2014. mTOR- and HIF-1 α -mediated aerobic glycolysis as metabolic basis for trained immunity. *Science* 345: 1250684
216. Song WM, Colonna M. 2018. Immune Training Unlocks Innate Potential. *Cell* 172: 3-5
217. Christ A, Gunther P, Lauterbach M, Duewell P, Biswas D, Pelka K, Scholtz C, Oosting M, Haendler K, Li Y, Fitzgerald M, Netea MG, Schultze J, Latz E. 2018. Western Diet Triggers NLRP3-Dependent Innate Immune Reprogramming. *Cell* 1: 162-75
218. Alexaki VI, Fodelianaki G, Neuwirth A, Mund C, Kourgiantaki A, Ieronimaki E, Lyroni K, Troullinaki M, Fujii C, Kanczkowski W, Ziogas A, Peitzsch M, Grossklaus S, Sonnichsen B, Gravanis A, Bornstein SR, Charalampopoulos I, Tsatsanis C, Chavakis T. 2018. DHEA inhibits acute microglia-mediated

inflammation through activation of the TrkA-Akt1/2-CREB-Jmjd3 pathway. *Mol Psychiatry* 23: 1410-20

219. Schulthess J, Pandey S, Capitani M, Rue-Albrecht KC, Arnold I, Franchini F, Chomka A, Ilott NE, Johnston DGW, Pires E, McCullagh J, Sansom SN, Arancibia-Carcamo CV, Uhlig HH, Powrie F. 2019. The Short Chain Fatty Acid Butyrate Imprints an Antimicrobial Program in Macrophages. *Immunity* 50: 432-45.e7